# ASSESSMENT OF AIR QUALITY DUE TO THE EMISSIONS FROM A COAL-FIRED POWER PLANT USING A DIFFUSION MODEL

**FARZANA FAIZA**

**M.Sc. ENGINEERING THESIS**

**DEPARTMENT OF CIVIL ENGINEERING**
**MILITARY INSTITUTE OF SCIENCE AND TECHNOLOGY**
**DHAKA, BANGLADESH**

**MARCH 2022**

# ASSESSMENT OF AIR QUALITY DUE TO THE EMISSIONS FROM A COAL-FIRED POWER PLANT USING A DIFFUSION MODEL

FARZANA FAIZA (SN. 1016110016)

A Thesis Submitted in Partial Fulfillment of the Requirements for the Degree of Master of Science in Civil Engineering

DEPARTMENT OF CIVIL ENGINEERING
MILITARY INSTITUTE OF SCIENCE AND TECHNOLOGY
DHAKA, BANGLADESH

MARCH 2022

ASSESSMENT OF AIR QUALITY DUE TO THE EMISSIONS FROM A COAL-FIRED POWER PLANT USING A DIFFUSION MODEL

M.Sc. Engineering Thesis

By

FARZANA FAIZA (SN. 1016110016)

Approved as to style and content by the Board of Examination on 24 March 2022:

| | |
|---|---|
| Dr Md Tauhid Ur Rahman<br>Professor of Civil Engineering<br>MIST, Dhaka | Chairman (Supervisor)<br>Board of Examination |
| Dr Tanvir Ahmed<br>Professor of Civil Engineering<br>BUET, Dhaka | Member (External)<br>Board of Examination |
| Maj Mohammad Shafiul Azam, PhD<br>Associate Professor of Environmental, Water Resources and Coastal Engineering<br>MIST, Dhaka | Member<br>Examination |
| Col Nasir Uddin Ahmed<br>Dean, Faculty of Civil Engineering<br>MIST, Dhaka | Member (Ex-Officio) |

Department of Civil Engineering MIST, Dhaka

ASSESSMENT OF AIR QUALITY DUE TO THE EMISSIONS FROM A COAL-FIRED POWER PLANT USING A DIFFUSION MODEL

## DECLARATION

I hereby declare that the study reported in this thesis entitled as above is my original work and has not been submitted before anywhere for any degree or other purposes. Further, I certify that the intellectual content of this thesis is the product of my own work and that all the assistance received in preparing this thesis and sources have been acknowledged and/or cited in the reference section.

Farzana Faiza
Student No. 1016110016

Department of Civil Engineering MIST, Dhaka

ASSESSMENT OF AIR QUALITY DUE TO THE EMISSIONS FROM A COAL-FIRED POWER PLANT USING A DIFFUSION MODEL

A Thesis

By

Farzana Faiza

# DEDICATION

Dedicated to my parents for supporting and encouraging me to believe in myself.

ABSTRACT

**Assessment of Air Quality due to the Emissions from a Coal-Fired Power Plant Using a Diffusion Model**

Barapukuria Thermal Power Plant is the very first coal-based power plant in Bangladesh established in the year 2006. Currently, various coal-run electricity generating plants are in pipeline in Bangladesh. On the other hand, coal-based thermal power plants are cited to be one of the major sources of pollution affecting human health and the environment. It is therefore important to assess the impact of the emission of coal-fired power plants on ambient air quality.

The objective of this study, therefore, is to simulate the dispersion and transport of pollutants emitted due to the operations of a coal-based power plant. For this study Barapukuria, Thermal Power Plant was selected. The assessment was made under two scenarios: (a) Scenario I: Plant Operating with 150 MW Capacity (3rd unit only) and (b) Scenario II: Plant Operating with 525 MW Capacity (Maximum Capacity). A dispersion model AERMOD was used to investigate the pollutant dispersion and ground level concentration at receptor grids over a 30 x 30 km domain for a one-year period. One year (2020) meteorological data was purchased from Lakes Environmental. An extensive field study was conducted to collect ambient air quality data for validation of the model. A questionnaire survey was also conducted among the people living in the vicinity of the power plant to assess the impact on human health.

Simulation results showed that the radius of impact of the emissions is approximately 5 km. The concentration of emissions at receptors located in the southwestern direction was found to be higher as the winds carried the pollutant clouds in their direction. The predicted peak concentrations of $SO_2$ in the area are 18.62 $\mu g/m^3$, 3.19 $\mu g/m^3$, and 0.82 $\mu g/m^3$ for 1-hr, 24-hr, and annual averaging periods respectively. Similarly, the predicted maximum concentrations of NOx in that area are found to be 33.56 $\mu g/m^3$, 5.75 $\mu g/m^3$, and 1.48 $\mu g/m^3$ for 1-hr, 24-hr, and annual averaging periods respectively. The peak concentrations of CO

are 9.32 μg/m$^3$, 1.59 μg/m$^3$, and 0.41 μg/m$^3$ for 1-hr, 24-hr, and annual averaging periods respectively. The predicted resultant concentration of NOx exceeds WHO guideline values whereas $SO_2$ and CO concentrations comply with Bangladesh air quality standards and WHO guideline values. The predicted peak concentration of pollutants ($SO_2$, NOx, and CO) over the modeled area increases about five times from scenario I (only the 3$^{rd}$ unit, operating with 150 MW capacity) to Scenario II (all units operating with 525 MW capacity).

Assessment of seasonal and diurnal variation of pollutants showed that change in pollutant behavior is largely dictated by meteorological parameters. Over a particular day, the peak concentration of pollutants is typically reached in the morning to noon. The dispersion model results were compared with the air quality data measured at the same location to validate the model. The performance evaluation, with the aid of statistical measures, revealed that the models' performance was acceptable.

From the model output results, the field measured ambient air quality data, and the questionnaire survey it can be concluded that the maximum emissions of air pollutants ($SO_2$, NOx, CO) due to the power plant operation is not harmful to the health of the people living in the vicinity of the plant.

# ACKNOWLEDGEMENT

First of all, the author would like to express her utmost gratefulness to the Almighty Allah for bestowing this opportunity to conduct the research endeavor and achieve desired results.

The author expresses her deepest thankfulness to her thesis supervisor, Dr. Md Tauhid Ur Rahman, Professor, Department of Civil Engineering, Military Institute of Science and Technology (MIST) for his continual support, immeasurable guidance, and ceaseless assistance throughout the execution of this thesis work. His valuable insights were of vital aid for the author in the completion of this research activity.

The author would like to express her special thanks to Dr. Tanvir Ahmed, Professor, Department of Civil Engineering, Bangladesh University of Engineering and Technology for his support in learning the modeling software.

The author expresses her gratefulness to all the faculty members and staff of the Department of Environmental, Water Resources, and Coastal Engineering, MIST for providing laboratory facilities and cooperation during the field visits. The author also expresses her gratitude to the members of Bangladesh Army for their cordial support to make the field visits successful.

The author would also like to thank the authority and members of Barapukuria Thermal Power Plant, Barapukurai Coal Mining Company Limited and Petrobangla for their assistance in collecting different data.

Lastly, the author expresses profound gratitude to her family for their endless love, unceasing prayers, and encouragement. Without them, the accomplishment of this thesis would not have been possible.

TABLE OF CONTENTS

LIST OF FIGURES

LIST OF TABLES

# ABBREVIATION

| | |
|---|---|
| BTPP | Barapukuria Thermal Power Plant |
| GLC | Ground Level Concentration |
| AERMOD | American Meteorological Society/Environmental Protection Agency Regulatory Model |
| AQI | Air Quality Index |
| DoE | Department of Environment |
| EIA | Environmental Impact Assessment |
| NOx | Nitrogen Oxides |
| $SO_2$ | Sulfur dioxide |
| CO | Carbon Monoxide |
| $PM_{10}$ | Particulate Matter Having diameter of 2.5 to 10 micrometer |
| $PM_{2.5}$ | Particulate Matter Having diameter smaller 2.5 micrometer |
| MW | Mega Watt |
| WHO | World Health Organization |
| EU | European Union |
| USEPA | United States Environmental Protection Agency |
| CASE | Clean Air and Sustainable Environment |
| CAMS | Continuous Air Monitoring Station |
| CEMS | Continuous Emission Monitoring System |
| BPDB | Bangladesh Power Development Board |
| BCMCL | Barapukuria Coal Mining Company Ltd. |
| IPP | Independent Power Producer |

| | |
|---|---|
| CPGCL | Coal Power Generation Company Ltd |
| APSCL | Ashuganj Power Station Company Ltd |
| CBL | Convective Boundary Layer |
| PDF | Probability Density Function |
| RH | Relative Humidity |
| ALR | Ambient Lapse Rate |
| DALR | Dry Adiabatic Lapse Rate |
| PBL | Planetary Boundary Layer |

# CHAPTER 1

# INTRODUCTION

## 1.1 General

Air is indispensable to all living beings in this world. Poor air quality affects human health as well as the environment. By reducing air pollution levels, the disease burden can be reduced from stroke, heart disease, lung cancer, and both chronic and acute respiratory diseases, including asthma. Industrial pollution is one of the most dominating sources among all anthropogenic sources of air pollution. Globally the power plant sector is considered an increasing threat to human health and the environment. To ensure clean and healthier air by reducing air pollutants emission, it is crucial to understand how the power production industry contributes to air pollution emissions.

## 1.2 Problem Statement

To ensure stable and universal access to electricity at affordable prices, like many developing countries Bangladesh is shifting to an electricity mix dominated by coal-fired power generation. At present, the country has a combined installed generation capacity of over 22,031 MW. Among these gas accounts for 51.97%, coal about 8.03%, fuel oil (furnace and diesel) 27.25%, and hydropower accounts for 1.04%. Coal-based power plants are supplying 1764 MW (BPDB, 2021). According to the power master plan Bangladesh has a target to generate 40000 MW by 2030 and 60000 MW by 2041. The plan suggests that 70% of the generation would come from coal and gas. Depending on different scenarios considered the contribution of coal can be somewhere between 15 to 55% (Power Division, 2016). As a part of the master plan, various coal-fueled megaprojects for electricity generation are under implementation in Bangladesh. The establishment of the Barapukuria Thermal Power Plant (BTPP) is such a type of endeavor for energy production starting in early 2006. The installed capacity of the power plant was 2X125 MW. Another unit with 275 MW was added to the national grid in 2018 (BPDB, 2020). By the year 2016-17, the plant consumes 5334153.994 tons of coal supplied from the nearby Barapukuria Coal Mining Company Ltd. (BCMCL, 2019).

Although, the presence of carbon, hydrogen and sulfur in coal facilitates the energy generation in coal combustion, some pollutants including $CO_2$, SOx, NOx, particulate matter (PM) and heavy metals accumulate in air and water and lead to severe environmental and health impacts (Munawer, 2017). The environmental costs of coal-based power plants and its economic benefits has been debated many times around the world which triggered numerous research on its adverse impacts (Shaikh et al., 2018).

The World Health Organization (WHO) considers clean air to be a basic requirement of human health and well-being. It recognizes ambient air pollution as a major environmental health problem affecting everyone in developed and developing countries. In the year 2020, air pollution ranked as second among all the risk factors of most death and disability in Bangladesh. The total number of annual deaths attributed to the exposure to $PM_{2.5}$ was 123,000 in Bangladesh in 2017 (Health Effects Institute, 2019).

Therefore, there is a critical need to evaluate the environmental impacts and health risks of the population living in the vicinity of the coal fired power plant of Barapukuria. This kind of study has been conducted in many other countries such as Mexico (Lo´pez et al., 2005), Cuba (Carbonell et al., 2007), Malaysia (Mokhtar et al., 2014), and India (Roy et al., 2019).

The outdoor air quality pattern can be indexed and predicted using air quality monitoring and air dispersion modeling. The air quality monitoring stations in Bangladesh consists of eleven Continuous Air Monitoring Stations (CAMS) in Dhaka, Narayanganj, Gazipur, Chittagong, Khulna, Rajshahi, Barisal and Sylhet (CASE, 2018), Installed by Department of Environment (DoE) of Bangladesh Government, which record the concentrations of $PM_{10}$, $PM_{2.5}$, CO, $SO_2$, NOx and $O_3$. Various air quality models such as ATMoS, CALPUFF, ISCST3, AERMOD etc. are commonly used to simulate the spatial and temporal dispersion of pollutants. These dispersion model simulations help to investigate the deterioration of ambient air quality owing to emissions from major sources.

Numerous studies have assessed the pollutant transportation, dispersion and health effects from thermal power plant emissions. Lopez et al. (2005) calculated annual average concentrations of primary and secondary (sulfates and nitrates) particulate matter by using the CALPUFF-CALMET modeling system. Mokhtar et al. (2014) studied ambient air quality around Kapar

Power Plant in Malaysia and predicted the ground level concentration of pollutants $SO_2$, Hg, As and Cr to assess the carcinogenic and non-carcinogenic health risks using AERMOD. Dai et al. (2019) investigated the emission of nitrogen oxides, sulfur dioxide and particulate matter from coal power plants in Anhui to assess the impact of control measures on the atmospheric emissions based upon continuous emission monitoring systems (CEMS). Carcinogenic and non-carcinogenic risks of $PM_{10}$ and $PM_{2.5}$ bound trace metals, using exposure pathways, in a critically polluted coal mining area, the Jharia Coalfield, India was analyzed by Roy et al. (2019). Adeniran et al. (2018) assessed air quality in major cement plant in Ibese Ogun State, Nigeria through ambient air quality monitoring and air dispersion modeling using AERMOD.

Limited studies have been conducted on air dispersion modeling in Bangladesh, among them most of the studies were focused on the air pollution from brick kiln and motor vehicles in Dhaka city (Guttikunda, 2019; Muntaseer Billah Ibn Azkar et al., 2012). In the last few years some studies have been conducted on air dispersion modeling for coal fired power plants as several coal fired power plants are in pipeline in Bangladesh at present. The Environmental Impact Assessment reports of coal fired power plants are most significant among them. The EIA reports of Matarbari 1200 MW Ultra Super Critical Coal Fired Power Plant and Payra 1320 MW Thermal Power Plant Project used different diffusion models to evaluate the impacts of emitted pollutants from the plant. Recently, Hossain et al. (2020) conducted a study on noncarcinogenic health risks associated with emissions from coal fired power plants developing in Payra,Bangladesh using AERMOD. But these studies were based on theoretical model assumptions as the power plants were not operating at that time.

The outcome of this study will evidently represent the dispersion of emissions from the operations of Barapukuria Coal Fired Power Plant and its effect on the ambient air quality in the surrounding area. The study uses a dispersion model, AERMOD, to investigate the dispersion of pollutants released from the plant. This study considers two scenarios: (a) 150 MW Running Load, (b) 525 MW Total Load. The outcome of this study will be crucial in assessment of possible health and environmental effect due to the operation of a coal fired power plant in Bangladesh.

### 1.3 Objective of the Research Work

This study is aimed at to demonstrate the power plant emission and its distribution with the change of space and time. The ultimate goal of the study is to find out the contribution of power plant emissions to the ambient air quality.

The specific objectives include:

- To predict ground level concentration of major pollutants ($SO_2$, NOx and CO) due to operation of the power plant using an advanced air quality model (AERMOD).
- To assess seasonal and diurnal variation of pollutants due to the meteorological conditions.
- To evaluate the model performance through specific statistical parameters and by comparing the simulated and observed concentrations distributions.

### 1.4 Organization of the Thesis

The thesis is presented in following five chapters comprising different aspect of the study.

Chapter 1 gives a general overview of the background information, specific objectives and structure of the thesis.

Chapter 2 reviews the basic information on air pollution, its sources and impacts. An overview of the air pollution status and air quality standards in Bangladesh have been presented. A detailed description of the present power generation situation of the country along with the associated hazardous pollutant emissions have been presented in this chapter. This chapter further summarizes the various air quality models used for modeling dispersion of air pollutants. This chapter further discusses the previous works in Bangladesh related to air dispersion modeling of coal fired power plant. This chapter also discusses the techniques used for evaluation of model performance.

Chapter 3 describes the methodologies adopted in the present study. This chapter provides a detailed description of the meteorological parameters and measured baseline ambient air quality in Barapukuria area. The procedure followed to model the dispersion of pollutants emitted from the power plants using AERMOD View 10.0.1 has been described in this chapter. It also highlights the procedures followed to validate the model.

Chapter 4 presents the spatial and temporal distribution of the pollutants. It also includes an elaborate evaluation of seasonal and diurnal variation of pollutant concentration, and their relationship with various meteorological parameters. The effects of the power plant emission on ambient air quality and contribution of the plant emission have been illustrated in this chapter. This chapter further evaluates the model performance results. The chapter concludes with the impact on human health of the power plant.

Chapter 5 summarizes the major conclusion from the present study. This chapter also presents the recommendations for future studies.

# CHAPTER 2

# LITERATURE REVIEW

## 2.1 General

This chapter provides comprehensive literature encompassing the air pollution, global air pollution due to power generation, Gaussian dispersion modeling, performance evaluation of air dispersion model, emission estimation and health effect of air pollutants.

## 2.2 Power Sector in Bangladesh

Incessant supply of power and energy is the prerequisite for the progress of an economy. The importance of energy is even more supplementary in the context of Bangladesh, an emerging economy that has been experiencing rapid economic growth but also has been experiencing prolonged period of energy crisis. Electricity is the main form of energy that is tapped on both private and commercial scales in Bangladesh. However, the country is still at a very low level of electrification. To meet the increasing demand for Power, the government of Bangladesh has undertaken massive steps towards increasing the power supply in the short span of time by encouraging private sector power production as well as import of power from native countries.

Bangladesh is known for its substantial stores of natural gas. About 52% of the nation’s electricity is generated from natural gas. As of 2020, the country’s total installed capacity was 22,031 MW (BPDB, 2021). The residential sector is the foremost user of grid electricity at about 51.0%, followed by industrial sector at 34.3%. Table 2.2 breaks down energy consumption by sector (SREDA, 2016). Most existing plants are gas fired and some are oil fired. Due to heavy usage of gas in the residential, utility, and transportation sector, the existing reserve of gas are decreasing (Hossain et al., 2020). The government is also trying to minimize the consumption of natural gas and seeking alternative ways to produce electricity. Currently the government is focusing on promoting renewable electricity production (Islam and Khan, 2017). The predicted transition of sources of electricity generation in Bangladesh from 2015 to 2021 has been shown in Figure 2.1.

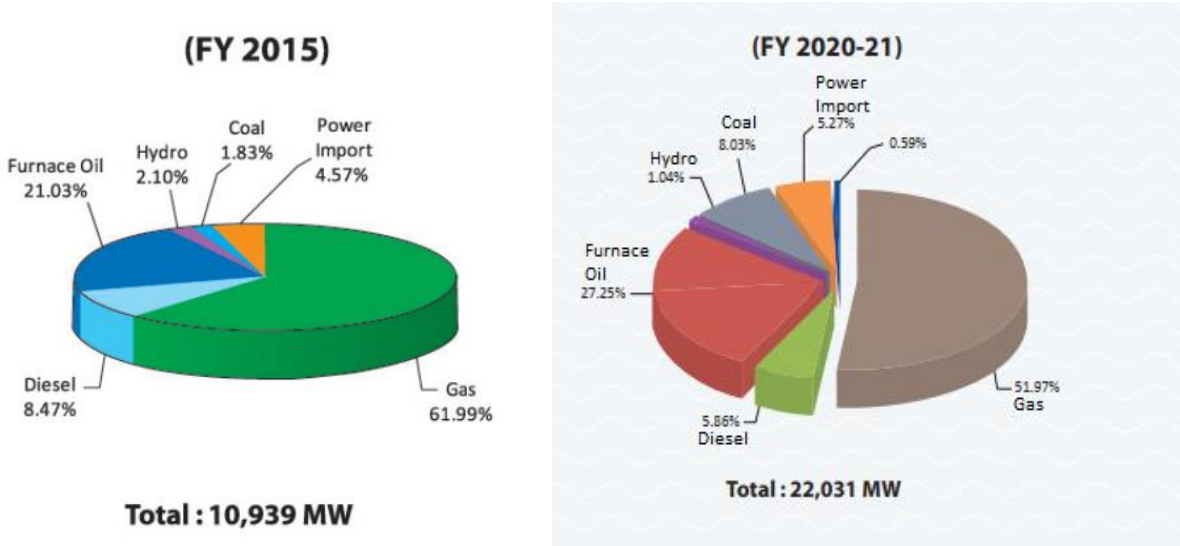


Figure 2.1: Transition of source of electricity generation in Bangladesh (2015-2021)
(Source: BPDB, 2021)

Bangladesh has only one hydro power plant, of 230 MW capacity, in Kaptai. Currently, a nuclear power plant of 2000 MW is under construction in Rooppur in collaboration with Russia.

Favorable Government policies have attracted private investment and Independent Power Producers (IPP). They are now producing 43% of total power in Bangladesh (BPDB, 2021). The country is also importing power from India.

The international price of coal is relatively more stable and has lower volatility compared with oil and natural gas, coal also has wider availability throughout the world and can provide a more diversified and stable supply. With this understanding the government has planned to set up coal based large base-load power plants. The plan was to produce 7500 MW from coal based power plant by 2021 (Islam and Khan, 2017). Six coal-run electricity generating plants are in the pipeline in Bangladesh upto the year of 2025, including Rampal Coal Fired Power Plant of 1320 MW capacity in Bagerhat district, Chattogram 2 x 612 MW Coal Fired Power Plant, Borishal 307 MW Coal Fired Power Plant, Patuakhali 1320 MW Ultra Super Critical Thermal Power Plant, Matarbari 1200 MW Ultra Super Critical Thermal Power Plant in Cox’s Bazar district and Payra, Patuakhali 1320 MW Coal Fired Power Plant ($2^{nd}$ phase).

Table 2.1 Grid electricity consumption by sector (SREDA, May 2016)

| Sector | Electricity Consumption % |
|---|---|
| Industry | 34.3 |
| Transport | 0.0 |
| Residential | 51.0 |
| Commercial | 9.9 |
| Agriculture | 4.8 |

### 2.3 Emission of Air Pollutants from Coal Fired Power Plants

Coal-fired power plants are set to be the future of power generation in Bangladesh, hence, emission from this source has become a major concern. Various studies across the globe have shown that emissions from coal-fired power stations can be harmful to the environment and human health (Adappa et al., 2017; Kravchenko and Lyerly, 2018; Yue et al., 2021)**.** The most important primary emissions associated with coal-fired power stations which are known for their adverse environmental and/or human health impacts include PM, $SO_2$, NOx, mercury (Hg) and GHG ( Baig and Yousaf, 2017; Zhao et al., 2008)**.**

In 2017, coal-fired power plants accounted for 4565 million tonnes (Mt) of $CO_2$ emissions, 1.2 Mt. of $SO_2$ emissions, 1.14 Mt. of nitrogen oxides emissions and 0.26 Mt. of $PM_{2.5}$ emissions in China (International Energy Agency, 2019). As the main cause of air pollution in China coal combustion is estimated to contribute 40% to the total $PM_{2.5}$ concentration at its national level (Wei et al., 2020).

India has the second largest planned expansion of coal burning capacity in the world (second only to China). This expansion if brought online, could significantly increase health risks in neighboring communities (Kopas et al., 2020). In fiscal year 2010-2011 alone, India’s coal fired plants caused as many as 80-115 thousand premature deaths at an estimated cost of USD 3.2-4.6 billion (Guttikunda and Jawahar, 2014).

Emissions from coal fired power plants have drawn significant concern due to their long range transport, harmful effects on human health, atmospheric visibility, vegetation, and cultural heritage (Liu et al., 2019; Wang et al., 2017). Therefore, controlling emissions from coal fired power plants plays a vital role in improving air quality.

### 2.4 Studies Related to Coal Fired Power Plants in Bangladesh

Five coal fired power plants each with 1320 MW generation capacity are expected to be installed by 2030 in areas within 5 km radius of Payra, situated in Patuakhali district. Pollutant concentration of these future power plants were predicted by Hossain (2019) using AERMOD air diffusion model in three different scenarios.

In the EIA (CPGCL, 2013) report of proposed Matarbari 1200 MW coal fired power plant, yearly average, 24-hour average and 1-hour average values of pollutant concentration were calculated using Gaussian diffusion model. Modeling study suggests that the predicted concentration of pollutants from exhaust gases, taking into account the background, will satisfy the ambient air quality standards of Bangladesh as well as environmental standards of the EU.

The Maximum Ground Level Concentration of $SO_2$ and NOx were calculated using SCREEN 3 model in the EIA (EQMS, 2015) report of proposed Payra 2x660 MW coal fired power plant, in Patuakhali district.

AERMOD air dispersion model was used for the prediction of emission of $NO_2$ from the proposed Ashuganj 400 MW combined cycle power plant (APSCL, 2016)

### 2.5 Environmental Impacts of Barapukuria Coal Fired Power Plant

The generation of electricity and consumption of energy in general, result adverse effects on the environment. Barapukuria is the only natural coal mine reserve in Bangladesh that is currently in operation. Barapukuria thermal power plant produces electricity from the reserved coal. The coal available in Bangladesh is of very high quality, with low ash content and high calorific value. Coal quality plays a vital role in environmental impact as well as gaseous emissions (Masud et al., 2014).

Hossain et al. (2015) assessed the environmental impacts of coal mine and thermal power plant to the surroundings of Barapukuria. The heavy metal, organic carbon and exchangeable cations of coal water mixed with the farmland soil suggest the deterioration of surrounding water and soil. Rahman et al. (2019) studied the water samples of Tillai River adjacent to the Barapukuria Thermal Power Plant. The study suggested that the river water quality is highly degraded as the drainage exit of the power plant is straightforwardly tumbled to the Tillai River.

Alam et al. (2011) evaluated the health impacts of SPM (suspended particulate matter) emitted from the combustion of coal in Barapukuria Thermal Power Plant and it was found that the cumulative analysis of the study that the impact was positive. Tamin et al. (2013) shows the analysis of fly ash of Barapukuria coal fired power plant. Fly ash is one of the common residues produced from combustion of coal. Rokonuzzaman et al. (2019) studied the total emission of $SO_2$, from Barapukuria Themal Power Plant and its impact on the surrounding area. Therefore, this study gives emphasis on the possible air pollutant emissions from Barapukuria Themal Power plant.

### 2.6 Air Pollution

Air pollution is the introduction of chemicals, particulates or biological material that cause discomfort, disease, or death to humans, damage other living organisms such as food crops, or damage the natural environment. The world Health Organization defines air pollution as 'the disequilibrium of air caused due to the introduction of foreign elements to humans' natural and manmade sources to the air so that it becomes injurious to biological communities. It has also been defined as the contamination of air by discharge of harmful substances, which can cause health problems including burning eyes and nose, itchy irritated throat and breathing problems (USEPA, 1995).

Pollution of the environment is one of the most concerning ecological crises the world is subjected today. The environment (air, land or soil and water) was in the past pure, virgin, undistributed, uncontaminated and basically most hospitable for living organisms but the situation is just the reverse today. Today, the environment has become foul, contaminated, undesirable and therefore, harmful for the health of living organisms, including man.

Atmosphere is a complex natural gaseous system that is essential to support life on planet Earth. Stratospheric ozone depletion due to air pollution has long been recognized as a threat to human health as well as to the Earth's ecosystems (Brancher, 2021). Due to enhanced human activities producing increased emissions atmospheric pollution in urban area has become a major issue in developing countries all over the world. The emission rates of increasing air pollutants in the cities of developing countries are higher than those of developed countries (Wang et al., 2022).

In 2019, air pollution is estimated to have contributed to 6.67 million deaths (95% UI:5.90 to 7.49 million) worldwide, nearly 12% of the global total deaths (Figure 2.2). Air pollution is the leading environmental risk factor for early deaths, with its total impact exceeded only by high blood pressure (10.8 million, 95% UI: 9.51 to 12.1 million), tobacco use (8.71 million, 95% UI: 8.1 to 9.3 million) and dietary risks (7.94 million, 95% UI: 6.5 to 9.8 million) (Health Effects Institute, 2020).

The pollution level is particularly serious in Asian countries: 86% of the most extreme concentrations (above 75 g/m$^3$) are experienced by population of China, India, Pakistan, Bangladesh (Ma and Takeuchi, 2020).

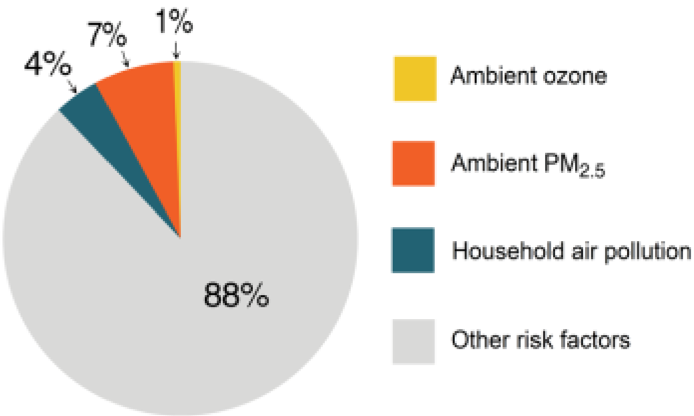


Figure 2.2: Percentage of global deaths attributable to individual pollutant (Health Effects Institute, 2020)

## 2.7 Effects of Air Pollution

**(a) Health Effect:** People exposed to high levels of certain air pollutants may experience: irritation of eyes, nose, throat, wheezing, coughing, chest tightness and breathing difficulties, worsening of existing lung and heart problems, such as asthma, increased risk of heart attack. Dust has been documented through the years as one of the biggest occupational killers (Petavratzi et al., 2005) and a wide range of occupational diseases may develop in mine workers depending on the properties of the inhaled dust. In addition, long term exposure to air pollution can cause cancer and damage to immune, neurological, reproductive and respiratory system. In extreme cases, it can even cause death (Kim et al., 2021).

**(b) Environmental effects:** Air pollution can cause a variety of environmental effects: acid rain is precipitation containing harmful amounts of nitric and sulfuric acids. These acids are formed primarily by nitrogen oxides and sulfur oxides released into the atmosphere when fossil fuels are burned. These acids fall to the Earth either as wet precipitation (rain, snow, or fog) or dry precipitation (gas and particulates). In the environment, acid rain damages tree and causes soils and water bodies to acidify, making the water unsuitable for some fish and other wildlife (Burns et al., 2016). It also speeds the decay of buildings, statues, and sculptures that are part of our national heritage.

Eutrophication is a condition in a water body where high concentrations of nutrients (such as nitrogen) stimulate blooms of algae, which in turn can cause death of fish and loss of plant and animal diversity. Air emissions of nitrogen oxides from power plants, cars, trucks, and other sources contribute to the amount of nitrogen entering aquatic ecosystems. Haze is caused when sunlight encounters tiny pollution particles in the air. Haze obscures the clarity, color, texture, and form of what we see. Some haze-causing pollutants (mostly fine particles) are directly emitted to the atmosphere by sources such as power plants, industrial facilities, trucks and automobiles, and construction activities.

**(c) Effects on wildlife:** Toxic pollutants in the air, or deposited on soils or surface waters, can impact wildlife in a number of ways. Like humans, animals can experience health problems if they are exposed to sufficient concentrations of air toxics over time. Studies show that air toxics are contributing to birth defects, reproductive failure, and disease in animals.

Persistent toxic air pollutants (those that break down slowly in the environment) are of particular concern in aquatic ecosystems. These pollutants accumulate in sediments and may biomagnify in tissues of animals at the top of the food chain to concentrations many times higher than in the water or air (Forero López et al., 2022).

**(d) Ozone depletion:** At ground level, ozone is a pollutant that can harm human health, in the stratosphere, however, ozone forms a layer that protects life on earth from the sun's harmful ultraviolet (UV) rays. But this "good" ozone is gradually being destroyed by man-made chemicals referred to as ozone-depleting substances, including chlorofluorocarbons, hydrochlorofluorocarbons, and halogens. These substances were formerly used and sometimes still are used in coolants, foaming agents, fire extinguishers, solvents, pesticides, and aerosol propellants. Thinning of the protective ozone layer can cause increased amounts of UV radiation to reach the Earth, which can lead to more cases of skin cancer, cataracts, and impaired immune systems (Brancher, 2021).

**(e) Crop and forest damage:** Ground-level ozone can lead to reductions in agricultural crop and commercial forest yields, reduced growth and survivability of tree seedlings, and increased plant susceptibility to disease, pests and other environmental stresses (such as harsh weather). Crop and forest damage can also result from acid rain and from increased UV radiation caused by ozone depletion. UV can damage sensitive crops, such as soybeans, and reduce crop yields (Shi et al., 2021).

**(f) Global climate change:** The Earth's atmosphere contains a delicate balance of naturally occurring gases that trap some of the sun's heat near the Earth's surface. This "greenhouse effect" keeps the Earth's temperature stable. Unfortunately, evidence is mounting that humans have disturbed this natural balance by producing large amounts of some of these greenhouse gases, including carbon dioxide and methane. As a result, the Earth's atmosphere appears to be trapping more of the sun's heat, causing the Earth's average temperature to rise - a phenomenon known as global warming (Brancher, 2021).

## 2.8 Air Pollution in Bangladesh

Air pollution is one of the major manmade environmental problems that had recently gained importance among environmental issues in Bangladesh (Ahmed and Hossain, 2008). Bangladesh has been ranked first among 106 countries with worst air quality in the air pollution monitoring report of IQAir (IQAir, 2020). Moreover, two Bangladeshi cities such as Manikganj and Dhaka have been put among the top 25 cities with poorest air. Air pollution of Bangladesh for outdoor and indoor is caused due to increasing population, associated motorization, industrial emissions and usage of biomass fuels during cooking with poor ventilation. Industries are mainly concentrated in major urban metropolitan areas such as Dhaka, Rajshahi, the seaport cities such as Khulna, the inland port city Narayanganj, and other divisional towns. Apart from unplanned industrial development in these areas, the severity of the pollution is increased mainly due to exhaust from two stroke engine and diesel run vehicles. In the rural areas of Bangladesh, the danger of outdoor air pollution has not yet turned into a point of concern. This is due to less motorized vehicles and industries in rural areas (Shindell et al., 2012). Agro based industries like sugar, pulp, paper, tanneries and value-added industries like textile, garments, pharmaceuticals, oil refineries and fertilizers and chemical industries are also contributing for air pollution. Other than industrial emission there are many brick making kilns which on being operating seasonally, mainly in dry seasons all over Bangladesh. Almost all of these kilns use coal and wood as their prime source of energy, resulting in the emission of particulate matter, oxides of sulfur, and volatile organic compounds. Rana et al. (2016) studied the trends of atmospheric particulate matter in Dhaka, Narayanganj and Gazipur: the observation revealed that the pollution levels followed the same pattern from November 2012 to march 2015 (Figure 2.3)

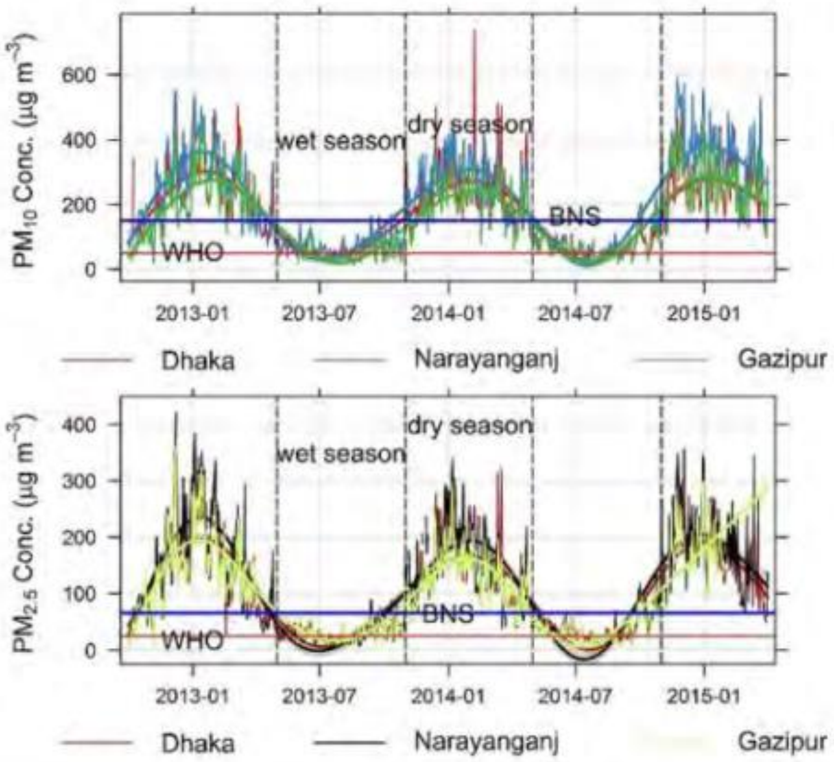


Figure 2.3: Time series plot of daily $PM_{10}$ and $PM_{2.5}$ concentrations captured at Dhaka, Narayanganj and Gazipur (Rana et al., 2016)

Studies in published literature indicate that increased mortality from CVD and respiratory diseases in Bangladesh are likely resulting from the high air pollution exposures (Massey et al., 2013). Air pollution ranked second among the all-risk factors of most death and disability in Bangladesh and high blood pressure ranked third (Institute for Health Metrics and Evaluation (IHME), 2018). According to a global state of air report, the number of annual deaths attributed to the exposure to $PM_{2.5}$ was 123,0000 in Bangladesh in 2017 (Health Effects Institute, 2019). In the last two decades, the mortality attributed to air pollution has been estimated to increase by 52% in Bangladesh. One recent reported that the total number of premature death attributed to $PM_{2.5}$ Exposure was 9051 (95% CI: 4596-12025), including 4435 (95% CI: 1721-5304) for ischemic heart disease (IHD), 2669 (95% CI: 1850-4135) for stroke, 1246 (95% CI: 684-1689) for chronic obstructive pulmonary disease (COPD), 500 (95% CI: 204-649) for lung cancer (LC), and 201 (95% CI: 137-248) for acute lower respiratory infection (ALRI) in Dhaka in 2016 (Maji et al., 2018).

Ambient air quality standards were first introduced in Bangladesh in 1997 under the Environmental Conservation Rules (ECR), 1997. Bangladesh released the draft Clean Air Bill in 2019, which sets the stage for preparation of the National Air Quality Management Plan as well as identification of critical air quality areas, among other measures (bdenvironment.com, 2013-2021). The country also undertook an extensive program (Clean Air and Sustainable Environment Project) to address air pollution from brick kilns and the transportation sector between 2009 and 2019.

## 2.9 Air quality Standards in Bangladesh

Air quality standards provide maximum limits on the amount of a specific pollutant in the air for precise averaging periods. These ambient standards primarily aim at human health protection and have been estimated to permit a margin for citizens susceptible to risk. These guidelines and standards are critical to efficient air quality administration, and they provide the link between the emissions source and the receptor that is provided in the downstream location. These values specify harmless daily exposure quantities for the greater part of the population, all over an individual's life period.

Table 2.2 lists the air quality standards of Bangladesh, United states Environmental Protection Agency (USEPA), and the World Health Organization (WHO).

From this table, it could be seen that Bangladesh standards are more or less same as those of the USEPA. The standards for the different pollutants are set considering the different averaging period, since health effect of air pollutants are directly related to exposure time. In order to analyze the air quality data of a city it is necessary to compare these values with already established standard.

Table 2.2: Air Quality Standards

| Pollutant | Averaging Period | Bangladesh Standard ($\mu g/m^3$) | WHO Guideline Values ($\mu g/m^3$) | US EPA Standards ($\mu g/m^3$) |
|---|---|---|---|---|
| $SO_2$ | Annual | 80 | - | - |
| | 24 hr | 365 | 20 | - |
| Pb | Annual | 0.5 | 0.5 | - |
| NOx | Annual | 100 | 40 | 100 |
| | 1 hr | | 200 | 188 |
| SPM | 8 hr | 200 | - | - |
| $PM_{2.5}$ | Annual | 15 | 10 | 15 |
| | 24 hr | 65 | 25 | 35 |
| $PM_{10}$ | Annual | 50 | 20 | |
| | 24 hr | 150 | 50 | 150 |
| $O_3$ | 1 hr | 235 | - | 235 |
| | 8 hr | 157 | 100 | 140 |
| CO | 8 hr | 10,000 | 10,000 | 10,000 |
| | 1 hr | 40,000 | 30,000 | 40,000 |

### 2.10 Air Dispersion Models

Air quality modeling is an extremely complex phenomenon involving a myriad of factors, including emission of pollutants, atmospheric reactions, and meteorological conditions. The dispersion models employ mathematical and numerical techniques to simulate the physical and chemical processes of air pollutants in the atmosphere. These models are designed to characterize primary pollutants that are emitted directly into the atmosphere and, in some cases, secondary pollutants that are formed as a result of complex chemical reactions within the atmosphere. The fundamental aim of the dispersion models is to accurately estimate the pollutant concentration downwind of any source based on inputs of wide range of meteorological conditions and source information like emission rates and stack height (Lakes Environmental Consultants Inc, 2003; USEPA, 2004).

There is a range of air dispersion models that have been used in different jurisdictions around the world to treat a wide array of modeling circumstances. They have been developed to assess various source types including point, area, and volume, various terrain (i.e., simple or complex), various locales such as urban, rural, various emission rates include plume, puff and various meteorological conditions. Air dispersion models have many features that cause them to be used in different investigations of air quality. They have the ability to elucidate the interactions of emission sources and the geophysical and meteorological conditions. Moreover, using the dispersion models, it is possible to: determine whether a permissible facility is obeying with state or federal necessities, evaluating where the best location site for an air monitor that reads actual data, etc., and finally, to estimate the possible environmental and health effects due to releases from industrial or trade locations.

There have been various review papers on atmospheric modeling and their approaches to dispersion of pollutants. Carqueira et al. (2019) simulated the dispersion of atmospheric pollutants from the Borborema thermal power plant in Brazil, using the AERMOD View program as a tool to evaluate the concentrations resulting from the simulation and to make comparisons with allowable levels according to current law.

Wang et al. (2022) simulated the dispersion of particulate matter from the in situ burning of spilled oil in the northwest Arctic area of Canada.

### 2.10.1 Need for air quality modeling

The atmospheric dispersion modeling can be useful in planning and designing urban setup, locating air quality monitoring stations, identifying maximum concentration occurring points. They play vital role in estimating future impact of the proposed expansion of any industrial activity or new industry**.** In general air quality model is a tool for:

a) Establishing emission control legislation, i.e., determining maximum allowable emission rates that will meet fixed air quality standards.
b) Evaluating proposed emission control techniques and strategies, i.e., evaluating the impact of future control.

c) Selecting location of future sources of pollution, in order to minimize their environmental impacts.
d) Planning the control of air pollution episodes, i.e., defining immediate intervention strategies, (i.e., warning systems and real-time short-term emission reduction strategies) to avoid severe air pollution episodes in a certain region. Establishing emission control legislation, i.e., determining maximum allowable emission rates that will meet fixed air quality standards.
e) Assessing responsibility for existing air pollution level, i.e., evaluating present source-receptor relationships.

Modeling of pollutant dispersion is employed for the following two main reasons:

a) Modeling can estimate pollutant concentration values at almost all locations wherever air monitoring network is not possible,
b) Models can also predict the impact of original sources prior to construction of the facility in addition to how novel pollution control and mitigation devices will influence the generation of the pollutant.

Air quality modeling is used to determine and visualize the significance and impact of emissions to the atmosphere. They are especially useful for the policy-makers to take effective abatement measure in managing air pollution.

### 2.10.2 Factors affecting dispersion of pollutants in atmosphere

Dispersion, i.e., the transport of pollutants from their source, consist of diffusion and advection processes. It determines whether a pollutant will accumulate or dilute in the atmosphere. Dispersion is influenced by several aspects including weather conditions and local topography (altitude, rivers and streams, etc.). Wind velocity and direction, atmospheric stability and location topography affect plume interaction in complex terrain and cause changes in the transport and dispersion of air pollutants. Drilling, loading and crushing of the ore at both primary and fine crushing plants generate dust which ends up being emitted in the atmosphere. Another possibility of generating dust at the processing plant is wind erosion from coarse and fine ore stockpiles especially during windy conditions. Wind erosion of tailings generates a high quantity of dust at mine. The magnitude of the problem becomes larger during windy conditions (Li et al., 2021).

Pollutant dispersion modeling helps as an extensive aid for visualizing the results of these complex interactions and assessing the quantity of ground-level pollution at different distances from origin. Dispersion causes convenient pollutant reduction near the source and harmful pollutant increases at the receptors.

Pollution dispersion in the air is affected by many factors:

- Dispersion from Emission Sources (stationary point, area, or mobile sources such as cars)
- Height of the pollutant emission sources
- Local topographical features Meteorological conditions
- Air Temperature Lapse Rates Atmospheric Boundary layer /Mixing Height Wind speed & direction
- Atmospheric air Inversions
- Humidity & Temperature
- Dispersion Coefficients
- Atmospheric stability

### 2.10.3 Classification of Dispersion Models

Air quality models can be classified by mathematical formulation or by objective. One formulation can meet more than one objective, just as one objective can be addressed with more than one formulation. This section discusses mathematical formulations and modeling objectives.

#### 2.10.3.1 Mathematical Formulations

Each mathematical formulation has inherent assumptions, advantages, limitations, and requirements for its implementation. This section presents information to help you select the formulation most appropriate to the requirements of your modeling study.

**i) Empirical or statistical**

An empirical model is an application of mathematics to a series of related data values for the purpose of establishing a relationship among dependent and independent variables. Various types of relationships (e.g., linear, exponential, logarithmic) can be tested to fit the data set. Statistics are applied to determine the values of parameters required for the specific formulation, as well as to estimate how well the resulting equation fits the data (i.e., goodness of-fit). Also, empirical models are based on mathematics instead of physical science. That is, the relationships developed within the data set may not have connections to principles of physics, chemistry, biology, or other physical sciences. These types of models, therefore, cannot be used to draw conclusions of how processes work in the underlying physical system.

**ii) Gaussian**

Gaussian models may be expanded in several ways. The surface of the Earth can be a perfect reflector such that any mass from the plume that touches the surface is reflected back up into the plume. Similarly, an elevated inversion layer in the atmosphere can be a perfect reflector. Some models allow a low-level inversion layer below the release height of the pollutant to be a perfect reflector, trapping the plume above the ground. When the low-level inversion layer breaks down after sunrise, then the plume is allowed to mix down to ground level in a process known as fumigation.

Also, Gaussian models are not limited to the plume paradigm. Some models have the source emit a series of puffs. Each puff has Gaussian characteristics as it disperses and travels downwind, but now all puffs are forced to travel in the same direction. This allows the model to use varying wind speed and direction within a Gaussian construct.

Steady-state Gaussian plume models should not be applied at distances greater than can be accommodated by the steady state assumptions inherent in such models. This limitation is generally considered to be 50 km. Long-range transport models should be used beyond this distance if a refined model is needed.

### iii) Lagrangian

Lagrangian models do not utilize the steady-state assumption. Instead, they are built on probability distributions for wind speed and direction. Therefore, they can support constant, time-varying, and intermittent emission sources. Lagrangian models require more computational resources (i.e., computer memory, CPU speed, and disk storage) than Gaussian models.

Two paradigms of Lagrangian models are particle and puff. In a particle model each particle is separately emitted from the emission source and separately moved throughout the modeling domain based on the probability of wind speed and direction. Each emitted particle may represent the same amount of mass when it is emitted, so more particles are emitted for higher emission rates and fewer particles for smaller emission rates. Deposition can be accommodated by changing the mass represented by a specific particle (Holmes and Morawska, 2006).

In a puff model each puff is emitted from the source with an initial length, width, and height and containing a specified number of particles, each of which represents the same amount of mass when it is emitted. The particles within the puff are separately moved based on the probability of wind speed and direction, but retain their identity within the same puff. Therefore, the puff changes shape as it moves throughout the modeling domain. A puff may be split into multiple puffs due to impaction with terrain features or buildings. Puffs that occupy the same space may be joined into one puff. Deposition can be accommodated by removing particles from puffs that impact the ground.

### iv) Eulerian

Eulerian models are typically used for urban-to-global scale air quality modeling studies and employ five-dimensional data sets. The modeling domain is divided into three-dimensional grid cells, each of which is homogeneous (e.g., a well-mixed reactor). Pollutants are advected between grid cells in the x- and y- directions (horizontal) and the z-direction (vertical), which are the first three dimensions. The fourth dimension is time and the fifth dimension is chemical species (Affum, 2015).

All relevant chemical species are included in the model in the form of a chemical mechanism. Therefore, Eulerian models are well-suited for full atmospheric chemistry. Some species are handled explicitly in the chemical mechanism, but most species are simulated using species unique to the chemical mechanism.

Eulerian models also require a vast amount of data, which spawns the need for numerous related models and pre- and postprocessors. Eulerian models are, however, customarily used to investigate air quality issues related to tropospheric ozone, $PM_{2.5}$ formation, secondary organic aerosols, and visibility.

#### 2.10.3.2 Objectives of Models

Many models have been built to meet specific modeling objectives. Therefore, it is important to select a model that meets the requirements of a specific air quality modeling study. This section discusses the types of models that are used most frequently. Examples of models that meet each of these objectives are also presented.

**i) Screening**

A screening model needs to quickly and easily estimate maximum downwind concentrations from an emissions source of nonreactive pollutants. The model must require less data than a more refined model. The results must be conservative; that is, the model must estimate higher concentrations than those estimated by a more refined model. Therefore, a screening model is typically a steady-state Gaussian plume model.

A screening model should be executed using a source's design capacity (i.e., 100% load), a higher load if the source may be able to operate at greater than design capacity, 75% load, and 50% load, and a range of operating conditions. The goal is to determine a set of conditions that cause the highest downwind concentration.

Examples of screening models are:

- SCREEN3 - This model is available from the USEPA
- AERSCREEN - new screening model under development. When promulgated this model will be available from the USEPA

**ii) Local scale modeling**

Local scale modeling is usually performed for new or expanding industrial sources, large industrial facilities, large construction projects, and major road construction projects. This type of modeling is more refined than screening models.

Local scale models are customarily built using Gaussian principles. Supported types of sources include elevated point (e.g., stack, flare), area, volume, and line. If the model does not directly support a line source, it is simulated as a series of adjacent area sources (e.g., road). These models typically include effects of buildings close to sources on elevated plumes (i.e., building downwash). When modeling the effects of a building on concentration, determine the projected length, width, and height of the building for each wind direction. Either the user's guide or the technical reference manual for the model should provide details on these calculations for the specific model.

Local scale models should also calculate effective plume height, which changes during the simulation based on the difference between ambient temperature and the exit temperature from the stack. The temperature difference causes buoyant plume rise. Exit velocity causes plume rise due to momentum or stack tip downwash due to low exit velocity in high wind conditions.

Examples of industrial source/facility models are:

- AERMOD – This is the most preferred Gaussian model of present time.
- Industrial Source Complex (ISC) – This model changed from a preferred model to an alternative model when AERMOD was promulgated.
- AUSPLUME – This model from the Environmental Protection Authority of Victoria in Australia is derived from the original ISC model (1979). This model supports stack,

area, and volume sources in flat terrain with simple winds (i.e., one wind direction in the entire modeling domain each hour).

- AUSPUFF – This non-steady-state Gaussian puff model is by Australia's Commonwealth Scientific and Industrial Research Organization (CSIRO). AUSPUFF uses a three-dimensional meteorology data set.
- Atmospheric Dispersion Modelling System (ADMS 4) – This model from Cambridge Environmental Research Consultants (CERC) supports point, area, volume, line, and jet sources.
- AirWare – This is a large modeling system from Environmental Software and Services of Austria.

**iii) Source Appointment**

The purpose of a source-apportionment model is to estimate the relative impact of specific types of sources at a designated location (i.e., a receptor). Also known as receptor models, chemical and physical characteristics of gases and particles that are measured at the source and receptor are used both to identify the presence of and to quantify source contributions to receptor concentrations. Because this type of model is typically based on linear algebra principles, this is a good example of a statistical model.

The primary assumption of source-apportionment models is that each type of source is associated with a unique combination of pollutants that are measured in the ambient air. This unique combination forms a fingerprint for that source type. Examples include gasoline evaporation, diesel truck exhaust, tanker engine exhaust, and painting.

A variety of source-apportionment models are available with differing data requirements, some of which include:

- Chemical Mass Balance Model
- Unmix
- Positive Matrix Factorization

### iv) Long range Transport

Long-range transport models are used when receptors are over 50 km from the source or when the plume of a large facility travels through mountains and valleys. Gaussian-type models are not appropriate for these conditions. Lagrangian or Eulerian models may be suitable for these distances.

Examples of long-range transport models are:

- CALPUFF
- Lagrangian Atmospheric Dispersion Model

### 2.10.4 Model Selection

The study area meteorological factor analysis showed fewer calm conditions and the terrain is not very complex. So, it was proposed to use the particle and grid based models. Of these entire models reviewed AERMOD (American Meteorological Society/Environmental Protection Agency Regulatory Model) seems to be promising. AERMOD is a new generation air modelling system used to support regulatory and nonregulatory modelling requirements worldwide. Hence a comprehensive review of the model was carried out in addition to considering other models.

By using AERMOD or any other advanced model, users/industries will be in a position to view, analyze, predict the current impacts and future impacts of the releases from one's facility and effectively devise control technologies and revise repeatedly based on the outcome of the atmospheric dispersion modeling results.

#### 2.10.4.1 Description of AERMOD

AERMOD is the recommended dispersion model from the USEPA, representing the current state-of-science in regulatory modeling. It is a steady-state plume model that incorporates air dispersion based on planetary boundary layer turbulence structure and scaling concepts. It assumes the concentration distribution to be Gaussian in both the vertical and horizontal. In the convective boundary layer (CBL), the horizontal distribution is also assumed to be Gaussian, but the vertical distribution is described with a bi-Gaussian Probability Density Function (PDF). The model tracks the dispersion of a pollutant emitted from a source as it travels through space over a defined receptor grid.

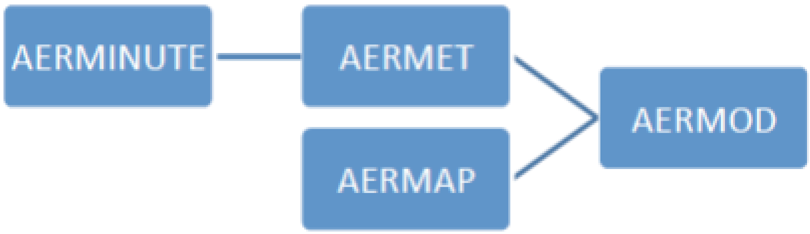


Figure 2.4: AERMOD model framework with preprocessors

The required inputs for AERMOD are: wind speed and direction, temperature profiles, mixing depth, turbulence parameters, plume characteristics, and degree of urbanization. Before these data are used in AERMOD, meteorological processors are used to format the data. Figure 2.4 depicts AERMOD and the two minimum preprocessors, AERMET and AERMAP, along with an optional preprocessor, AERMINUTE.

AERMET uses meteorological data and surface characteristics to calculate boundary layer parameters and creates two output files: a surface data file and a profile data file. Surface characteristics in the form of albedo, surface roughness and Bowen ratio, plus standard meteorological observations (wind speed, wind direction, temperature, and cloud cover), are input to AERMET (USEPA, 2016). AERMET then calculates the PBL parameters: friction velocity($u^*$), Monin-Obukhov length (L), convective velocity scale ($w^*$), temperature scale ($\theta^*$), mixing height ($z_i$), and surface heat flux (H). These parameters are then passed to the INTERFACE (which is within AERMOD) where similarity expressions (in conjunction with measurements) are used to calculate vertical profiles of wind speed (u), lateral and vertical turbulent fluctuations ($\sigma_v$, $\sigma_w$), potential temperature gradient ($d\theta/dz$), and potential temperature ($\theta$).

AERMINUTE, the wind preprocessor is needed for wind speeds that are considered "calm", <1 m/s. Calms are assigned a value of 0 and AERMOD cannot simulate dispersion under missing wind conditions. AERMINUTE processes 1-minute wind data to generate hourly average winds for input to AERMET.

The AERMOD terrain pre-processor AERMAP uses gridded terrain data to calculate a representative terrain-influence height ($h_c$), also referred to as the terrain height scale. The terrain height scale $h_c$, which is uniquely defined for each receptor location, is used to calculate the dividing streamline height (USEPA, 2004). The gridded data needed by AERMAP is selected from AERMET and creates a file suitable for use within an AERMOD control file.

#### 2.10.4.2 Input Data Requirement of AERMOD

AERMOD simulates necessary atmospheric processes and presents the refined pollutant concentration estimates over the modeling domain. As pollutants enter the atmosphere, they undergo various physical and chemical changes prior to reaching a receptor, sometimes resulting with serious effects to people's health and to the environment. So, modeling and predicting pollution intensity becomes necessary. For this purpose, the required data are as follows:

**i) Source Data**

Location of the power plant, type of source (point, area or line source) emission rates of respective power plants, exit gas velocities etc. constitute the source data. The information on the boiler stack consists of the stack details like height, diameter, exit temperature, flue gas flow rate, plume rise and elevation etc. Information on the sources that considerably result in pollutant concentration at chosen monitoring station is necessary to run the models.

**ii) Terrain Data**

Terrain and land-use land cover data are necessary for AERMET in order to generate the wind profile fields and additional meteorological factors like:

- Albedo
- Bowen ratio
- Terrain elevations
- Land use categories
- Vegetation leaf area index
- Surface roughness length
- Soil heat flux parameter

These required data were derived from terrain and land use data and processed into individual gridded fields within the modeling domain. Terrain altitudes can hugely affect the pollutant dispersion and deposition and consequently the estimates of potential risk to human health and the environment (USEPA, 2022) .

**iii) Receptor Data**

AERMOD computes the concentrations of substances based on user-specified spatial points, commonly referred to as receptors. Receptor selection is critical to capturing the maximum point of impact and proper placement of receptors can be achieved through several approaches. AERMOD support a variety of receptor types that allow for considerable user control over calculating pollutant concentrations (North Carolina Department of Environment and Natural Resources, Devision of Air Quality, 2014). The major receptor types and grid systems are described in the following sub-sections.

**Cartesian Receptor Grids:** Cartesian receptor grids are receptor networks that are defined by an origin with receptor points evenly (uniform) or unevenly (non-uniform) spaced receptor points in x and y directions. Figure 2.5 illustrates a sample uniform Cartesian receptor grid.

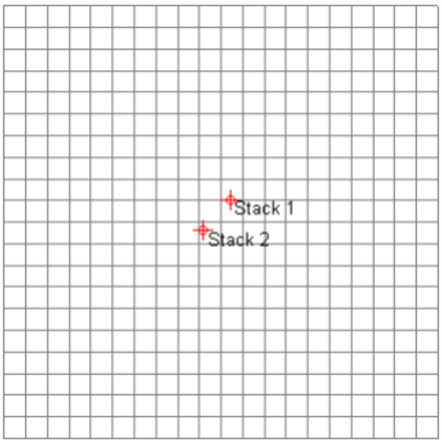


Figure 2.5: Cartesian Grid

**Polar Receptor Grids:** Polar receptor grids are receptor networks that are characterized by an origin with receptor points defined by the intersection of concentric rings, which have defined distances in meters from the origin, with direction radials that are separated by a specified degree spacing. Figure 2.6 illustrates a sample uniform polar receptor grid.

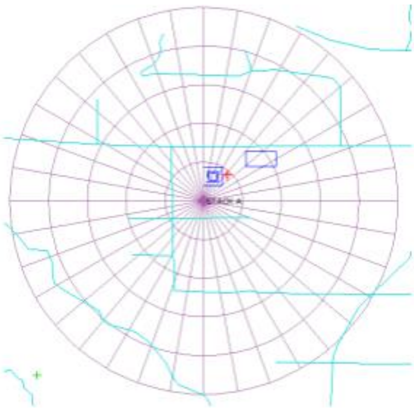

Figure 2.6: Polar Grid

Polar grids are a reasonable choice for facilities with only one source or one dominant source. However, for facilities with a number of significant emissions sources, receptor spacing can become too coarse when using polar grids.

**Multi-Tier Grids:** Each receptor point requires computational time. Consequently, it is not optimal to specify a dense network of receptors over a large modelling area; the computational time would negatively impact productivity and available time for proper analysis of results. An approach that combines aspects of coarse grids and refined grids in one modelling run is the multi-tier grid. Figure 2.7 provides an example of a multi-tier grid.

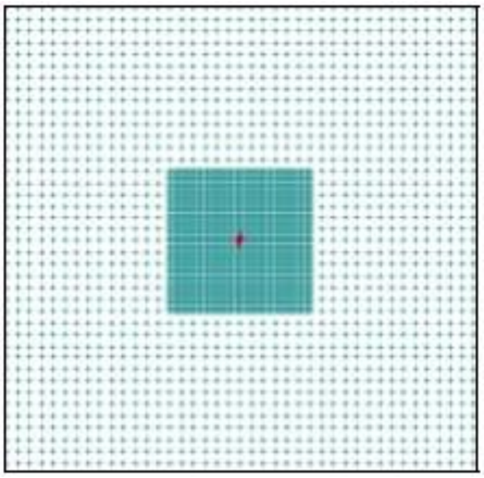

Figure 2.7: Multi-Tier Grid

**Fenceline Receptors:** Receptors must be placed along the plant boundary to demonstrate compliance at the nearest reportable geographical locations to the sources. A receptor network based on the shape of the property boundary that has receptors parallel to the boundaries is often a good choice for receptor geometry. The receptor spacing can then progress from fine to coarse spacing as distance increases from the facility, similar to the multi-tier grid.

**Discrete & Sensitive Receptors:** Receptor grids do not always cover precise locations that may be of interest in modelling projects. Specific locations of concern can be modelled by placing single receptors, or additional refined receptor grids, at desired locations. This enables the modeler to achieve data on specific points for which accurate data is especially critical. In particular, for elevated receptors the maximum concentrations can be larger than found at ground level. Common locations of sensitive receptors can include, among others, the following: Apartments, Residential zones, Schools, Apartment buildings, Day care centers, Air intakes on nearby buildings, Hospitals, Parks etc.

**iv) Meteorological data**

Downwind air pollution concentrations are a function of the meteorological and synoptic measurable parameters. The pollutants transport occurs along the direction of wind known as downwind direction. The pollutants concentration in ambient air is governed by the wind speed, wind direction, relative humidity, temperature etc (USEPA, 2022).

**Ambient temperature profile:** For the air quality assessments, the maximum and minimum ambient temperatures pertaining to the site account for the variations in possible plume rise. The vertical distribution of temperature in the atmosphere changes with season, location's latitude and longitude, from day to night as well.

**Relative humidity:** Humidity measurements at the Earth's surface play vital role in meteorological analysis, due to their significance as it represents the changes in state of water in the atmosphere. Relative humidity (RH) is the fraction in percent of the pragmatic vapor pressure to the saturation vapor pressure with respect to water at the identical temperature and pressure. Evidently, relative humidity is a fraction of tangible amount of water vapor in the atmosphere compared to the maximum water vapor, the atmosphere could hold at that same temperature. RH is inversely proportional to the ambient temperature and is higher at higher surfaces and is lower at ground. RH is maximum at sunrise (minimum temperature) and minimum during late afternoon (Maximum temperature).

**Atmospheric stability and Wind characteristics (Wind speed and direction):** For dispersion modeling purposes, these levels of atmospheric stability are classified into six classes based on six surface wind speed categories, three daytime insolation types and two night time cloudiness forms (Table 2.3).

Table 2.3: Pasquill-Gifford Stability Categories (Hossain, 2019)

| **Wind Speed (m/s)** | **Solar Insolation** | | | **Night Time** | |
|---|---|---|---|---|---|
| | **Strong** | **Moderate** | **Slight** | **This overcast or>1/2 low clouds** | **<3/8 cloudiness** |
| <2 | A | A-B | B | - | - |
| 2-3 | A-B | B | C | E | F |
| 3-4 | B | B-C | C | D | E |
| 4-6 | C | C-D | D | D | D |
| >6 | C | D | D | D | D |

Atmospheric Stability serves as measure to analyze the atmosphere's propensity to support or put off vertical motion. The relationships between the ambient lapse rate (ALR) and the dry adiabatic lapse rate (DALR) vitally institute the air stability and the speed with which pollutants can disperse. These stability classes are known as Pasquill-Gifford stability classes (Hossain, 2019), or categories: very unstable–A; unstable–B; slightly unstable–C; neutral–D; slightly stable–E; stable–F and very stable conditions–G.

Atmospheric stability is determined by wind and heating effects. In Gaussian models, plume transport/dispersion away from the centerline is characterized by plume dispersion coefficients, $\sigma_y$ (horizontal) and $\sigma_z$ (vertical). A, B, and C represent the unstable conditions during daytime hours; stability D denotes the overcast days or nights with neutral conditions, similarly, stabilities E and F suggest nighttime, stable conditions, with class 'A' being the nearly unstable or mainly turbulent class, and class 'F' the most stable or least turbulent classes (Hossain, 2019). In general, stability classes F and G are combined into one class, F (Table 2.3).

**Wind speed:** Wind is the significant meteorological feature in the transport and dispersion of air pollutants, as they move predominantly downwind. Any change in direction of wind over the plume depth (wind shear) will result in a notable lateral dispersion which can contribute to a noteworthy additional effect on the horizontal expanse of the plume. Wind speed records are represented as a wind rose, a graphical depiction of wind speeds and the direction from which the wind blows. Wind roses have 16 spokes representing the directions from which winds blow for the given duration of period. The colors reveal the various categories of wind speeds. The dotted circles convey information concerning the wind speed frequency occurrence and direction classes.

**Plume dispersion coefficients ($\sigma_y$ and $\sigma_z$):** Dispersion coefficients explain the rate of dispersion of pollutants in the plume in the horizontal and vertical directions (pollutant plume width and height). Horizontal dispersion, also referred to as transport, relating to wind speed and direction and it depends on location, elevation above ground, and to some extent on time of day. Degree of the horizontal dispersion on a given day depends greatly on the synoptic (regional) scale air flow and raises as atmospheric conditions turn into less stable (set out from F to A). Transport of elevated sources is rapid in the nighttime, whereas for low level sources transport is faster during the daytime. As a result, the horizontal dispersion of elevated sources exceeds the dispersion from low level sources.

**Mixing height:** Generally, the meteorological conditions that influence the dispersion prevail in the Planetary Boundary Layer (PBL or Mixing height), approximately at the lower 1000m of the atmosphere. The mixing height (MH) is depth of the boundary layer, which decides the volume available for the dispersion of pollutants and is necessary input data for estimating and forecasting the air quality. The most common methods for determining the mixing height are employment of remote sounding systems, radio-soundings and Parametrization methods. Monin–Obukhov length (L) describes the effects of buoyancy on turbulent flows in the environment, mainly in the lower tenth of the atmospheric boundary layer.

The mixing height is calculated based on the following criteria:

a) During the day, when the Monin–Obukhov Length is negative, it is approximated as the larger of the convective or the mechanical mixing heights.

b) During the night, when the Monin–Obukhov Length is positive, it is equivalent to the mechanical mixing height.

**Cloud cover:** Cloud cover is the part of the sky obscured by clouds**,** as it is seen from a particular position. Okta is the unit of the cloud cover measurement. Sky cover circumstances are estimated in terms of how many eighths of the sky is covered with clouds, ranging from 0 Oktas (complete clear sky) through to 8 Oktas (completely cloudy). Information of cloud cover levels is used to present estimates of the solar insolation at a specific location.

**Solar insolation and other data:** Depending upon on the equation of the sun's position in the sky throughout the year, the greatest amount of solar insolation on a particular surface at a particular tilt angle can be calculated as a function of latitude and Julian day of the year using surface energy balance method. Radiative Fluxes (Shortwave Radiation, Long wave Radiation) and Turbulent Fluxes (Latent heat flux (e.g. evaporation) Sensible heat flux (heating surface)) are used in approximating solar insolation and satellite data is widely used. Determination of solar radiation and cloud cover is the common practice from satellite images.

**Surface roughness length:** In the logarithmic wind profile, the roughness length is defined as the height at which wind speed is zero. It presents an estimate of the average roughness elements (Topographic features, buildings or vegetation) of the surface. With vegetated surfaces, as the vegetation itself offers a particular amount of roughness, the logarithmic wind profile reaches zero at a height equal to the displacement height plus the roughness length.

### 2.10.5 Gaussian Plume Dispersion Models

The Gaussian model forms the basis for the majority of air pollution models, and is the most well-known and documented approach. The model presupposes that the dispersion associated with the polluting species can be described by a modified gaussian or normal distribution curve as shown in Figure 2.8.

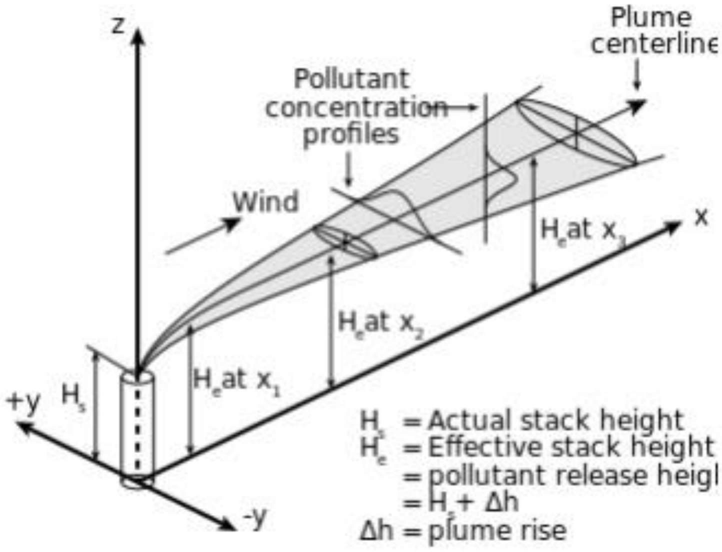


Figure 2.8: Visualization of a buoyant Gaussian air pollution dispersion plume (Holmes and Morawska, 2006)

A three- dimensional axis system is employed to provide a downwind, crosswind and vertical resolution. The species concentration is defined as being proportional to the emission rate of the source, diluted by the wind velocity at the source of emission. The dispersion behavior of a pollutant is determined by the standard deviations associated with the Gaussian distribution function. These standard deviations are related to the turbulent diffusivities are typically functions of atmospheric stability, localized turbulence and distance downwind from the source (Holmes and Morawska, 2006).

The model equation is derived from basic considerations of the diffusion of gaseous matter in three-dimensional space as shown in equation.

$$C = \frac{Q}{2\pi u \sigma_y \sigma_z} \exp\left(\frac{-y^2}{2{\sigma_y}^2}\right) [\exp\left(\frac{-(h-z)^2}{2{\sigma_y}^2}\right) + r_G \exp\left(\frac{-(h+z)^2}{2{\sigma_y}^2}\right)$$

Where,

C (x,y,z) = contaminant concentration at the specified coordinate [$ML^{-3}$],

x = downwind distance [L],

y = crosswind distance [L],

z = vertical distance above ground [L],

Q = contaminant emission rate [$MT^{-1}$],

$\sigma_y$ = lateral dispersion coefficient function [L],

$\sigma_z$ = vertical dispersion coefficient function [L],

u = wind velocity in downwind direction [$LT^{-1}$],

H = effective source height [L]

The effective source height (H) or plume rise is the height to which an emission will initially rise as a result of thermal buoyancy and vertical momentum. The upward movement of the plume is retarded on mixing with ambient air reaching an equilibrium point when the internal energy of the plume is equal to that of the surrounding atmosphere (Affum, 2015). The limitations of gaussian model precludes its use in cases where the short-term prediction of species concentrations (i.e., sub-hourly average values), or the prediction of species concentrations relative to complex environmental constraints are required.

### 2.11 Air Quality Index

The AQI is a tool for reporting daily air quality of any city or country. It provides information about how clean or polluted the air is, and what associated health effects might be a concern for public. The AQI focuses on health effects that one might experience within a few hours or days after breathing polluted air. The AQI value is a yardstick (Table 2.4) that runs from 0 to 300.The higher the AQI value, the greater the level of air pollution and the greater the health concern. For example, an AQI of 50 represents good air quality with little potential to affect public health, while an AQI value of 300 represents hazardous air quality.

An AQI value of 100 generally corresponds to the national air quality standard for the pollutant, which is the level that set by the mandated Environment Protection Agency (e.g., for Bangladesh, Department of Environment) to protect public health. AQI values below 100 are generally thought of as satisfactory. When AQI values are above 100, air quality is considered to be unhealthy-at first for certain sensitive groups of people, then for everyone as AQI values get higher. The main purpose of air quality index is Daily release of air quality conditions to the public, Convey the health implications of air quality, protect public interest and take actions to reduce emissions and Forecast air pollution level.

In Bangladesh, the AQI is based on 5 criteria pollutants; Particulate Matter ($PM_{10}$ and $PM_{2.5}$), $NO_2$, CO, $SO_2$ and Ozone ($O_3$). The Department of Environment (DoE) has also set national ambient air quality standards for these pollutants. These standards aim to protect against adverse human health impacts. The AQI standard for Bangladesh is given as under.

Table 2.4: Approved Air Quality Index (AQI) for Bangladesh

| Air Quality Index (AQI) Range | Category | Color | Cautionary Statement |
|---|---|---|---|
| 0-50 | **Good** | **Green** | **little potential to affect public health** |
| 51-100 | **Moderate** | **Yellow Green** | **Unusually sensitive individuals** |
| 101-150 | **Caution** | **Yellow** | **Identifiable groups at risk – different groups for different pollutants** |
| 151-200 | **Unhealthy** | **Orange** | **General public at risk; sensitive groups at greater risk** |
| 201-300 | **Very Unhealthy** | **Red** | **General public at greater risk; sensitive groups at greatest risk** |

## 2.12 Model Performance Evaluation

Air quality modeling can be considered as a useful tool to predict air quality in the future and determine the control strategies of emission abatement. It is imperative that these dispersion models be properly evaluated with observational data before their predictions can be used with confidence, because the model results often influence decisions that have large-public health and economic consequences (Venkatram et al., 2001).

A comprehensive model evaluation methodology makes use of scientific assessments of the model technical algorithms, statistical evaluations using field or laboratory data, operational assessments by users in real-world applications. The focus of the current paper is on the statistical evaluation components (Chang and Hanna, 2004).

There can be three components to the evaluation of air quality model: scientific, statistical and operational. In a scientific evaluation the model algorithms, physics, assumptions and codes are examined in detail for their accuracy, efficiency and sensitivity. This exercise usually requires in depth knowledge of the model. For statistical evaluation, model predictions (such as concentrations and cloud widths) are examined to see how well they match observations. It is possible for a model to produce the right answers, but as a result of compensating errors. The operational evaluation components mainly consider issues related to the user-friendliness of the model, such as the user's guide, the user interface, error checking of model inputs, diagnostic of interim model calculations, and processing and display of model outputs (Chang and Hanna, 2004). The focus of this paper is mainly on statistical model evaluation.

The kind of data needed for verifying model output, will depend on the model itself and the user's needs. In any case, a consistent procedure should be applied in order to evaluate the model performance. In this respect, some statistical performance measures namely: fractional bias (FB), normalized mean square error (NMSE) and index of agreement (IOA) were proposed in different studies (Affum, 2015; Chang and Hanna 2004; Rood, 2014).

The NMSE measures the random spread of the values around the mean. It characterizes the amount of deviation between predictions and observations. A good model will have an NMSE value of 0. The IOA reflects the degree to which the observed variable is accurately predicted. The IOA varies from 0 (the theoretical between minimum for an inadequate prediction) to 1 (perfect accuracy between the predicted and observed values). However, IOA value of 0.5 is considered as good. The FB is a measure of the systematic bias of the model and ranges from +0.5 to -0.5. It indicates the tendency and the sign of deviation. A negative FB value indicates model over prediction and a positive value indicated under prediction. Thus, a perfect model will have the FB and NMSE values to be zero (Rood, 2014).

Dispersion is primarily controlled by turbulence in the atmospheric boundary layer. Turbulence is random by nature and thus cannot be precisely described or predicted, other than by means of basic statistical properties such as the mean and variance. As a result, there is spatial and temporal variability that naturally occurs in the observed concentration field. On the other hand, uncertainty in the model results can also be due to factors such as errors in the input data, model physics, and numerical representation. Because of the effects of uncertainty and its inherent randomness, it is not possible for an air quality model to be ever be “perfect”, and there is always a base amount of scatter that cannot be removed (Rood, 2014).

# CHAPTER 3

# METHODOLOGY

## 3.1 General

The study is mainly based on ambient air quality modeling to assess the effect of the operation of the coal fired powerplant in Barapukuria on ambient air quality in the surrounding area. AERMOD dispersion model was considered for the modeling purpose for this work. Different applications of this model were exercised to predict ambient air quality. Ground level concentration of pollutants were also measured experimentally using suitable equipment. From the comparison of the experimental data and model generated data, performance of the modeling software was ensured.

The study's methodology is described in this chapter. This chapter begins by describing the power plant's location in Dinajpur District and its surroundings. The chapter then goes on to detail the various sorts of data that were gathered for this study from various sources. Finally, a description of the Air Quality Index computation process is provided. Chapter 4 provides a thorough explanation of the Dispersion model's development.

## 3.2 Description of Study Area

Barapukuria coal mine and coal fired power plant is located in flat peddy land of the north-western part of Bangladesh at about 45 km east of the district headquarters of Dinajpur and 20 km east from the border of India. It is physiographcally located in the Dinajpur Shield of Bangladesh, surrounded by the Himalayan foredeep to the north Shillong shield to the east and Indian Peninsular shield to the west (Safiullah, et al., 2011). The coal mine and power plant are located in the Hamidpur Union of Parbatipur Upazila in Dinajpur District, and the coordinates of the observation object is at $25.551200^0$ N and $88.947579^0$ E. Land use in the immediate vicinity of the project area is mainly rural. The location of the study area has been shown in Figure 3.1.

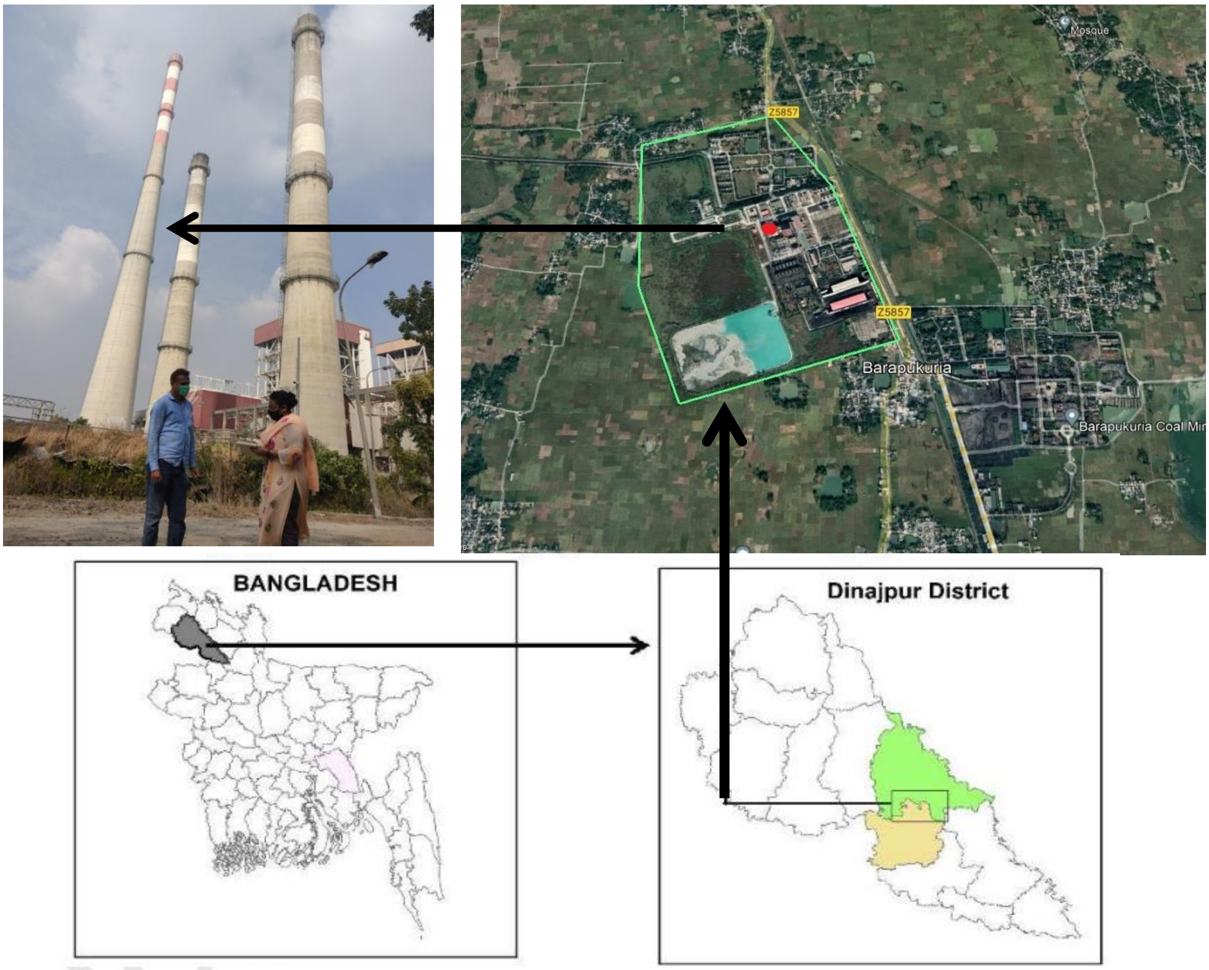


Figure 3.1: Location of the power plant

Figure 3.2: Emission from the stack of Barapukuria Thermal Power Plant

### 3.2.1 The Climate

The climate of Bangladesh is a subtropical monsoon climate which can be characterized by seasonal rainfall, warm temperature and high humidity (Khatun et al., 2016). According to the Bangladesh Meteorological Department (BMD) the climate of Bangladesh is partitioned into four seasons namely pre-monsoon (March, April, May), monsoon (June to September), post monsoon (October and November) and winter (December, January and February). Generally maximum summer temperatures range between 30°C to 40°C. The annual rainfall recorded is between 1600 mm and 2000 mm. April is the warmest month in most part of the country and January is the coldest month when average temperature for most of the country is about 10°C.

The power plant is in Dinajpur district which falls under the North-western climatic zone of Bangladesh. It has a tropical dry climate. The region has a distinct monsoonal season with an annual average temperature of 25 °C and monthly means varying between 12 °C in January and 33 °C in July.

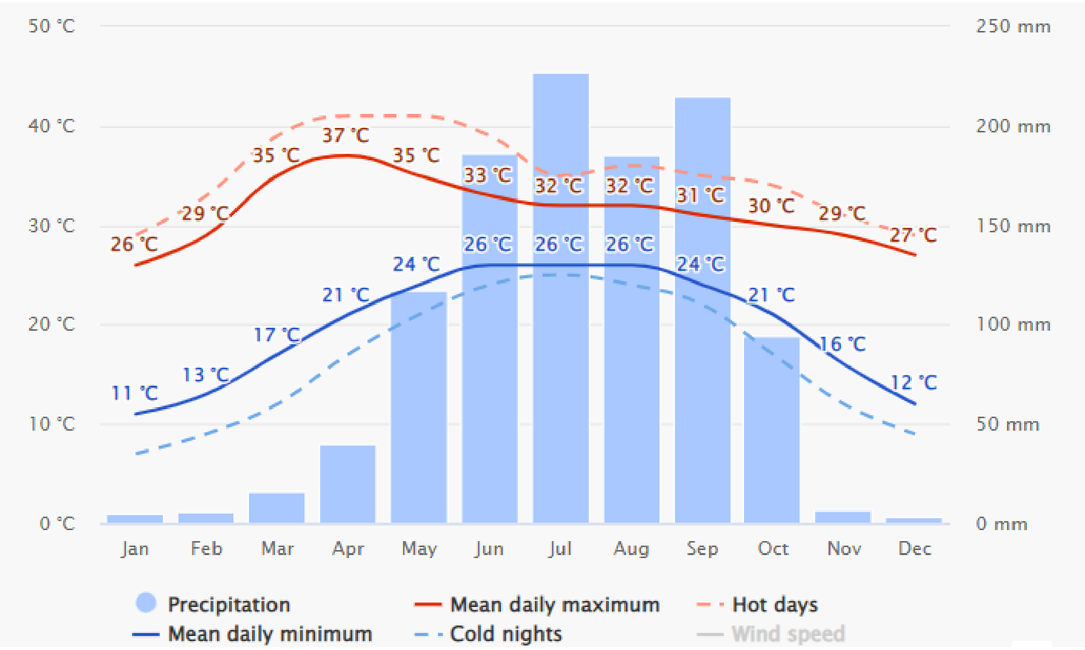


Figure 3.3: The maximum temperature, the average precipitation, the average minimum temperature, the average hottest day and the coldest night are shown every month of Dinajpur District (Source: meteoblue, 2022)

The wind direction is dominated by monsoon wind. Wind direction and speed exhibit seasonal variation. The annual wind rose shows that the predominant wind directions are mainly from ENE and from SE. During pre-monsoon (March-May), the predominant wind direction is NE to SW and during monsoon season (June-September), it is SSE to NNW whereas during the post-monsoon (October-November) predominant wind direction is SE to NW and during the winter season (December-February) it is NE to SW.

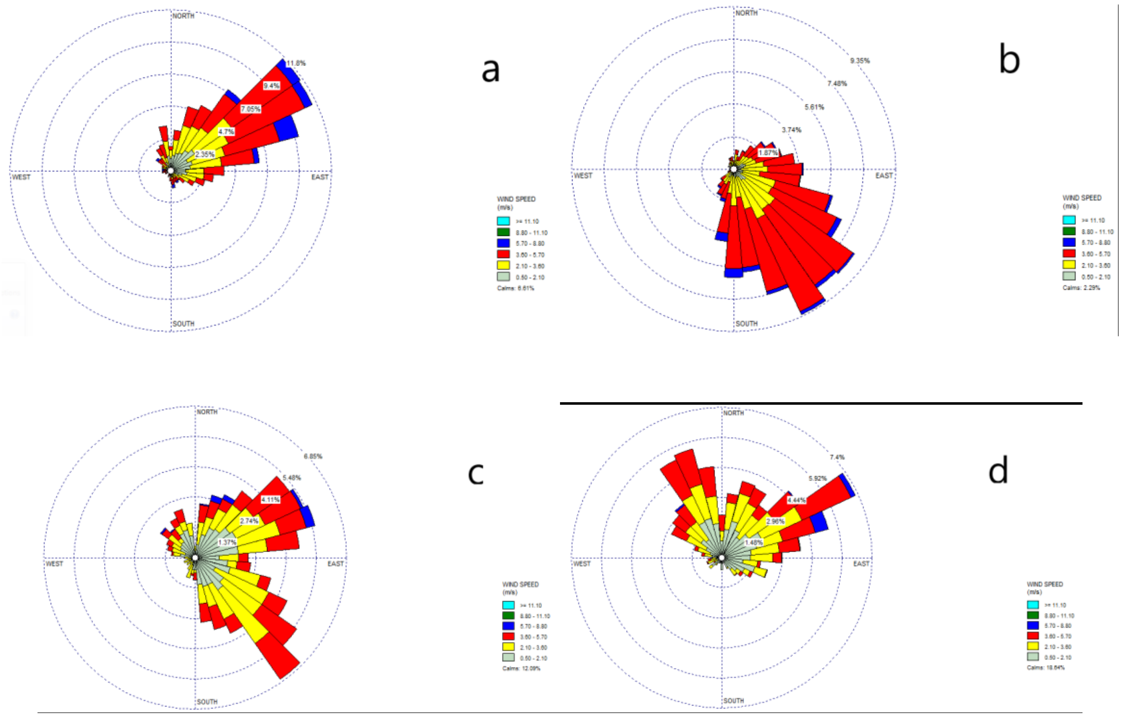


Figure 3.4: Distribution of wind speed and wind direction (a) Pre-monsoon, (b) Monsoon, (c) Post-monsoon, (d) Winter season

### 3.3 Data Collection

This thesis covers both primary and secondary data. Here the primary and secondary data sources are used to investigate the emissions and their effects from Barapukuria Thermal Power plant.

#### 3.3.1 Primary Data

The Primary data for this study were collected through field visits.

##### 3.3.1.1 Ambient Air Quality Data

For this study a 30x30 km domain was selected for observation. 11 sensitive points were selected for collecting ambient air quality data which covers the whole project area. As the wind direction in dry season is from NE to SW, observation sites located in the south western site of the plant were the focal points. Sampling locations with distance from the source are listed in Table 3.1.

Field data were collected in two phases.

- Phase 1: 01 to 04 November 2020 – Continuous 1 hour data collected at 11 sensitive locations.

- Phase 2: 05 to 07 December 2021 – Continuous 24 hour data collected at 3 downwind locations from source. These three locations are marked in yellow color in Table 3.1.

Table 3.1: Sampling locations with distance from source

| Label | Sampling Location | X Coordinate m | Y Coordinate m | Distance from source (km) | Direction | Duration of data collection (hr) |
|---|---|---|---|---|---|---|
| 1 | Base of stack | 695783.21 | 2827630.56 | 0 | - | 1 |
| 2 | Phulbari Primary School | 696239.77 | 2826124.61 | 1.5 | S | 1 |
| 3 | Sherpur Bhabanipur Govt college | 694960.36 | 2830595.21 | 3 | N | 1 |
| 4 | Shibnogor playground | 693139.68 | 2825442.8 | 3 | SW | 1 |
| 5 | Phulbari Model High School | 696110.53 | 2822477.62 | 5 | S | 1 & 24 |
| 6 | Rangamati jame mosque | 692612.34 | 2822298.35 | 6 | SSW | 1 & 24 |
| 7 | Bhagulpur Bazar | 701079.54 | 2824282.49 | 6 | SSE | 1 |
| 8 | Parbatipur Upazila Health Complex | 88.919392° | 2836360.9 | 9 | N | 1 & 24 |
| 9 | Ambari Bazar Road | 683935.50 | 2826279.88 | 12 | W | 1 |
| 10 | Shuchnipara primary school | 694369.96 | 2813064.05 | 14 | S | 1 |
| 10 | Lohanipara High School | 710921.12 | 2831815.4 | 15 | ENE | 1 |

These data include ambient concentration of Sulphur dioxide ($SO_2$), Nitrogen oxides (NOx), and Carbon Monoxide (CO). The concentrations of pollutants are measured using Haz Scanner. Sampling sites are shown in Figure 3.5.

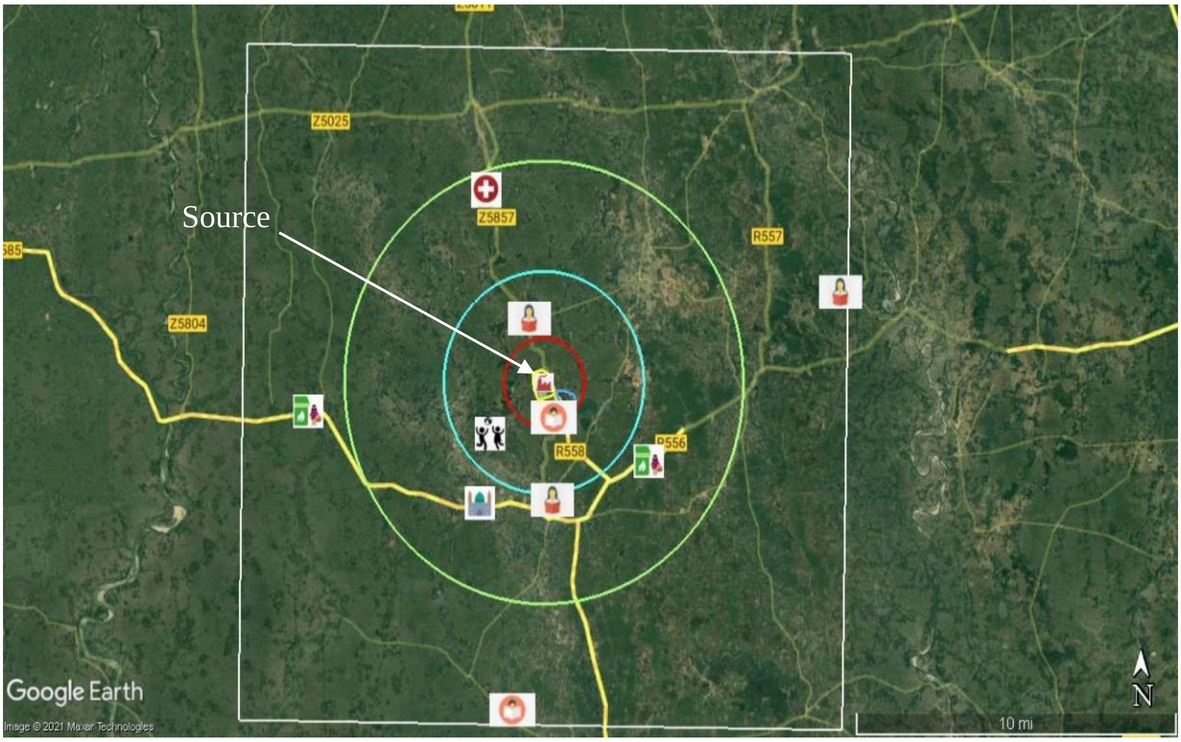


Figure 3.5: Study area with all the sampling locations

Location: Base of stack

Location: Bhabanipur college

Location: Rangamati Jame Mosque

Figure 3.6: Collection of field data

### 3.3.2 Secondary Data

The secondary data collected for this study were collected from different sources.

#### 3.3.2.1 Meteorological Data

One year (2020) meteorological data has been purchased from Lakes Environmental in MM5 version ($5^{th}$ generation Mesoscale Model) for this study. Which provides two files: Hourly Surfa Data file (SAMSON Format) and Upper Air data (TD-6201 format).

#### 3.3.2.2 Source information

The emission rates of different pollutants from the power plant have been collected from the power plant authority for a continuous 7day period. (Appendix A-1) Only the 3rd unit of the plant has Continuous Emission Monitoring System (CEMS). Therefore, emission rate can be collected for 3rd unit only. The average emission rate is shown in the Table 3.2.

During this period the highest load of the power plant was 150 MW. Due to the shortage of coal the plant is running at 150 MW or a less load now a days. The average emission rate is shown in the table.

Source parameters for model input has also been collected from the power plant authority. (Table 3.3).

Table 3.2: Exhaust gas emission from stack of the power plant (Source: BTPP)
(Period: 29 Nov 2021 to 05 Dec 2021)

| **Pollutant** | **Emission rate** | |
|---|---|---|
| | $mg/m^3$ | g/s |
| **NOx** | 362.90 | 92.54 |
| **$SO_2$** | 201.46 | 51.37 |
| **CO** | 100.83 | 25.71 |

Table 3.3: Source parameters for Air Dispersion Modeling (Source: BTPP)

| Stack Parameters | Unit | Stack 03 |
|---|---|---|
| Stack Height | m | 220 |
| Stack Top diameter | m | 5.6 |
| Stack Exit Temperature | K | 397 |
| Flue Gas Velocity | m/s | 12.9 |
| Gas Exit Flow rate | $m^3/s$ | 255 |
| | ton/hr | 1150 |
| Pollution control measure | | Electrostatic precipitator<br>Low NOx Burner |

### 3.3.2.3 Coal Composition

Barapukuria Thermal Power Plant is based on the coal collected by Barapukuria Coal Mine. So, the composition of this coal was collected directly from Barapukuria Coal Mining Company Ltd.

### 3.3.2.4 Baseline Ambient Air Quality

The Baseline ambient air quality of the study area was extracted from the EIA report of the Extension of Barapukuria Coal Fired Thermal Power Plant. Table 3.4 shows the concentration of SOx and NOx at different monitoring locations in the project area. The resultant concentration of a certain pollutant will be determined using the result shown in Table 3.4. (i.e by summation of baseline concentration with the predicted concentration from air dispersion modeling)

Table 3.4: Ambient air quality in the study area (CEGIS, 2013)

| Ser | Sampling Location | Ambient Concentration (μg/m$^3$) (24-hour avg) | |
|---|---|---|---|
| | | SOx | NOx |
| 1 | In front of 3rd unit | 38.12 | 42.15 |
| 2 | In front of administrative building | 35.15 | 40.25 |
| 3 | Besides north boundary wall | 32.20 | 38.20 |
| 4 | In front of rest house | 31.10 | 37.15 |
| Ambient air quality of the study area | | 34.14 | 39.44 |

### 3.4 Dispersion Modeling

Lakes Environmental's AERMOD View version 10.0.1 has been used in this study for modeling dispersion of $SO_2$, NOx, and CO. Chapter 4 describes the details of model assumptions, model domain for the study and procedures followed for running the model.

### 3.5 Scenarios Considered

The air quality in the vicinity of the power plant have been predicted using the dispersion model AERMOD under two different scenarios:

I. 150 MW in operation: Only the third unit's emissions statistics were gathered. The plant's maximum load throughout the data collection period was 150 MW. Therefore, the first scenario only included pollution for the plant's 150 MW capacity.
II. 525 MW in operation: Taking into account the power plant's overall capacity of 525 MW, the second scenario forecasted the pollutants for all 3 units.

### 3.6 Air Quality Index Calculation

AQI index value for this study was calculated for ambient concentration of $SO_2$ and $NO_X$ to check the ambient air quality for these two air pollutants. Air quality index (AQI) is used by government agencies to communicate to the public how polluted the air currently is or how polluted it can become. As the AQI increases, an increasingly large percentage of the population is likely to experience increasingly severe adverse health effects. AQI values are derived from air quality data readings, which allows for more meaningful comparison of pollutants affecting air quality.

The index is derived using the following formula:

$$AQI = \frac{\text{Pollutants Data Reading}}{\text{Standard Limit}} \times 100$$

# CHAPTER 4

# MODEL DEVELOPMENT

## 4.1 General

The next section of this chapter discusses the procedure used to produce pollutant dispersion behavior using the AERMOD View 10.0.1, as well as the processing of topography and meteorological data using its two preprocessors, AERMET and AERMAP, respectively. It also draws attention to all the information utilized as input to the model, including source parameters, pollutant types, and averaging time options. This chapter also discusses the steps taken to validate the model that was created.

## 4.2 Model Assumptions

The main model assumptions considered in this study are as follows:

1) Power plant operation is continuous for twenty-four hours over a 365-day year.
2) Gaussian distribution for pollutant dispersion in both vertical and horizontal directions.
3) Source emission rates are continuous and constant for 24 hours and 365 days.
4) All the pollutants liberated into the atmosphere stay in the atmosphere.
5) The boiler stack is modeled as point source.
6) AERMOD is capable of estimating building downwash. But these effects are assumed to be negligible in the model setup due to absence of tall building in the surrounding.

## 4.3 Model Grid

The modeling domain of 30x30 km was selected with the reference point positioned at 2827427 m Northing and 695653 m Easting. This reference point is selected such that the emission source was located at the center of the model domain. This domain includes all source and receptors. Figure 4.1 gives a regional view of the modeling area along with emission source.

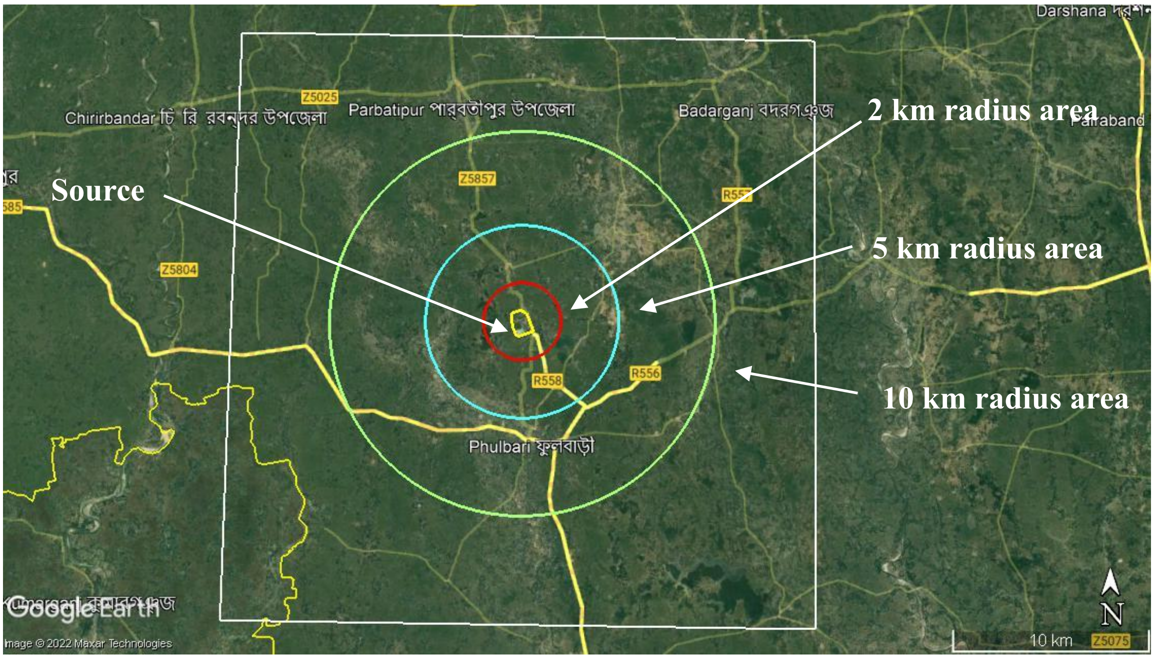


Figure 4.1: Modeling domain

### 4.4 Air Dispersion modeling with AERMOD View

An overview of the modeling approach and general steps for using AERMOD View is provided below. The general process for performing an air dispersion study using AERMOD includes:

- Meteorological data processing- AERMET
- Obtain digital terrain elevation data
- Final site characterization- complete source and receptor information
- AERMAP – perform terrain data preprocessing for AERMOD air dispersion model
- AERMOD – run the model
- Visualize and analyze result

As can be seen above, the AERMOD modeling system is comprised of 3 primary components as outlined below and illustrated in Figure 4.2.

1. AERMET – Meteorological data preprocessor
2. AERMAP – Digital terrain preprocessor
3. AERMOD – Air dispersion model

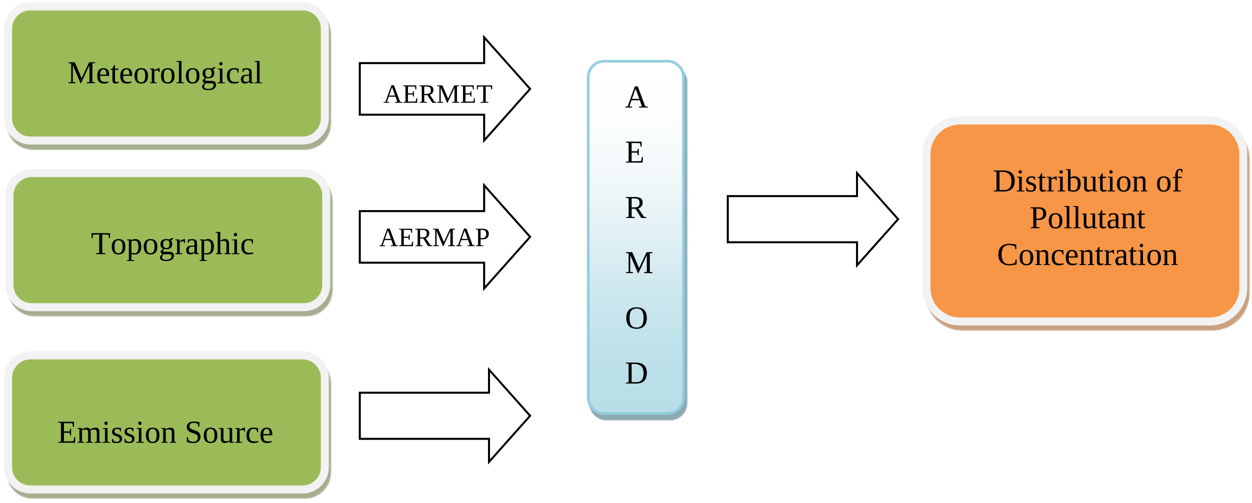


Figure 4.2: Modeling system of AERMOD with involvement of preprocessor and data

### 4.5 Data processing in AERMET

AERMET is used to calculate parameter of boundary layer (important in estimating profiles of wind, turbulence and temperature) with the help of acquired meteorological data. Surface characteristics in the form of albedo, surface roughness and Bowen ratio, plus standard meteorological observations (wind speed, wind direction, temperature and cloud cover) are input to AERMET (Idris et al., 2019). For this study one year (2020) meteorological data has been purchased from Lakes Environmental in MM5 version ($5^{th}$ generation Mesoscale Model). Which provides two files: Hourly Surface Data file (SAMSON Format) and Upper Air data (TD-6201 format). The meteorological data were processed using the AERMET pre-processor in order to get it in the correct format for model input files. These data were then merged with location specific user-defined values for the bowen ratio, albedo and surface roughness. These parameters can be varied spatially over a selection of directional sectors (depending on wind direction) and/or temporally, representing annual, seasonal and even monthly values. Wind class frequency distribution has been generated in AERMET with the help of WRPLOT View and hourly boundary layer parameters (Figure 4.3). In Figure 4.4, the wind rose plot of the region has been presented based on meteorological data. As can be observed in the figure, the direction of the dominant wind is from Northeast to Southwest.

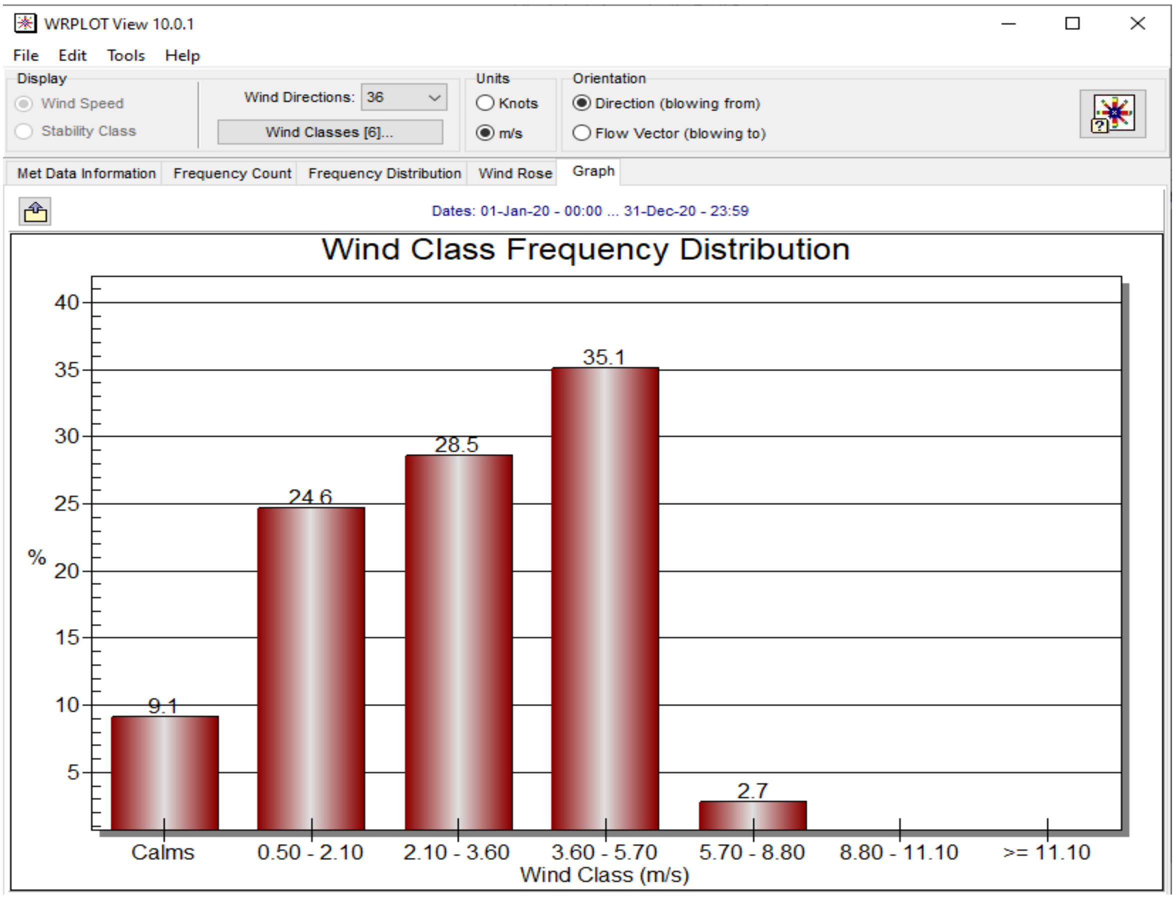


Figure 4.3: Wind Class Frequency Distribution

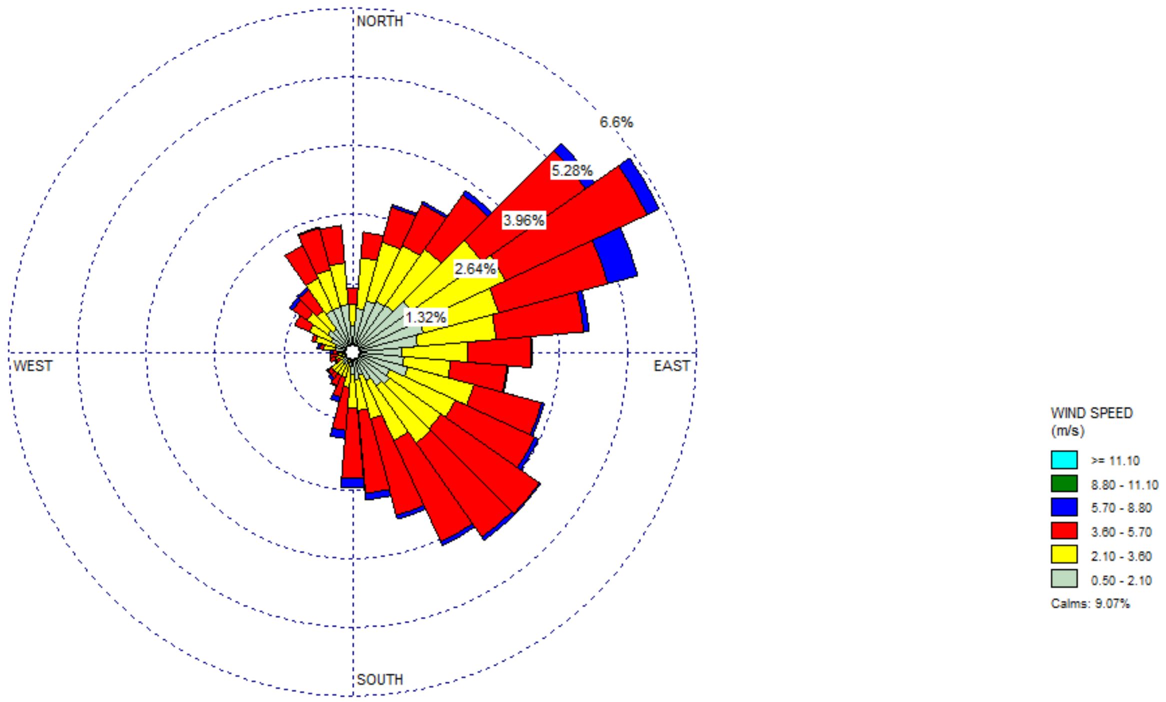


Figure 4.4: Wind rose plot prepared by meteorological data of the study area

### 4.6 Data processing in AERMAP

The function of AERMAP in this model is to compute terrain height of modeled area. This AERMAP preprocessor will determine the ground altitude beneath all the sources, receptors and height scale of every receiver that can influence the pollutant distribution value (Fadavi, Abari and Nadoushan, 2016). For this study the ground elevation data required by the AERMAP were obtained from Shuttle Radar Topography Mission (SRTM1). The Combination of AERMAP, AERMET and emission data are supporting the generation of air quality model from AERMOD.

### 4.7 Running AERMOD View

The Universal Transverse Marcator was selected as project coordinate system. According to the projection system and its corresponding datum, study area lies in WGS-84 corresponding to SRTM1 and the project site comes under the UTM zone 456Q, for the radius of influence of the modeling area selected. Then the location of reference point (center of model domain) was selected such that the power plant is positioned at the center of the domain and modeling area dimensions were selected. The entire data of the model domain was then exported to Google earth for obtaining the satellite view of selected area and a base map was generated. Finally, the base map was imported to AERMOD View as the modeling domain. After the simulation run, simulated outputs for all pollutants (hourly, daily, monthly, seasonal and annual) were plotted.

### 4.8 Modeling Procedure

The necessary input data for AERMOD View and the desired output derivatives can be given using the following options.

- Control pathway/option (CO)
- Source pathway/option (SO)
- Receptor pathway/option (RE)
- Terrain grid pathway/option (TG)
- Meteorological pathway/option (ME)
- Output pathway/option (OU)

#### 4.8.1 Control pathway

In control pathway dispersion options (concentration, wet and dry deposition), type of pollutant, pollutant averaging time options, terrain options, land use category are specified.

The following inputs have been specified for the present study.

- Regulatory option: Default
- Terrain: Elevated
- Pollutant: $SO_2$, NOx, CO
- Averaging period: 1-hour, 24-hour, annual (depending on the air quality standard of a particular pollutant)
- Dispersion option: Concentration
- Land use category: Rural

#### 4.8.2 Source pathway

Sources of pollutant emission can be defined here. The model can deal with multiple emission sources (i.e., point, area and/or volume). Numerous source groups can be considered in a single run, along with different source contributions come together for each group. Source emission rates are considered as constant during the modeling run time, or varying by hour, day, or based on seasonal, annual or any other required period.

The study area being located far away from the city, significant urban impacts were nonexistent near Barapukuria power plant. Emission sources and their locations (UTM coordinates), emission rates, base elevation, gas exit temperature and velocity, release height, flow rate and stack inside diameter were given as the source pathway input (Table 4.1).

Table 4.1: Source parameters for Air Dispersion Modeling (Source: BTPP)

<table>
<tr><th>Stack Parameters</th><th>Unit</th><th>Stack 3</th></tr>
<tr><td>X coordinate</td><td>m</td><td>695653.69</td></tr>
<tr><td>Y coordinate</td><td>m</td><td>2827427.91</td></tr>
<tr><td>Height</td><td>m</td><td>220</td></tr>
<tr><td>Top diameter</td><td>m</td><td>5.6</td></tr>
<tr><td>Stack Exit Temperature</td><td>K</td><td>397</td></tr>
<tr><td>Flue Gas Velocity</td><td>m/s</td><td>12.9</td></tr>
<tr><td rowspan="2">Gas Exit Flow rate</td><td>$m^3/s$</td><td>255</td></tr>
<tr><td>ton/hr</td><td>1150</td></tr>
<tr><td>Pollution control measure</td><td></td><td>Electrostatic precipitator<br>Low NOx Burner</td></tr>
</table>

#### 4.8.3 Receptor pathway

This pathway is utilized to find out the impact of air quality at different receiver locations. Multiple receptor locations can be specified in a single run and we could as well combine cartesian and polar grid receptor networks in the same run. Also, receptor coordinates can be specified by the user in either universal transverse mercator (UTM) coordinate system or any other user coordinate system (North Carolina Department of Environment and Natural Resources, Devision of Air Quality, 2014).

For this study a typical receptor grid was followed which is:

a. Medium receptor grid of 500 m spacing upto 10 km from center point location and
b. Coarse receptor grid of 800 m spacing after 10 km distance from center point location.

As a result, 1793 receptors were generated to predict the Ground Level Concentration (GLC) which is sufficient to resolve the maximum impacts and any potential significant impact area. Caution was taken such that coarse grid was placed over the entire chosen modeling field, but with denser grid where highest impacts are expected i. e. within 10x10 km area from modeling grid reference point.

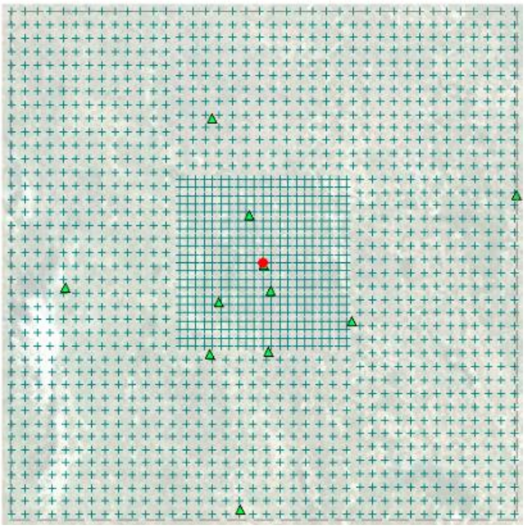

Figure 4.5: Multi-tier grid of modeling domain with discrete receptors and source

In addition to the multi-tier receptor, 11 discrete receptors labeled from 1 to 11, (Table 4.2) were set up within 15-km radius to estimate the maximum ground-level concentrations at those point. These receptors are schools, colleges and markets which may be sensitive to changes. These receptors correspond to the ambient air quality monitoring sites in order to facilitate the model to monitor comparison that is a part of model validation process. Concentration of air pollutants were predicted at these receptors also. Figure 4.5 showed the multi-tier grid with 11 discrete receptors.

Table 4.2: Location and other details of receptors

| Label | Receptor/Sampling Location | X Coordinate m | Y Coordinate m | Base elevation (m) | Distance from source (km) | Direction |
|---|---|---|---|---|---|---|
| 1 | Base of stack | 695783.21 | 2827630.56 | 32.87 | 0 | - |
| 2 | Sherpur Bhabanipur Govt college | 694960.36 | 2830595.21 | 36.86 | 3.07 | N |
| 3 | Shibnogor playground | 693139.68 | 2825442.8 | 39.46 | 3.4 | SW |
| 4 | Phulbari Model High | 696110.53 | 2822477.62 | 39.27 | 5.18 | S |
| 5 | Rangamati jame mosque | 692612.34 | 2822298.35 | 34.6 | 6.2 | SSW |
| 6 | Ambari Bazar Road | 683935.50 | 2826279.88 | 38.85 | 12 | W |
| 7 | Shuchnipara primary school | 694369.96 | 2813064.05 | 32.62 | 14 | S |
| 8 | Parbatipur Upazila Health Complex | 88.919392° | 2836360.9 | 36.64 | 9 | N |
| 9 | Bhagulpur Bazar | 701079.54 | 2824282.49 | 37.32 | 6.2 | SSE |
| 10 | Lohanipara High School | 710921.12 | 2831815.4 | 38.42 | 15 | ENE |
| 11 | Phulbari Road Bazar | 696239.77 | 2826124.61 | 36.15 | 1.5 | S |

Elevations of receptors were taken from the Shuttle Radar Topography Mission (SRTM1) with a resolution of 1 arc second (30 meters). This SRTM1 data was processed with AERMAP in combination with receptor layout and emission sources taken for modeling. The terrain elevations of all receptors and sources were run in AERMAP model. After this model run was completed, elevation of all sources and receptors were imported to the model.

### 4.8.4 Meteorology pathway

This pathway is utilized for giving input data related to meteorological conditions and additional meteorological parameters, as well as period to be processed from the meteorological file. Surface and raw upper air data for the year 2020 were obtained from the Lakes Environmental Databases. AERMET processed these files to produce two files for input into AERMOD. The surface met file (*.SFC) contains observed and calculated surface observations, boundary layer scaling parameters and reference-height winds and temperature. The profile met file (*.PFL) contains one or more levels (profile) of wind, temperature and standard deviation of the fluctuating components of the wind. These files are arranged such that every receptor block of data holds all of the observations for a 24-hour period.

### 4.8.5 Terrain pathway

In terrain grid pathway, we can specify grid data. The terrain elevations of all receptors and sources were run in AERMAP model. AERMOD View simulated the plume dispersion in horizontal direction in stable conditions as well. The predicted results were exported to obtain a natural view of isopleths. This feature is useful to observe to what degree the pollutants are dispersed around the emission source with satellite imaging. Gridded terrain data is required in computing deposition in elevated topography (USEPA, 2004).

### 4.8.6 Output pathway

The isopleths plot are the plotted contours of constant ground level pollutant concentration that reflect the pollutant dispersion with respect to distance, time and topography. Figure 4.6 shows the plot for $SO_2$ 24-hr average plume as an example.

Maximum estimated GLC (Ground Level Concentration) for the specified time period, over the whole duration were also obtained from these isopleths. These isopleths imply that, even if a maximum day concentration is predicted to transpire a distinct receptor, it will only be true for that one day in the total simulation duration. For all the pollutant, isopleth plots were created, entailing only the worst-case scenario (highest predicted GLCs) for all the significant averaging periods.

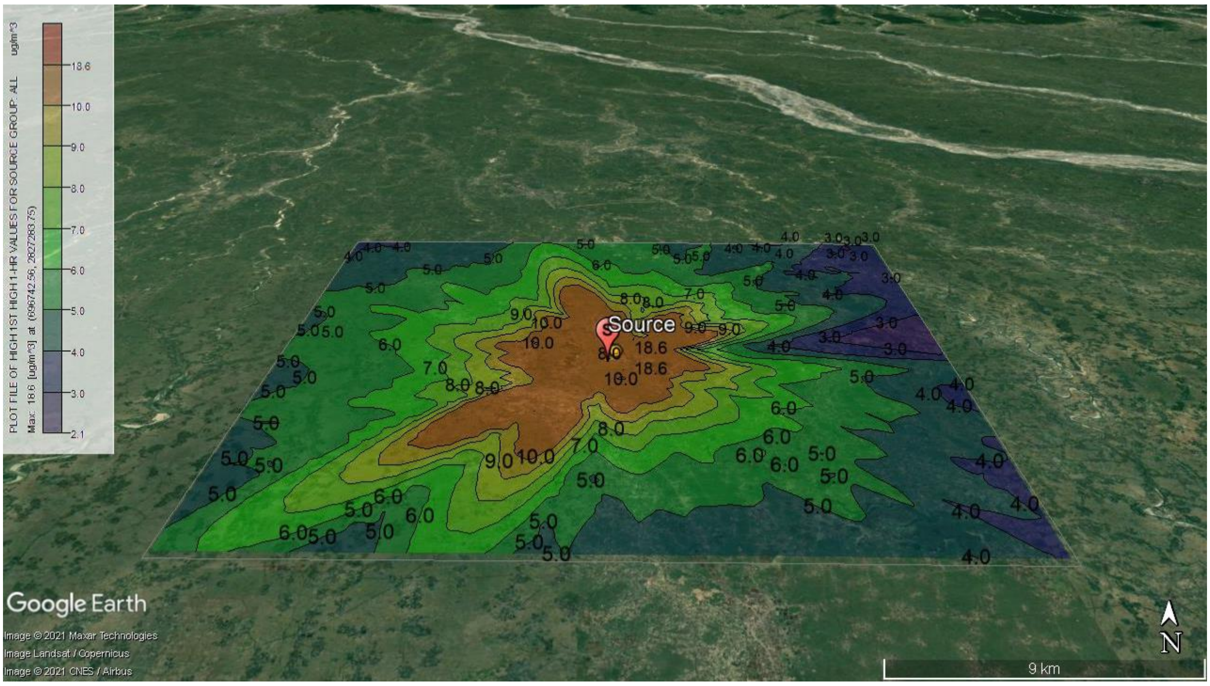


Figure 4.6: A plot showing 24 hr average plume of $SO_2$ for the operation of Barapukuria Power Plant

### 4.9 Scenarios Considered

The air quality in the vicinity of the power plant have been predicted using the dispersion model AERMOD under two different scenarios:

III. 150 MW in operation: Only the third unit's emissions statistics were gathered. The plant's maximum load throughout the data collection period was 150 MW. Therefore, the first scenario only included pollution for the plant's 150 MW capacity.

IV. 525 MW in operation: Taking into account the power plant's overall capacity of 525 MW, the second scenario forecasted the pollutants for all 3 units.

### 4.10 Validation of Model

Model validation substantiates that a simulation model possesses a satisfactory range of accuracy consistent with the intended application of the model. For this a comparative analysis has been carried out between the measured values from monitoring sites and model predicted values.

This study also employed three statistical indicators to verify the model performance through USEPA 1992 modeling guidance. These include fractional bias (FB), normalized mean square error (NMSE) and Index of agreement (IOA) as shown in Eqs. (1) to (3).

$$\text{FB} = \frac{2\ X\ (\overline{C_o} - \overline{C_p})}{\overline{C_o} + \overline{C_p}} \tag{1}$$

$$\text{NMSE} = \frac{(\overline{C_o - C_p})^2}{\overline{C_o}\ X\ \overline{C_p}} \tag{2}$$

$$\text{IOA} = 1 - \frac{\sum(C_p - \overline{C_o}\ )^2}{\sum(\mid C_p - \overline{C_o}\ \mid + \mid C_o - \overline{C_o}\ \mid)^2} \tag{3}$$

Where $C_o$ and $C_p$ are observed and predicted concentrations, respectively. $\overline{Co}$ and $\overline{Cp}$ are the mean values of the observed and predicted concentrations, respectively.

FB is a dimensionless value used to evaluate the biasness of data sets and ranges from +2 to -2. The positive and negative FB values indicate underpredictions and overpredictions, respectively (Chang and Hanna, 2004). Also, NMSE measures variance and scattering values between modeled and measured data. Thus, a perfect model will have the FB and NMSE values to be zero (Rood, 2014). Similarly, the IOA is used to rate the accuracy of models and ranges from 0 to 1. An ideal model will have IOA to be equal to 1 with 0 being the least value. However, IOA value of 0.5 is considered as good (Affum, 2015). Due to influence in varied meteorological factors, these may lead to a large range of values between modeled and observed data (Chang and Hanna, 2004).

# CHAPTER 5

# RESULTS

## 5.1 General

This chapter explains the results of modeling carried out using AERMOD in the form of isopleths concentrations and discusses the effects of the operation of Barapukuria Thermal Power Plant on ambient air quality. This chapter first presents the emission rates of different pollutants from the power plant considered in this study. Then the results of model simulations under different scenarios have presented and discussed. Specifically, this chapter presents the spatial variation of pollutant concentration due to the operation of the power plant. Then the chapter presents an evaluation of compliance with Bangladesh and European Union air quality standards and WHO guidelines. The seasonal and diurnal variation of pollutants have been illustrated and its correlation to meteorological factors have been presented and discussed. Finally, the performance evaluation of the dispersion model is analyzed.

## 5.2 Emission Rates from The Power Plant

The emission rates of different pollutants from the power plant are presented in this section. These data have been collected from the power plant authority for continuous a 7-day period. (29 Nov 2021 to 05 Dec 2021) The average emission rate is shown in the Table 5.1.

Table 5.1: Exhaust gas emission from stack of the power plant (Source: BTPP)

| **Pollutant** | **Emission rate** | |
|---|---|---|
| | **$mg/m^3$** | **g/s** |
| NOx | 362.90 | 92.54 |
| $SO_2$ | 201.46 | 51.37 |
| CO | 100.83 | 25.71 |

Environmental Conservation Rules 1997 specified emission standards for sulfur dioxide, and nitrogen oxides are 200 $mg/m^3$ and 350 $mg/m^3$ respectively. Even though, sulfur dioxide emission is in compliance with the standard, nitrogen oxide emission exceeds the standard slightly.

### 5.3 Windrose Construction

Figure 5.1 describes the wind characteristics such as magnitude and direction of the study area. It was plotted with the help of WRPLOT view using the meteorological data in background. In this analysis wind rose is prepared for the whole data period of the meteorological data. This wind rose diagram is saved in circular format showing the patterns of wind flow including direction and magnitude over a particular time period. Predominant wind directions are mainly from ENE and from SE as can be seen from the wind rose diagram. Hence, the plume can travel towards SW and NW directions.

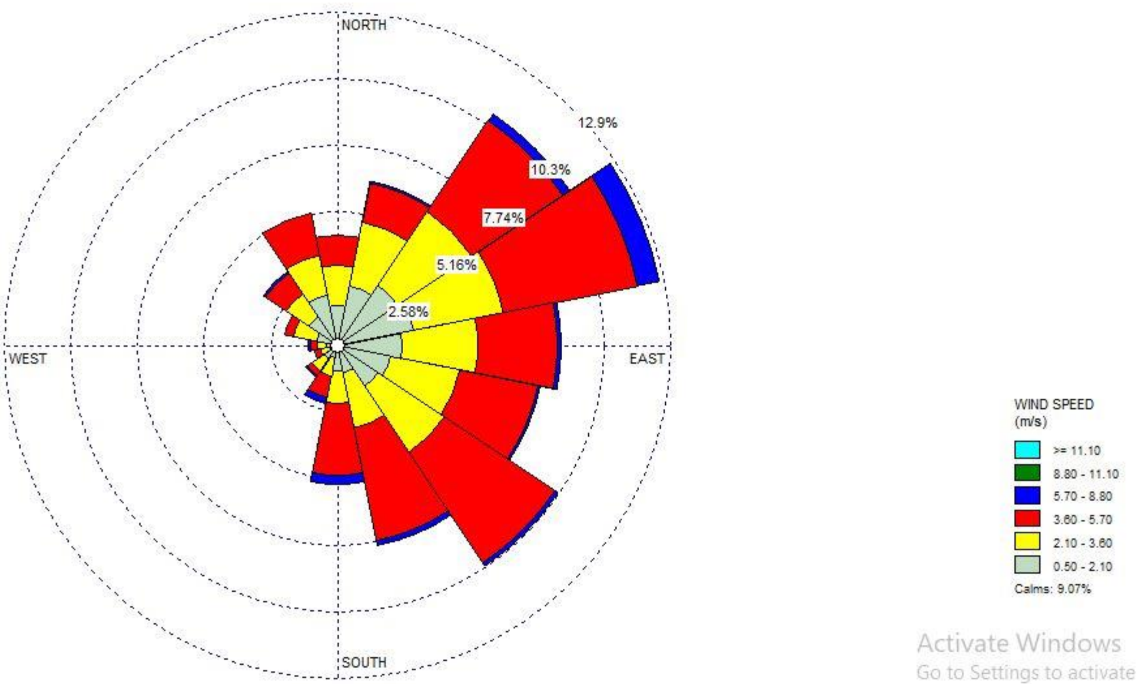


Figure 5.1: Wind rose diagram of the study period

### 5.4 Spatial Distribution of Pollutant Concentration

In this study, the dispersion of $SO_2$, NOx, CO has ben simulated under two perspective scenarios:

I. 150 MW in operation: The first scenario simulated pollutants only for 150 MW capacity of the plant (3rd unit only).

II. 525 MW in operation: The second scenario predicted the pollutants for all 3 units considering the full capacity of the power plant which is 525 MW.

In this study, hourly, daily and annual concentrations were predicted using AERMOD at each of the 1804 receptors within the model grid assuming that the power plant is operational all around the year.

Concentration contours are very important in determining the spatial distribution of pollutants over the modeled area. From model predictions, concentration contours were generated, and these contours have been used to determine the spatial and temporal locations for which the Bangladesh and European Union Standards and WHO guideline value for any pollutant concentration is approached or exceeded. This section discusses the spatial distribution of pollutants.

### 5.4.1 Scenario I: Plant Operating with 150 MW Capacity (3rd unit only)

Figure 5.2, 5.3 and 5.4 represents the hourly steady spatial distribution of $SO_2$, NOx, CO concentration emitted from stack of the power plant. The hourly iso concentration curves of $SO_2$, NOx, and CO follow the same pattern of pollutant dispersion. It is observed that the maximum concentration occurs at the south west direction of the power plant for each of the pollutants. The peak ground level concentration (GLC) of $SO_2$ (18.62μg/$m^3$) occurs at 1.5 km downwind direction of southeast and this concentration gradually diminishes to minimum level in the wind direction. The peak concentration is reached on 19 April 2020 at 9 am.

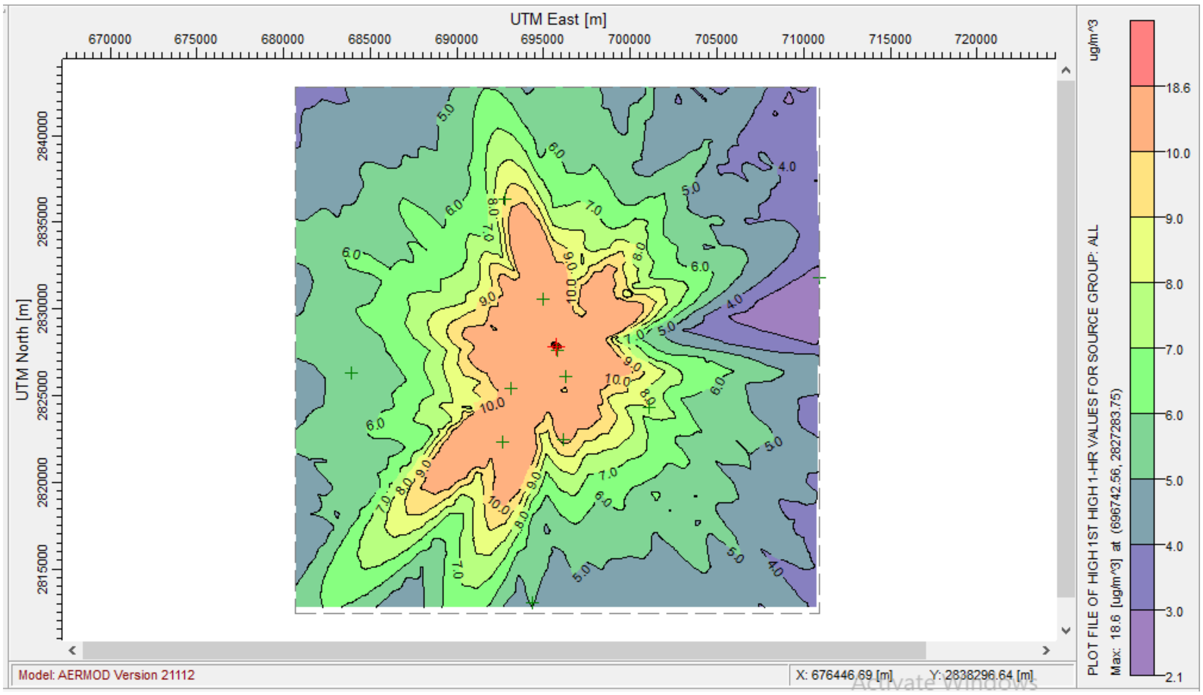


Figure 5.2: One hour average concentration curve of $SO_2$

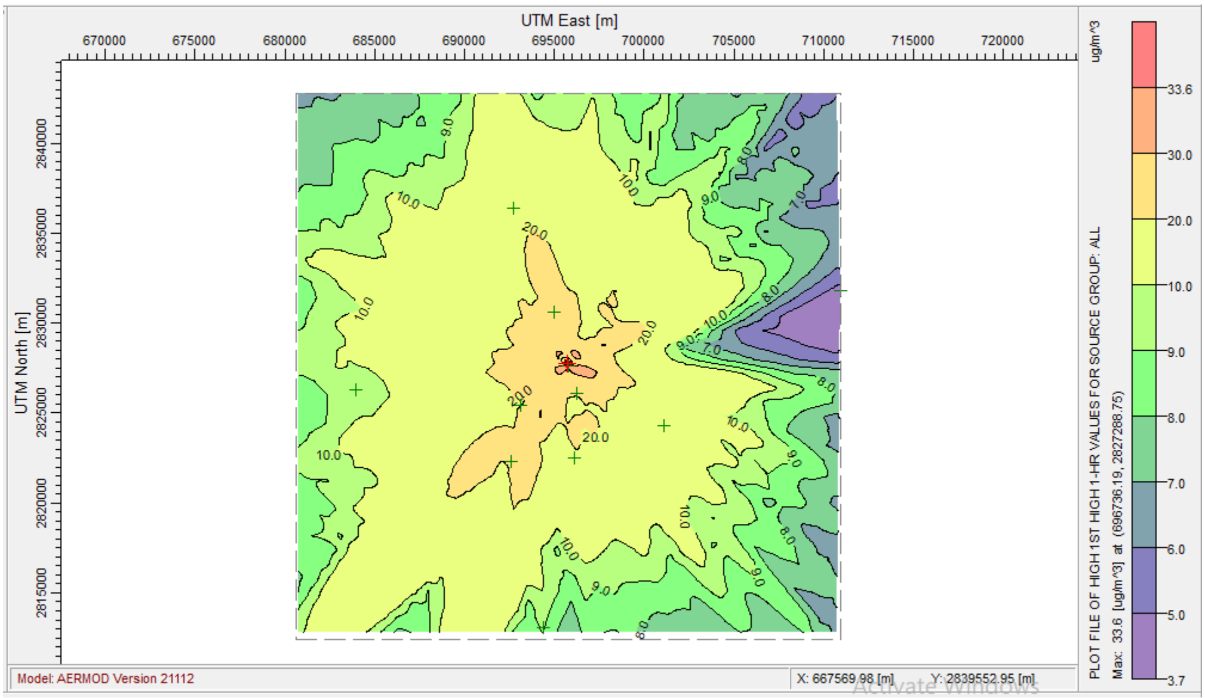


Figure 5.3: One hour average concentration curve of NOx

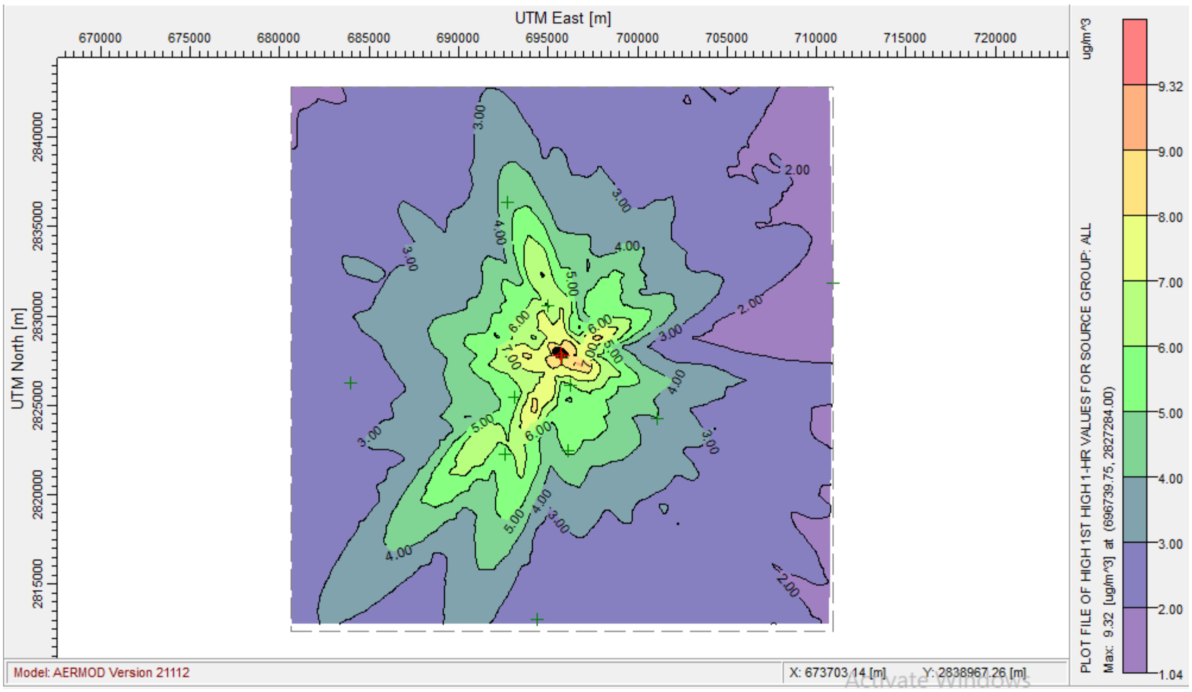


Figure 5.4: One hour average concentration curve of CO

The peak concentration of NOx is 33.56 µg/m$^3$ which is observed on 19 April 2020 at 9 am at a distance of 1.5 km from the stack towards southeast direction. Figure 5.4 represents the spatial distribution of CO emitted from the plant. The maximum concentration of CO (9.32 µg/m$^3$) occurs on the same date as $SO_2$ and NOx. The direction of peak concentration is southeast from the powerplant and the distance is about 1.42 km from stack. Among these pollutants only CO has one hour standard (40000 µg/m$^3$ in Bangladesh air quality standard). The predicted peak one hour concentration (due to plant operation) is much lower than the standard. However, monitored one hour concentration of CO is found to be significantly higher than the predicted value.

The wind rose diagram of 19 April 2020 is shown in Figure 5.5. It is observant from the diagram that the results are in agreement with the dominant wind direction.

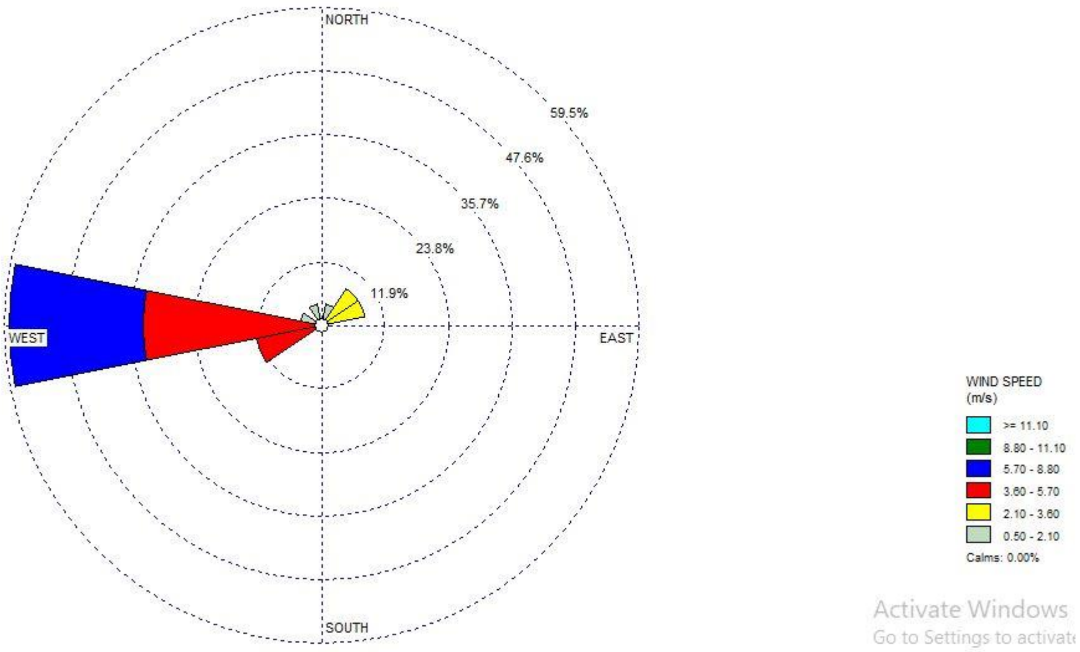


Figure 5.5: Wind rose diagram on 19 April 2020.

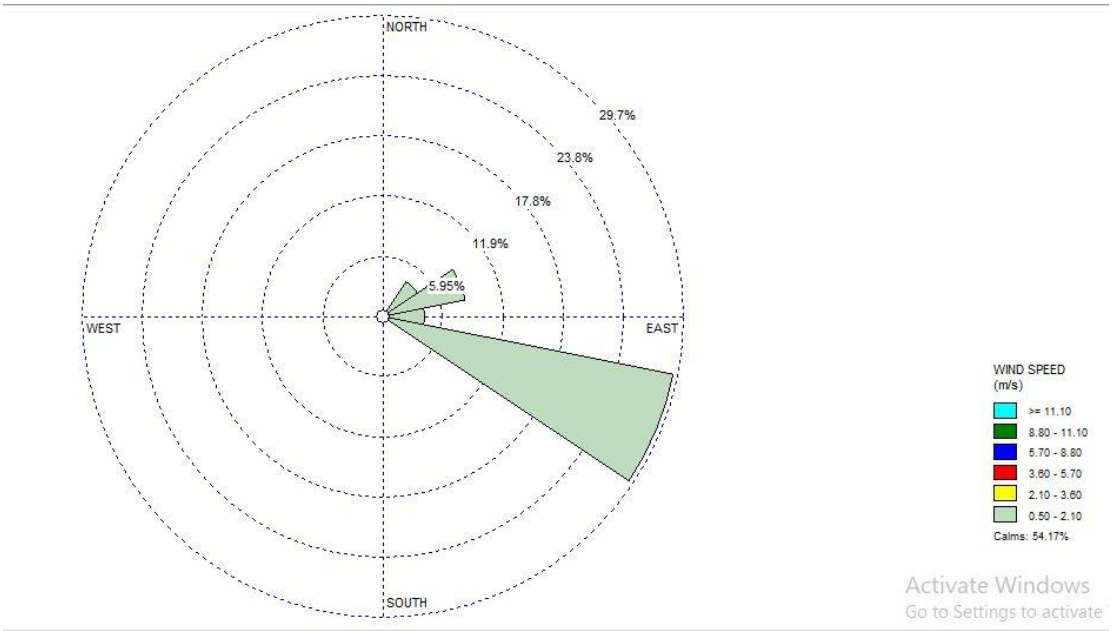


Figure 5.6: Wind rose diagram on 16 January 2020.

The daily iso-concentration curves are shown in Figure 5.7, 5.8 and 5.9. These are derived from the model computation at each grid point followed by a calculation of their average over a day and retaining only the highest concentrations of the 365 days study period. The peak concentrations for 24 hour averaging time are lower than the corresponding hourly averages as expected. After the exhaust gas emissions from the stack are dispersed for 24 hours the maximum concentration of $SO_2$, NOx, CO are found to be 3.19 $\mu g/m^3$, 5.74 $\mu g/m^3$, 1.59 $\mu g/m^3$ respectively. The maximum concentration occurs on 16 January 2020 at a location of UTM 695238.13m and 2828286.50 m which is at a distance of 0.71 km from the emission source. The peak concentration shifts towards the north western direction which agrees with the wind rose diagram of 16 January (Figure 5.6) that shows the maximum prevailing wind is from the ESE direction. Of all the pollutants, NOx seems to spread in higher concentration over a wider zone. Emissions are coming out of the stack are directly dispersed so that the concentration decreases and then continues to increase until reaches the maximum concentration. After that the concentration will continues to decrease. For $SO_2$, the concentration decreases below 2 $\mu g/m^3$ after reaching a distance about 7.5 km from the source in the prevailing wind direction. In case of NOx after 6 km from the source the concentration decreases below 4 $\mu g/m^3$. For pollutant CO the higher concentration spreads over about 7 km around the powerplant which decreases below 1 $\mu g/m^3$ after a distance of 7 km. The predicted peak concentration of $SO_2$ for 24 hour average period are well below the Bangladesh standard and also complies with WHO standard as well. NOx and CO does not have any standard value for 24 hour averaging period.

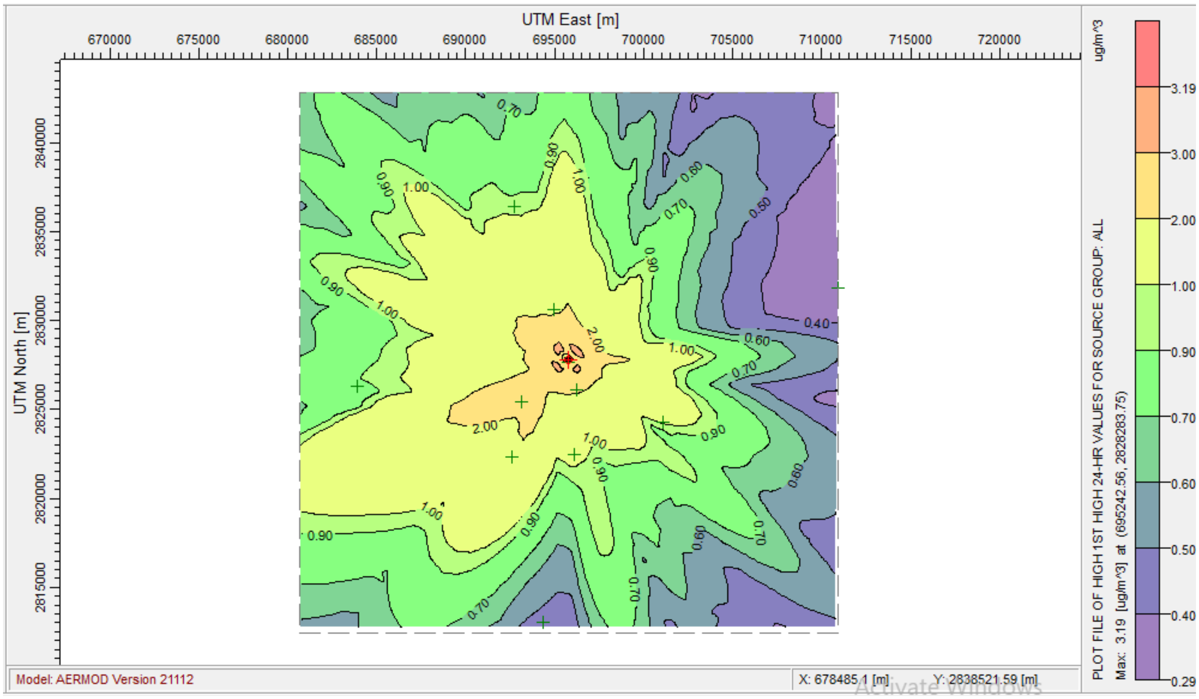


Figure 5.7: 24 hour average concentration curve of $SO_2$

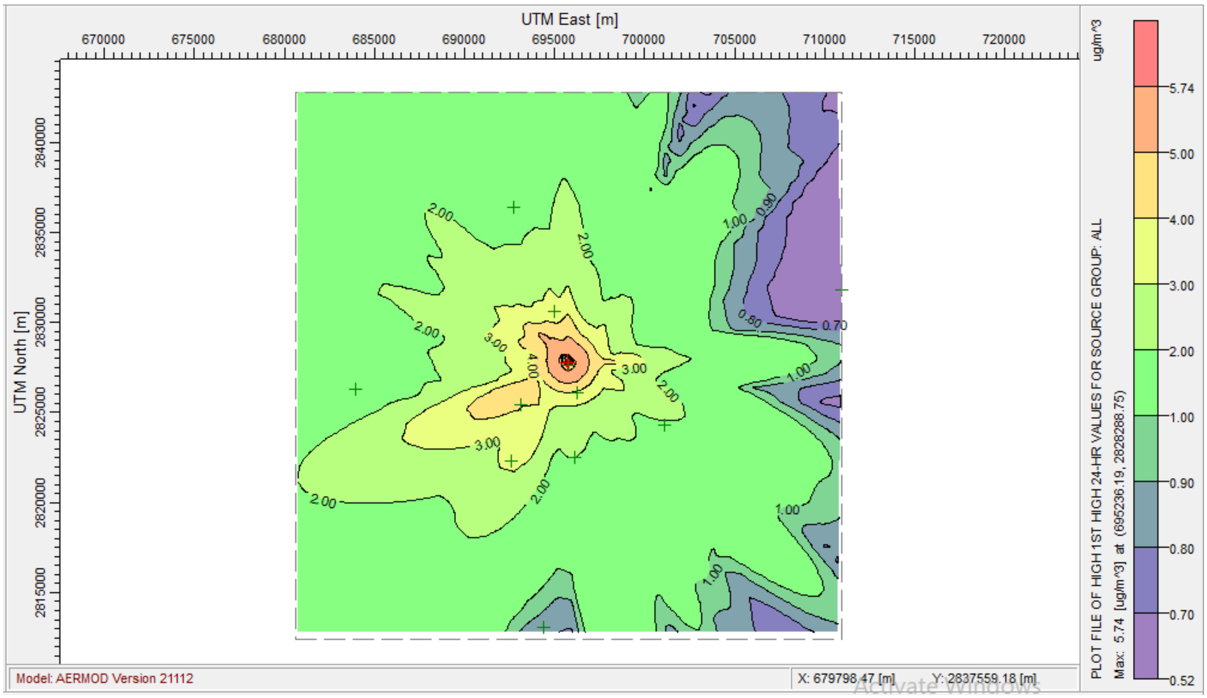


Figure 5.8: 24 hour average concentration curve of NOx

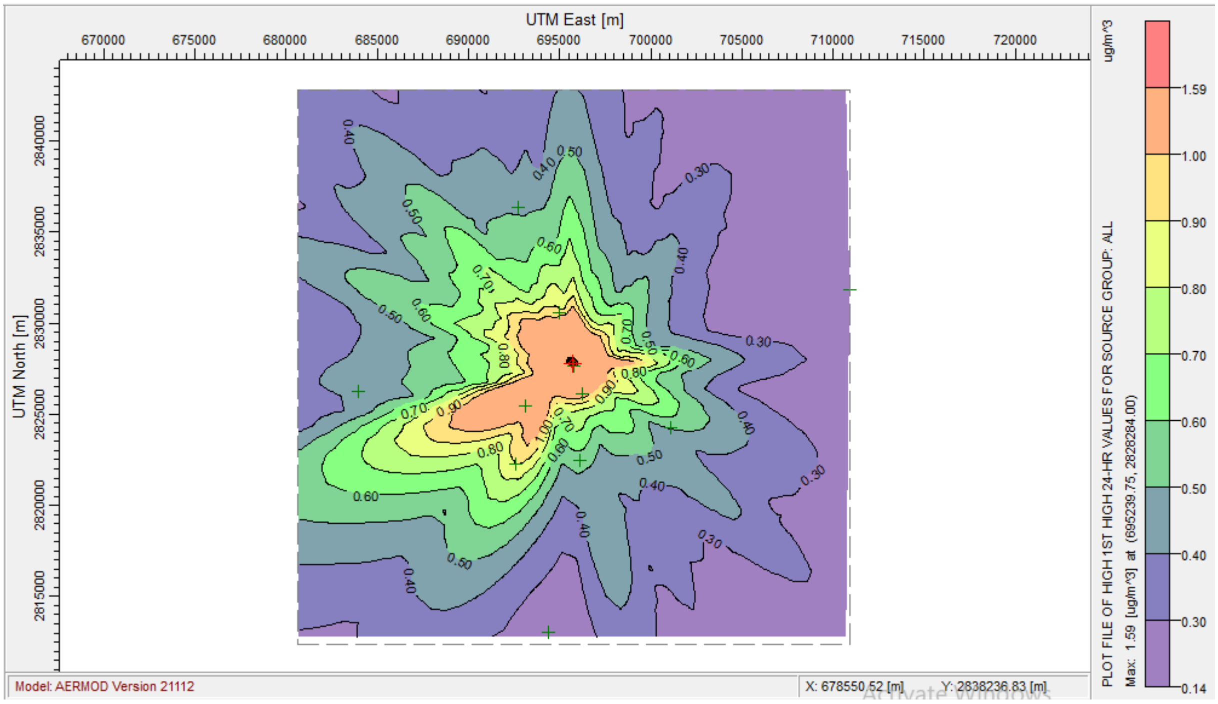


Figure 5.9: 24 hour average concentration curve of CO

The process to draw the annual iso-concentration curves was slightly different. In fact, the AERMOD model computes the average of all hourly concentration modeled over the year, and then connects the points of same concentration. In this case, no maximum value is retained to calculate the annual average at a given point. Figure 5.10, 5.11 and 5.12 shows the annual iso concentration curves of pollutants and the pollutant concentration is seen to drop vastly compared to the hourly average or daily average concentrations. The annual average concentrations of the pollutants are negligible.

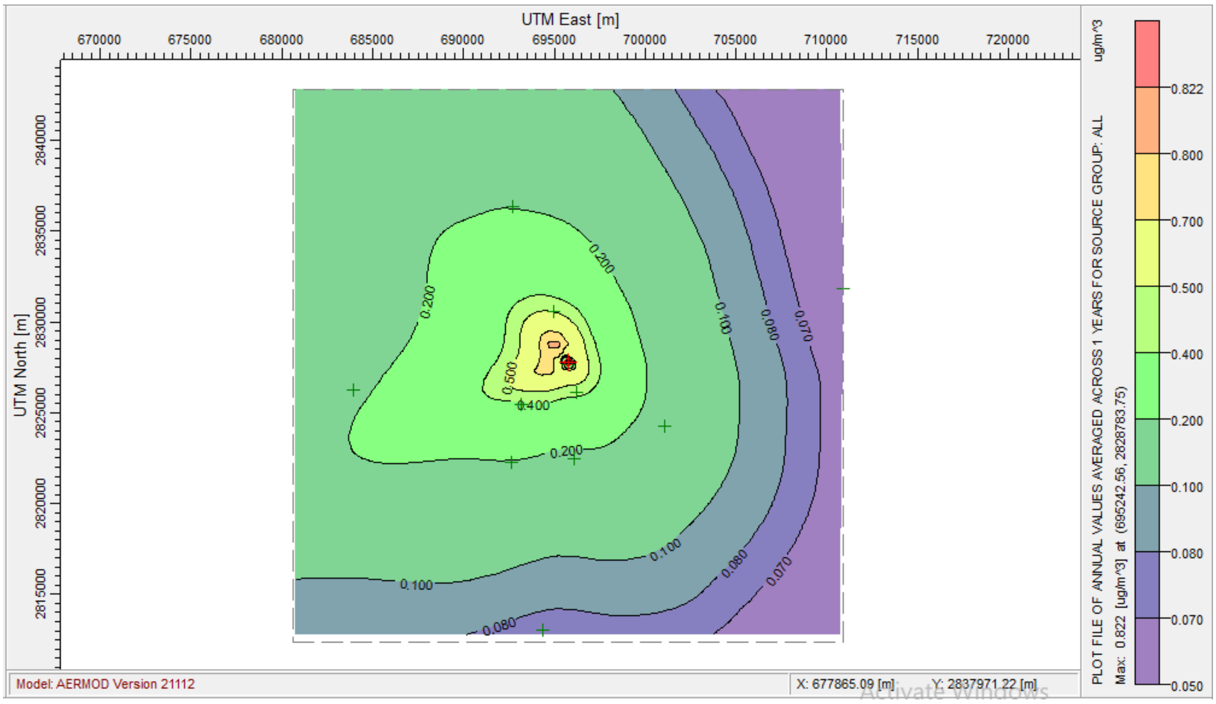


Figure 5.10: Annual concentration curve of $SO_2$

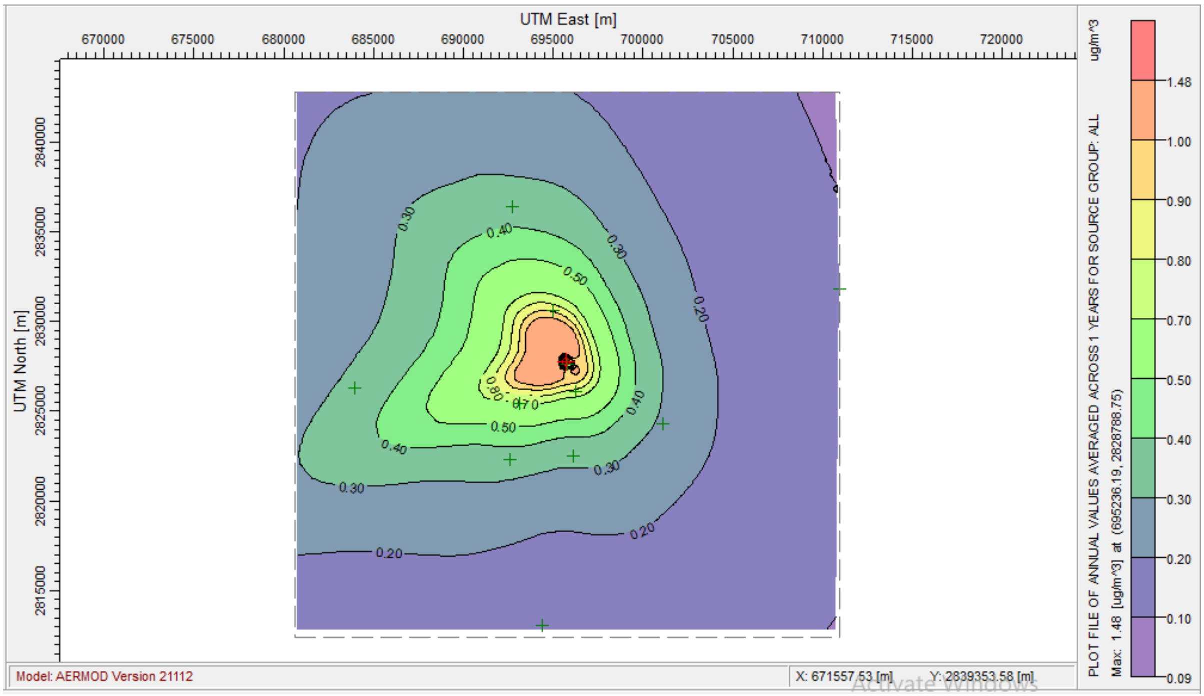


Figure 5.11: Annual concentration curve of NOx

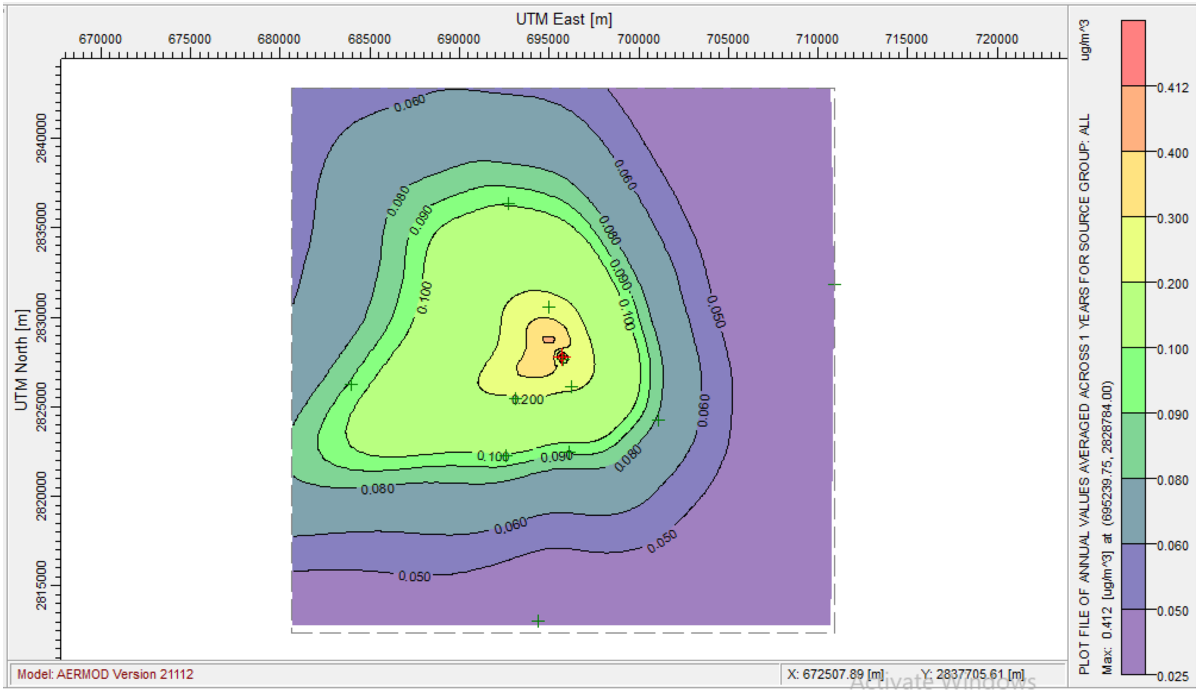


Figure 5.12: Annual concentration curve of CO

The annual iso concentration curves clearly suggests that people living in Western part (Phulbari and Chirirbandar Upazila) of the study area are likely to bear consequences of combined emission of the power plant.

Table 5.2: Dispersion model Results for $SO_2$, NOx, CO (Scenario I)

| Ser | Period | Pollutant | Peak Concentration (µg/m$^3$) | Peak Concentration distance from stack (km) | Date and time | Coordinates | |
|---|---|---|---|---|---|---|---|
| | | | | | | X | Y |
| 1 | Hourly | $SO_2$ | 18.62 | 1.5 to ESE | 19 April 2020, 0900 | 696742.56 | 2827283.75 |
| 2 | | NOx | 33.56 | 1.5 to SE | | 696736.19 | 2827288.75 |
| 3 | | CO | 9.32 | 1.42 to SE | | 696739.75 | 2827284.00 |
| 4 | Daily | $SO_2$ | 3.19 | 0.71 to NW | 16 Jan 2020, 2400 | 695242.56 | 2828283.75 |
| 5 | | NOx | 5.74 | 0.71 to NW | | 695236.19 | 2828288.75 |
| 6 | | CO | 1.59 | 0.71 to NW | | 695239.75 | 2828284.00 |
| 7 | Annual | $SO_2$ | 0.82 | 1.32 to NNW | | 695242.56 | 2828783.75 |
| 8 | | NOx | 1.48 | 1.44 to NNW | | 695236.19 | 2828788.75 |
| 9 | | CO | 0.41 | 1.42 to NNW | | 695239.75 | 2828784.00 |

### 5.4.2 Scenario II: Plant Operating with 525 MW Capacity (Maximum Capacity)

The spatial distribution of pollutants in Scenario II has been determined to be similar to that in Scenario I (described in Section 5.4.1). Like Scenario I, CO concentrations were found to be extremely low over the model grids, however $SO_2$ and NOx concentrations were found to be relatively high.

The peak hourly concentration trend of $SO_2$, NOx and CO for Scenario II is comparable to that of Scenario I, but the peak pollutant concentration increases by about five times, as shown in Figure 5.13, 5.14 and 5.15. For instance, the peak $SO_2$ concentration under Scenario I was 18.62 µg/m$^3$, while the peak under Scenario II was 88.5 µg/m$^3$. For NOx, the peak concentration of Scenario I was 33.56 µg/m$^3$, while the peak concentration of Scenario II was 159 µg/m$^3$. The peak CO concentration was 9.32 µg/m$^3$ under Scenario I while the peak under Scenario II was 44.3 µg/m$^3$. The dispersion radius has noticeably increased. However, the peak concentration of $SO_2$ only spans a limited area in Scenario II while in Scenario I the peak hourly iso-concentration curves of $SO_2$ spans over larger area. In case of NOx and CO the peak concentration covers a larger region in Scenario II.

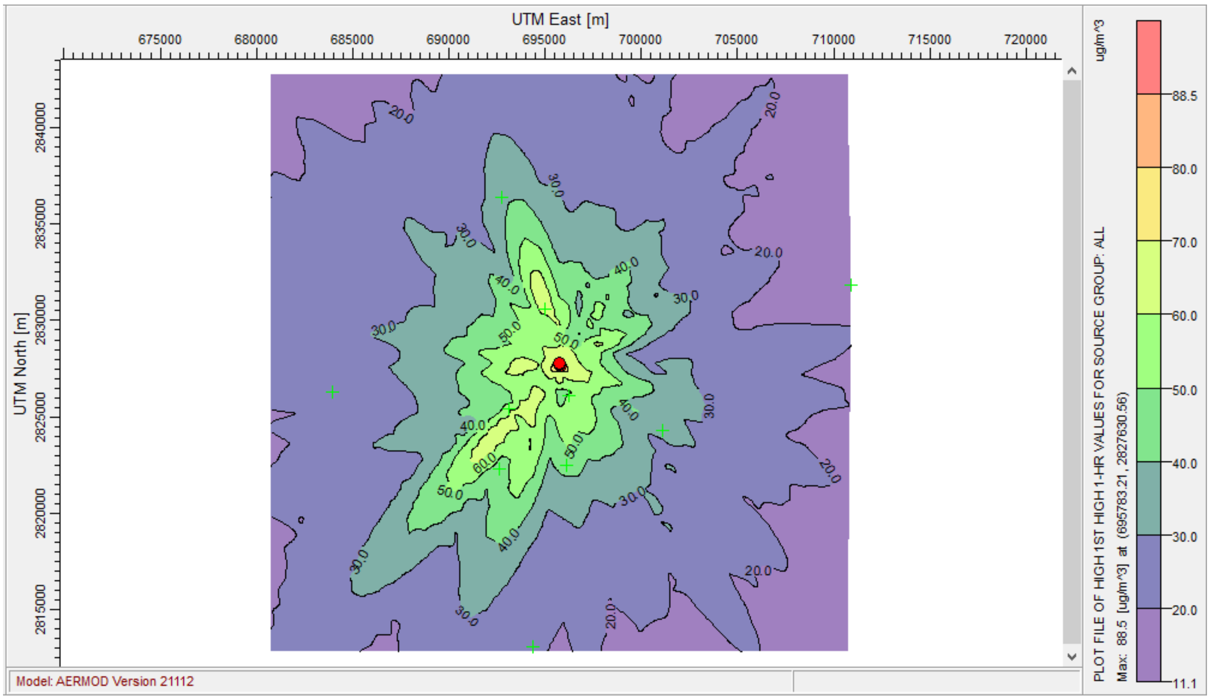


Figure 5.13: One hour average concentration curve of $SO_2$ (Scenario II)

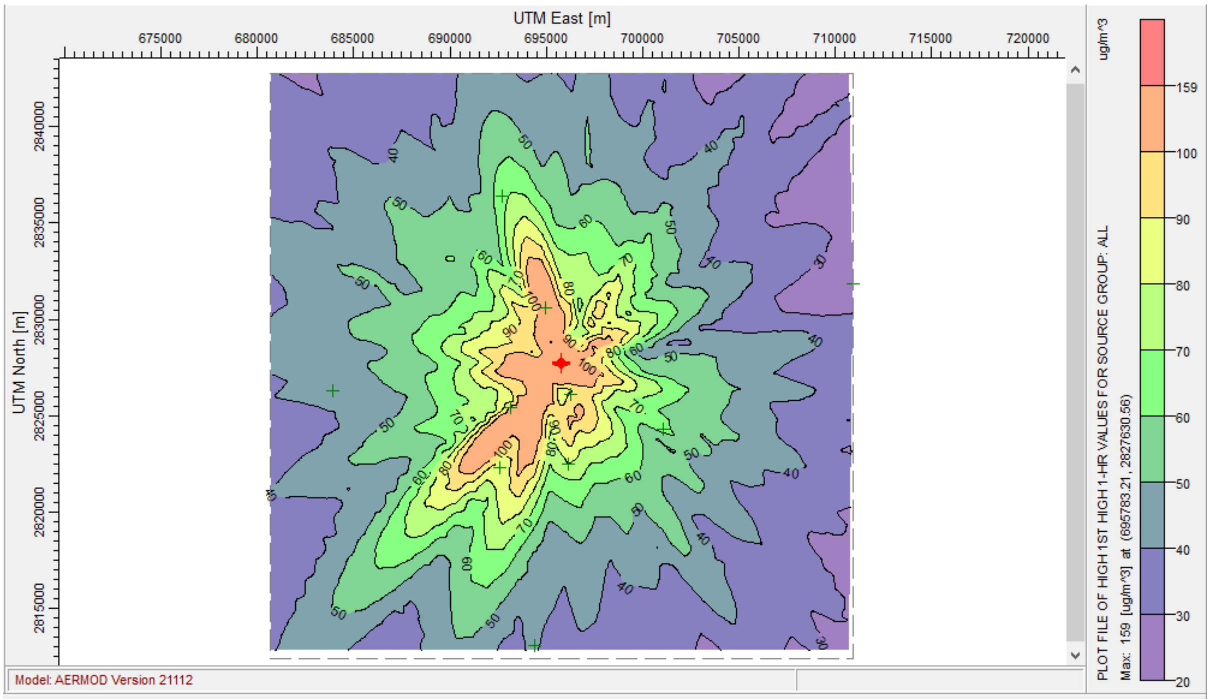


Figure 5.14: One hour average concentration curve of NOx (Scenario II)

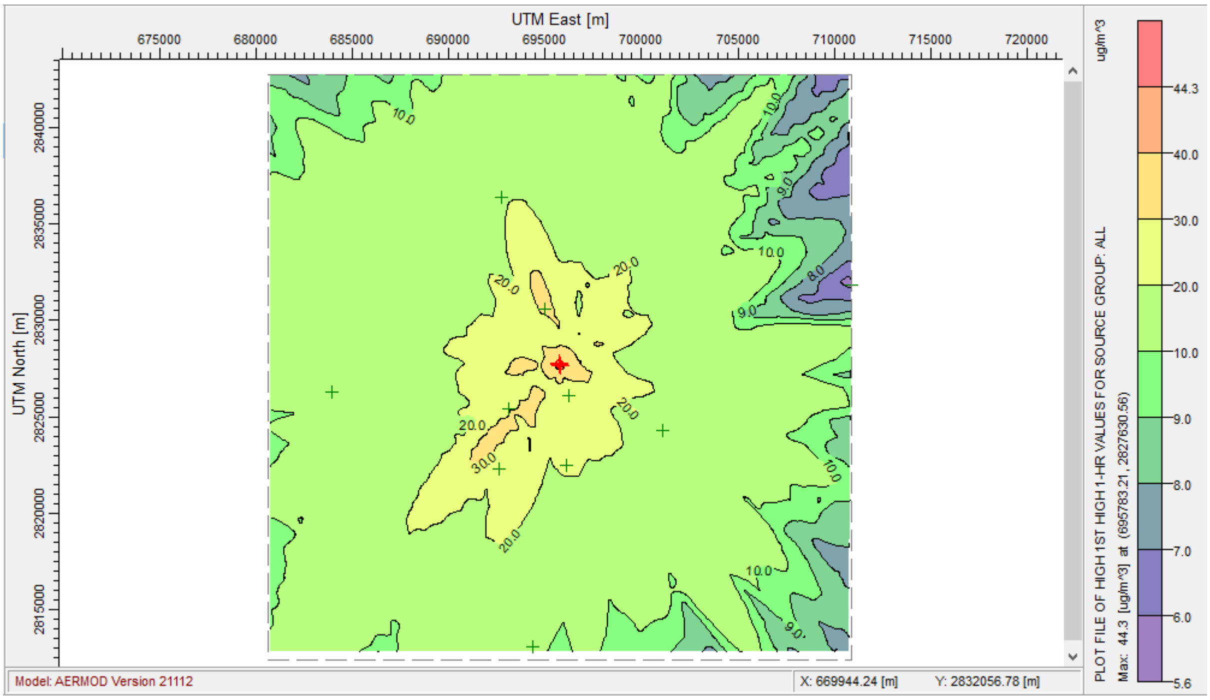


Figure 5.15: One hour average concentration curve of CO (Scenario II)

The daily and annual average iso-concentration curves for $SO_2$, NOx and CO are shown in following figures (Figure 5.16 to 5.21). These data demonstrate a considerable increase in the pollutant concentration in ambient air following the addition of 375 MW. Under Scenario II, the amount of pollutants in the surrounding areas grew more than five times as much as it did under Scenario I. For instance, the peak average concentrations of $SO_2$, NOx and CO during a 24-hour period in Scenario-II are 16.9, 30.4 and 8.48 $\mu g/m^3$ respectively, whereas in Scenario-I, these pollutants' highest concentrations were 3.19, 5.74 and 1.59 $\mu g/m^3$, respectively. Forecasted peak $SO_2$ concentration over a 24-hour period complies with WHO and Bangladesh Standards.

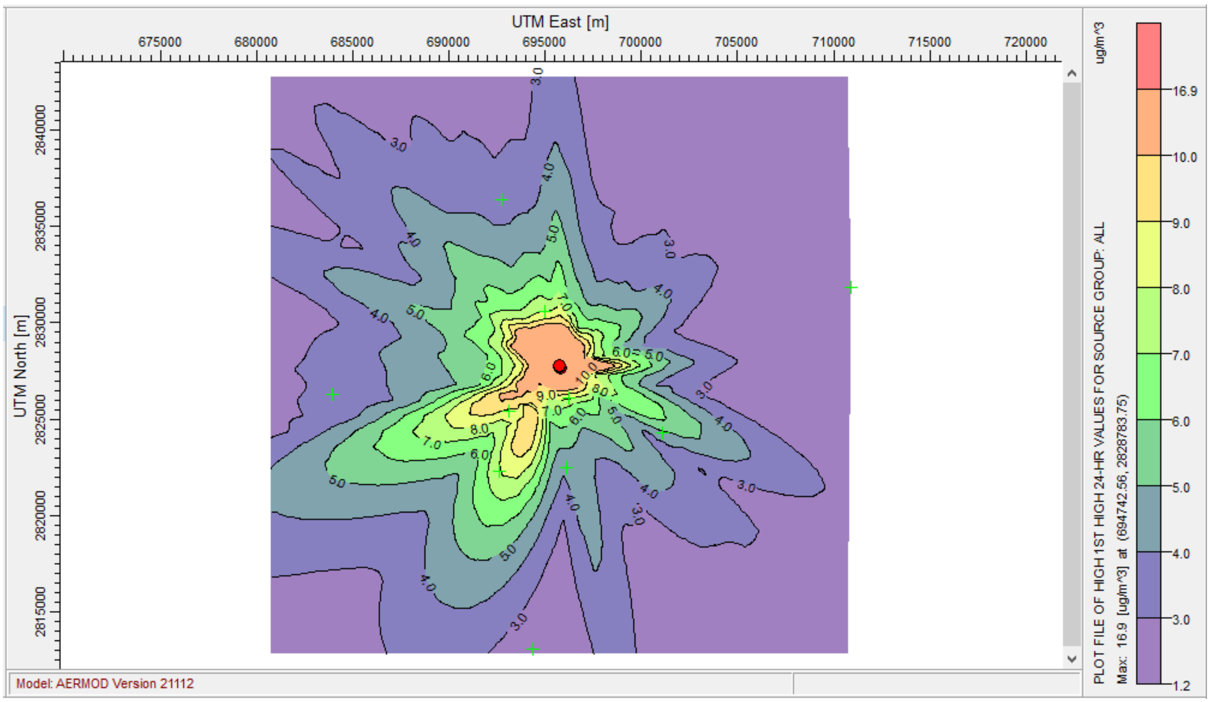


Figure 5.16: 24 hour average concentration curve of $SO_2$ (Scenario II)

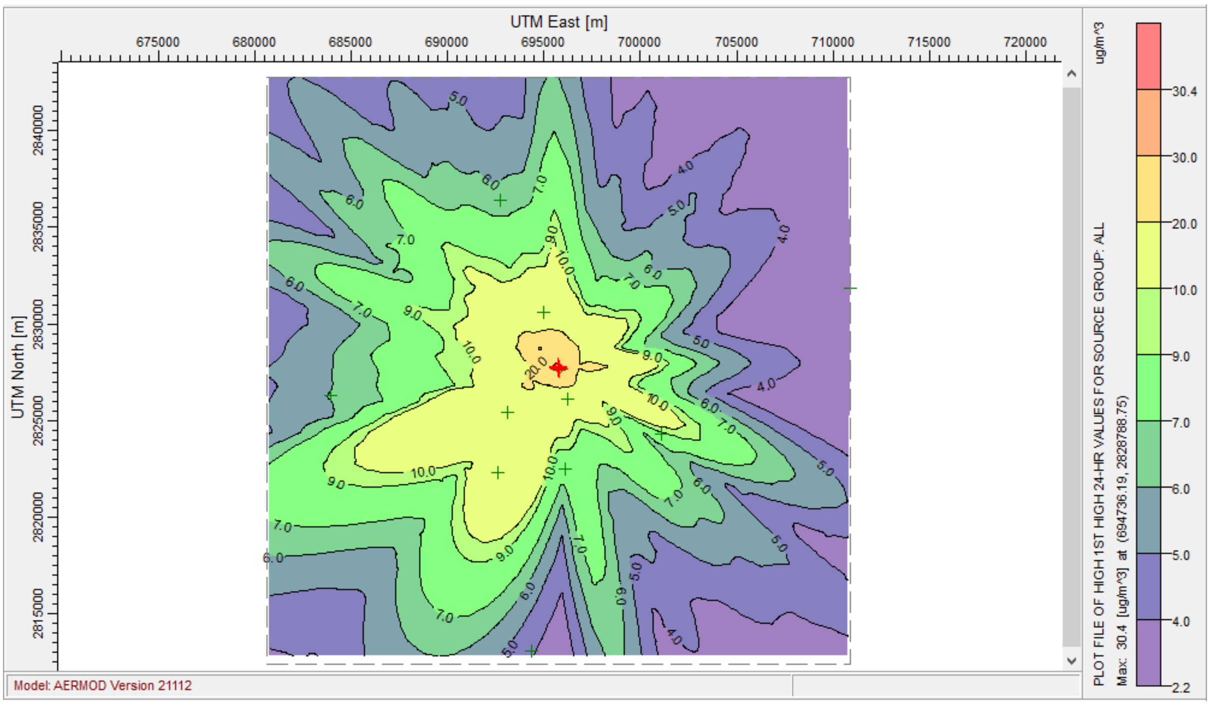


Figure 5.17: 24 hour average concentration curve of NOx (Scenario II)

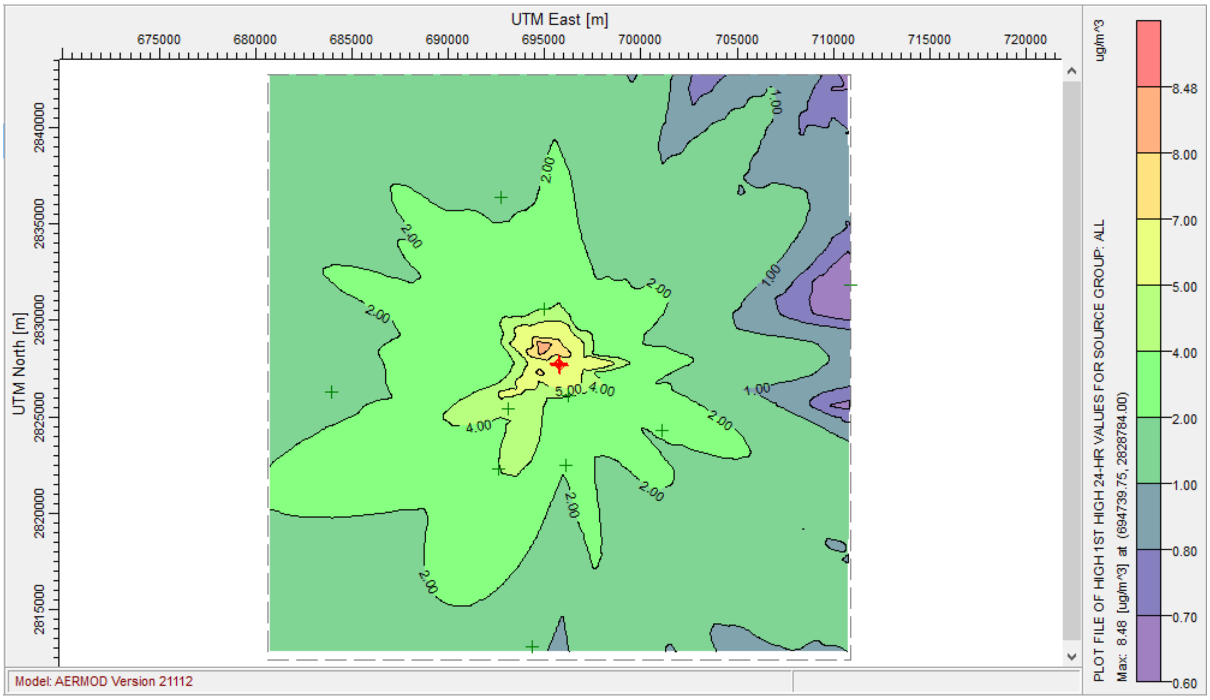


Figure 5.18: 24 hour average concentration curve of CO (Scenario II)

The maximum yearly $SO_2$, NOx, and CO values in Scenario-II are 4.64, 8.36, and 2.32 μg/$m^3$, respectively, which are far lower than the corresponding standards. The direction of the plume has not been seen to shift.

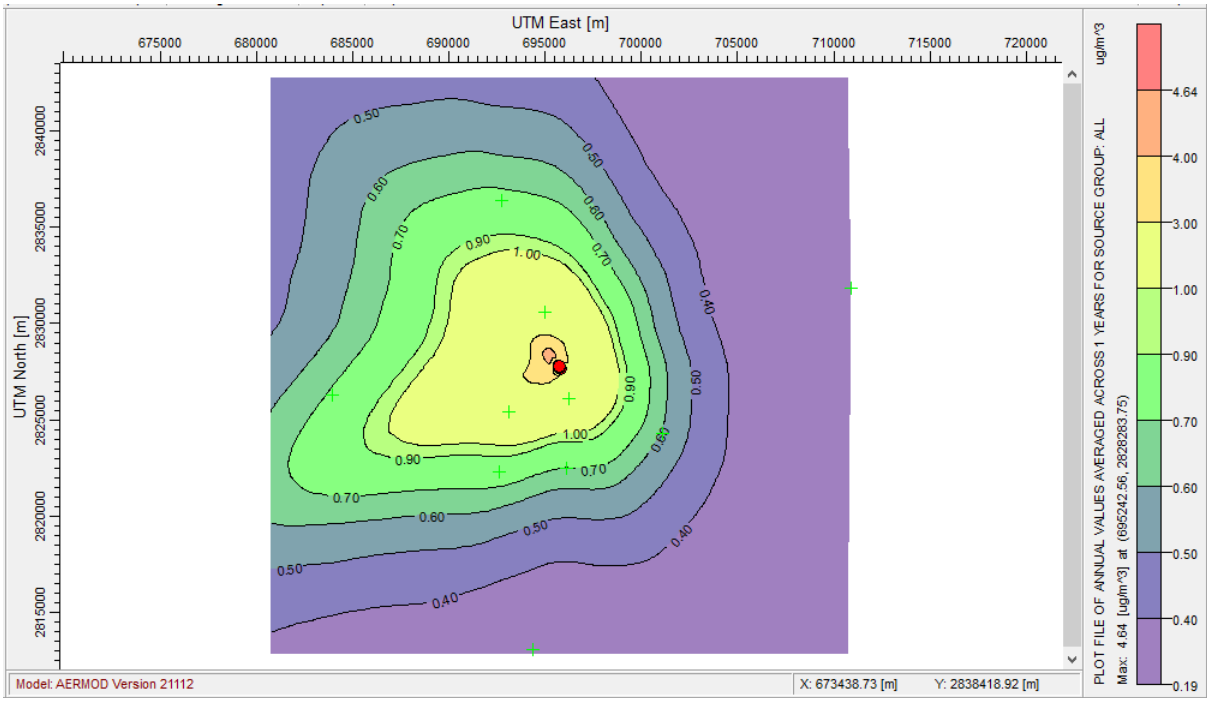


Figure 5.19: Annual concentration curve of $SO_2$ (Scenario II)

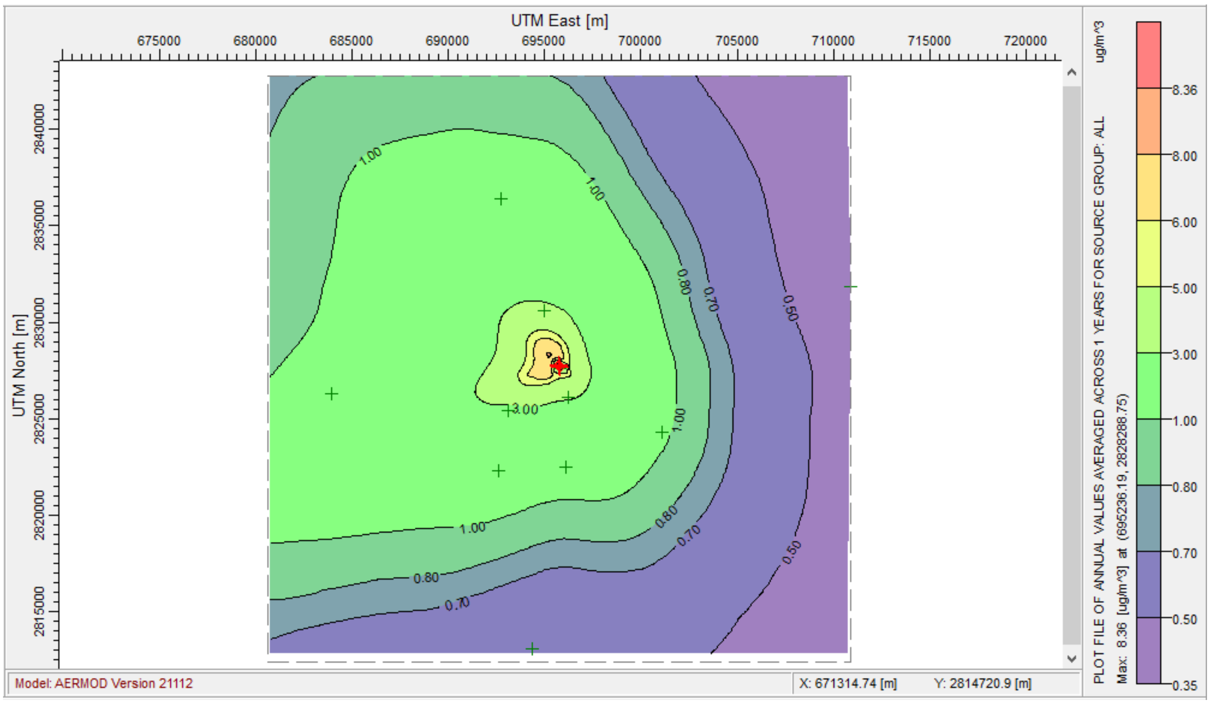


Figure 5.20: Annual concentration curve of NOx (Scenario II)

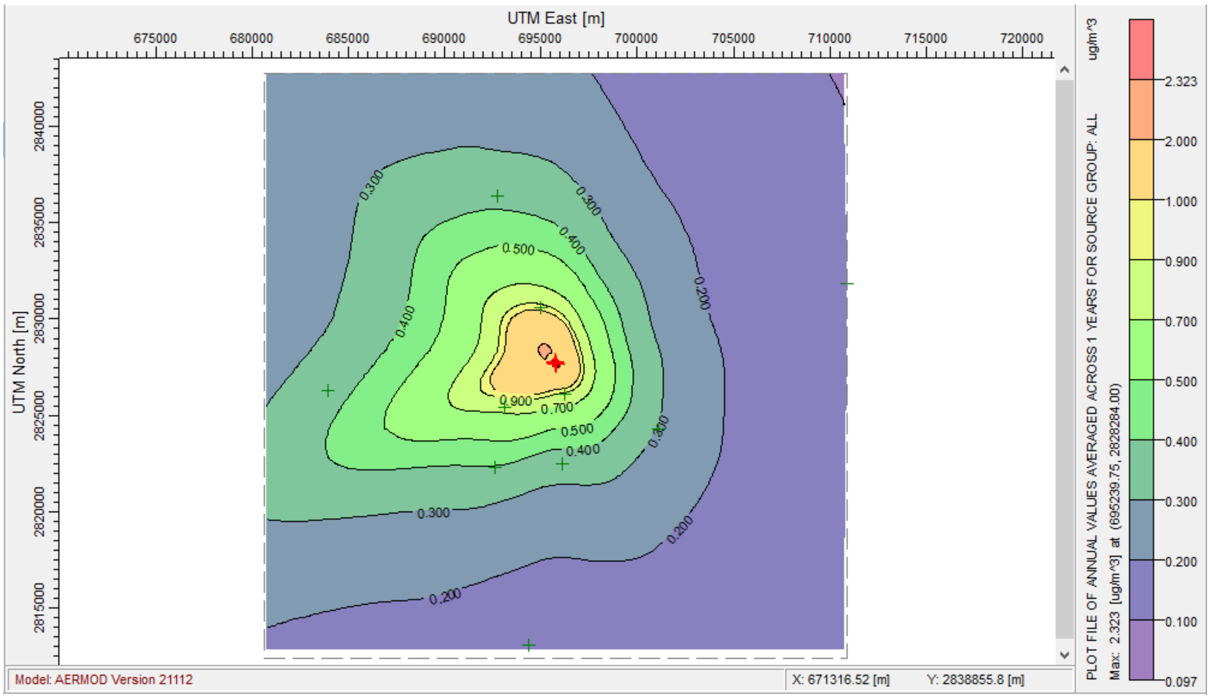


Figure 5.21: Annual concentration curve of CO (Scenario II)

## 5.5 Zone of Maximum Concentration

Hourly average concentration of $SO_2$, NOx and CO were simulated as 18.62 µg/m$^3$, 33.56 µg/m$^3$ and 9.32 µg/m$^3$ respectively. The zone of maximum concentration of pollutants can be identified within 5 km area of the source emitted from the power plant. The zone of maximum concentration 5 km of source location can be identified as mostly concentrated zone (Z-1) which is 5 km radial near the source with the concentration of $SO_2$> 10 µg/m$^3$, NOx> 20 µg/m$^3$ and CO>5 µg/m$^3$. Z-2 is 10 km radial area surrounding the source with the concentration of $SO_2$> 6 µg/m$^3$, NOx> 10 µg/m$^3$ and CO>3 µg/m$^3$. Furthermore, receptors located on south western parts of the plant showed relatively higher pollutant concentrations than other parts of the study domain as a result of the predominant north eastern winds in the project area during the study period.

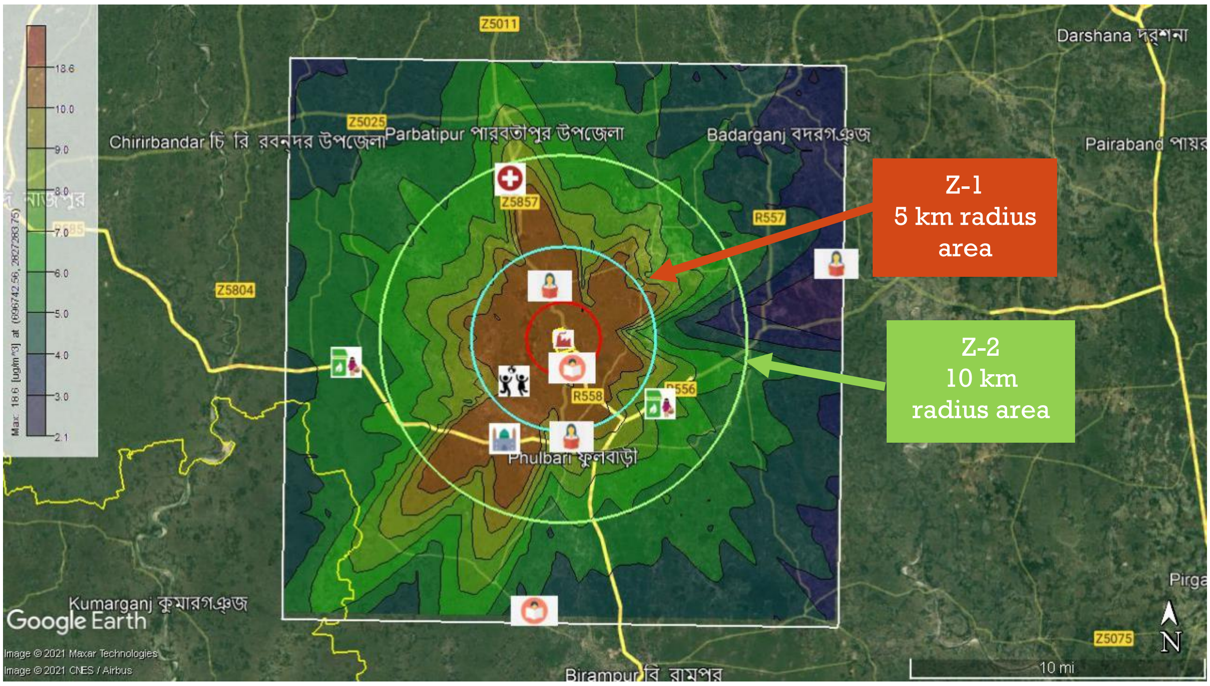


Figure 5.22: One hour average concentration curve of $SO_2$ with exposure zone

### 5.6 Evaluation of Power Plant Emissions on Ambient Air Quality

The predicted peak concentrations of pollutants in the vicinity of the coal-based power plant were obtained from AERMOD simulations. But what about the ambient pollutant concentration that already exists in the study area. To evaluate the resultant concentration, the ambient pollutant concentrations of $SO_2$ and NOx from the EIA report of Barapukuria Thermal Powerplant (3$^{rd}$ Unit), 2013 has been used as the baseline ambient concentration. As the ambient concentration of CO was not measured during the preparation of EIA report, the resultant concentration of CO is not evaluated here. The reported baseline concentrations of pollutants were averaged and considered to represent ambient air quality of the surrounding area. For calculating annual concentration of baseline pollutant from 24 hr average values, conversion factor for averaging time is used (Ministry of Environment, Toronto, Ontario, 2004).

A comparison was then made between cumulative ground level concentration (i.e. summation of peak predicted concentration due to power plant activity and baseline concentration) and the existing WHO, Bangladesh and European Union Standards to ensure compliance with the standards.

Table 5.3: Maximum Predicted Ground Level Concentration (GLC). (Worst-case scenario)

| Pollutant Parameter | Averaging Period | Baseline ambient concentration of pollutant (μg/m$^3$) | Max predicted GLC (μg/m$^3$) | Max predicted resultant values of GLC (μg/m$^3$) | Bangladesh Standard (μg/m$^3$) | WHO guideline values (μg/m$^3$) | European Union Standard (μg/m$^3$) |
|---|---|---|---|---|---|---|---|
| $SO_2$ | 24 Hr | 34.14 | 3.19 | 37.33 | 365 | 40 | 125 |
| | Annual | 10.49 | 0.82 | 11.56 | 80 | - | |
| NOx | 24 Hr | 39.44 | 5.74 | 45.18 | - | 25 | |
| | Annual | 12.11 | 1.48 | 13.59 | 100 | 10 | 40 |

In the worst case scenario the peak 24 hour and peak annual predicted concentrations of $SO_2$, $NO_x$ were compared with the corresponding air quality standards.

Table 5.3 shows that for both the averaging periods, resultant ground level concentration of NOx exceeds WHO guideline values. Thus, additional low NOx burners can be used to comply WHO guideline values. However, both the pollutants comply with the respective Bangladesh and European Union standards. Annual concentrations of the pollutants are well below the Standards.

Therefore, FGD will not be required if the quantity (1450 ton per day) and quality (average S content - 0.57%) is maintained in future operations. In case of operating at a higher load, a rise in pollutant concentration can be expected.

### 5.7 Contribution of $SO_2$ and NOx from Barapukuria Power Plant

AERMOD dispersion model simulated ground level concentration (1 hr) at 11 receptor (sampling) locations for $SO_2$ and NOx. These data were tabulated along with the observed concentration (1 hr) of $SO_2$ and NOx at those locations (Appendix A-2). Contribution of

Barapukuria coal fired power plant emission was then calculated for each point and finally the contribution for 11 points were averaged to show the average concentration of the plant emission to the ambient airshed.

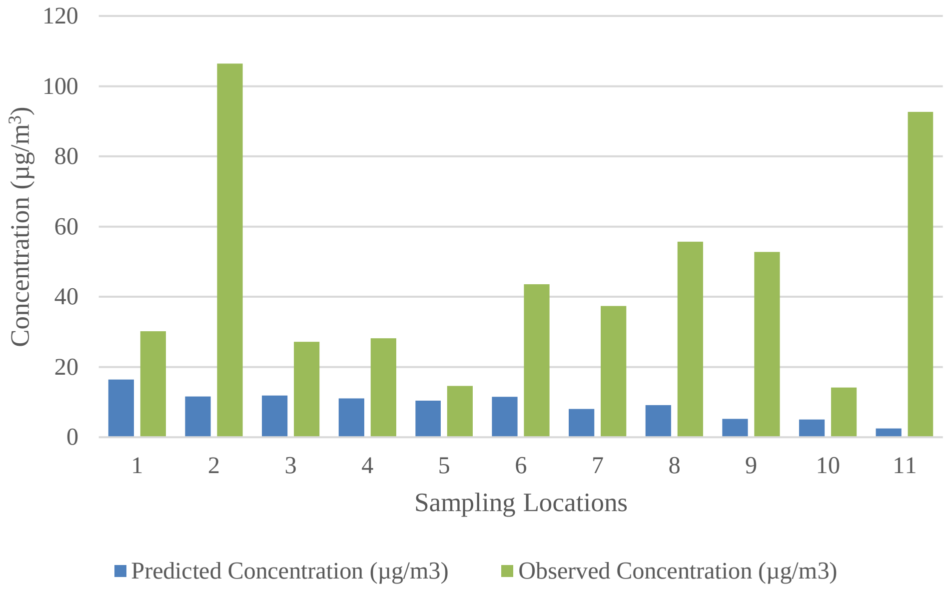


Figure 5.23: Contribution of plant $SO_2$ emissions to the ambient $SO_2$ concentration

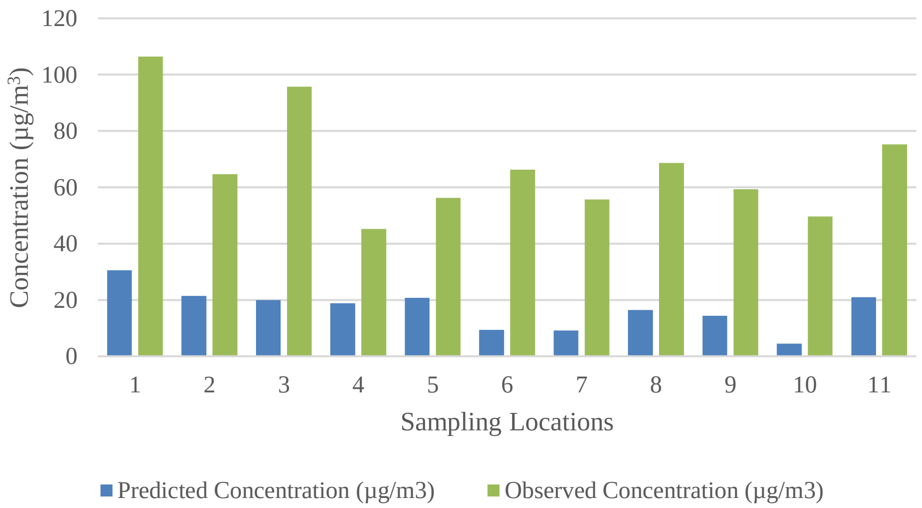


Figure 5.24: Contribution of plant NOx emissions to the ambient NOx concentration

Figure 5.23 and Figure 5.24 shows the contribution of power plant emission to the ambient air quality. Comparing the observed data with the simulated data, it was found that 29.4% of total ambient $SO_2$ is contributed by the power plant emission and 25.2% of total ambient NOx is contributed by the power plant emission.

### 5.8 Dispersion Variation with Distance and Direction

Figure 5.25 illustrates the ground level concentration for $SO_2$ along SW, NW and eastern direction. It is observed that maximum concentration of $SO_2$ i.e 16.46 μg/m$^3$ is found to be along south west direction at 1.5 km distance.

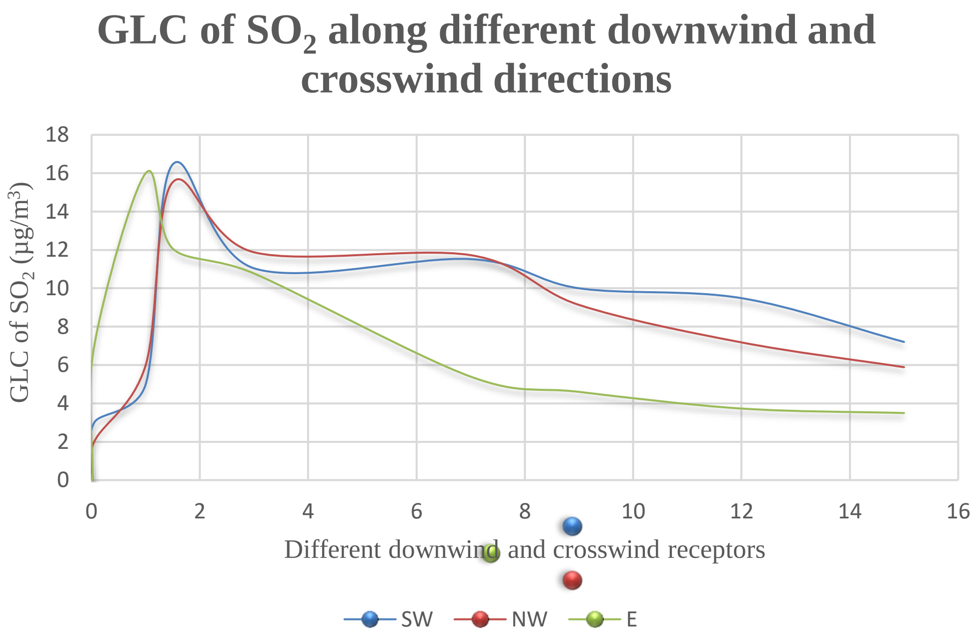


Fig 5.25: GLC of $SO_2$ along different downwind and crosswind directions

Figure 5.26 represents the ground level concentration for NOx along SW, NW and eastern direction. It is observed that maximum concentration of NOx i.e 30.25 μg/m$^3$ is found to be along south west direction at 1.5 km distance.

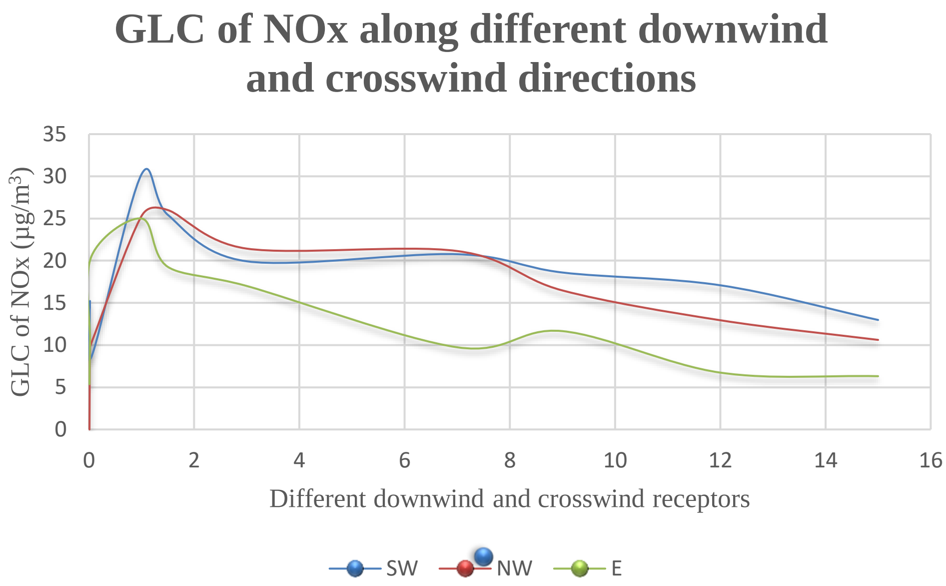


Fig 5.26: GLC of NOx along different downwind and crosswind directions

Figure 5.27 represents the ground level concentration for CO along SW, NW and eastern direction. It is observed that maximum concentration of CO i.e 8.79 µg/m$^3$ is found to be along south west direction at 0.05 km distance.

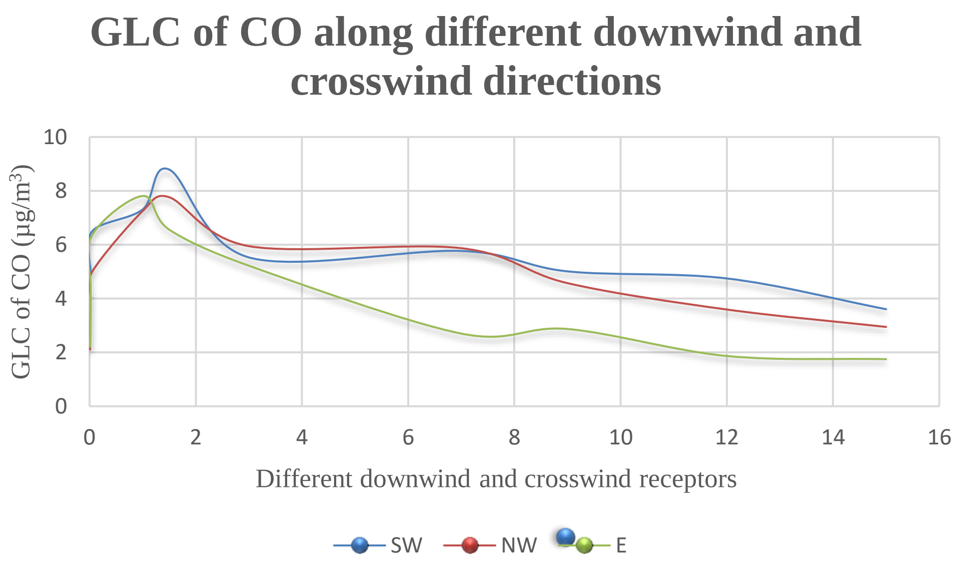


Fig 5.27: GLC of CO along different downwind and crosswind directions

### 5.9 Seasonal Variation of Pollutant Concentration

The seasonal variability of pollutant concentration within the model domain was assessed by predicting peak 1-hr concentrations of pollutants for the summer (March-June), monsoon (July-October), and winter (November–February) seasons as shown in Table. The maximum 1 hour concentrations for the pollutants occurred during summer, while lowest 1 hour concentrations were predicted during monsoon. The highest concentration of pollutants in summer is due the effects of meteorological parameters such as wind speed and solar radiation, which also affects mixing heights. During monsoon pollutant concentrations are expected to be low due to scavenging of particulate pollutants from the atmosphere due to rainfall and also due to higher relative humidity, which reduces re-suspension of dust (Stern, 1976). Thus, changes in seasonal concentration of the pollutants depend on daily climates, which are influenced by seasonal winds and land-sea breeze (Mousavi et al., 2021).

Table 5.4: Seasonal concentration of pollutants due to plant activity

| **Season** | **Peak concentration- 1 hr average ((μg/m$^3$)** | | |
|---|---|---|---|
| | **$SO_2$** | **NOx** | **CO** |
| Winter | 17.68 | 31.85 | 8.85 |
| Summer | 18.62 | 33.56 | 9.32 |
| Monsoon | 16.46 | 30.55 | 8.27 |

The predicted peak 1-hr $SO_2$ concentration for the three seasons are shown in Figures 5.28 (a-c).

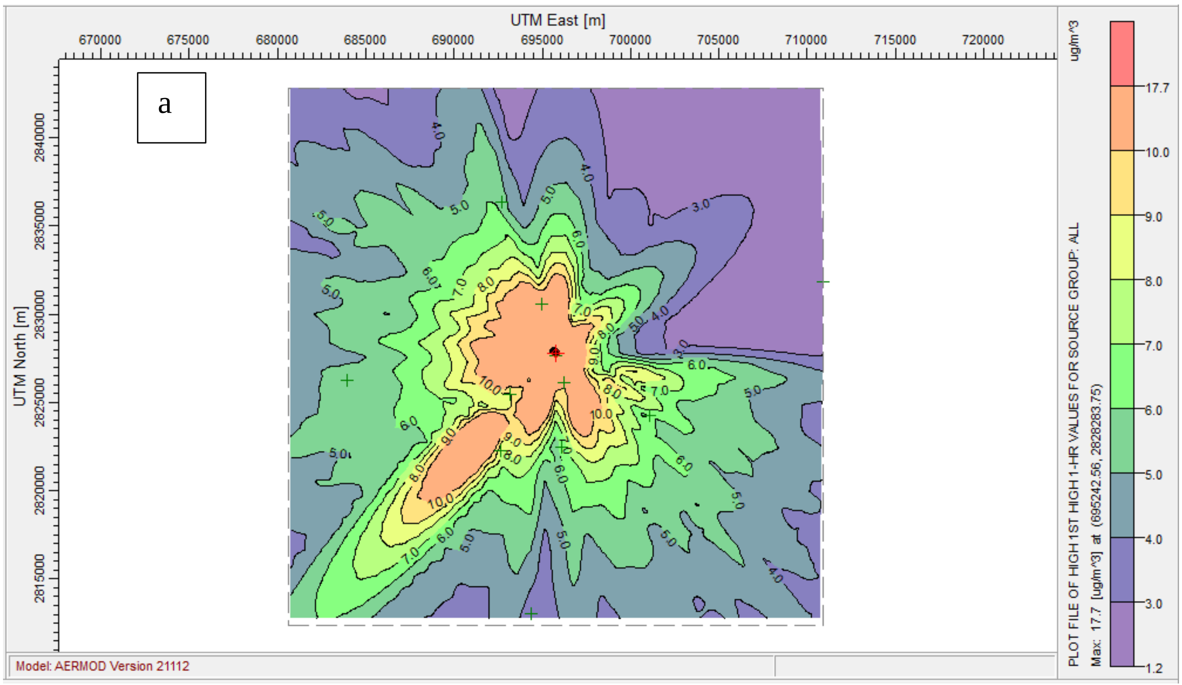


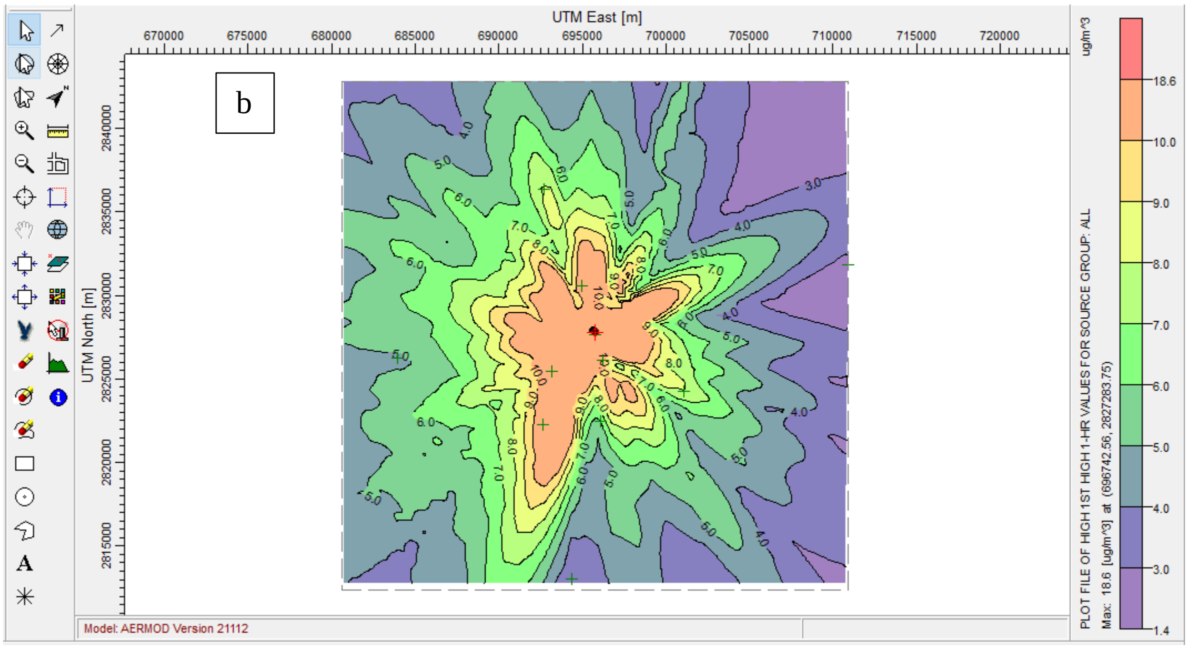

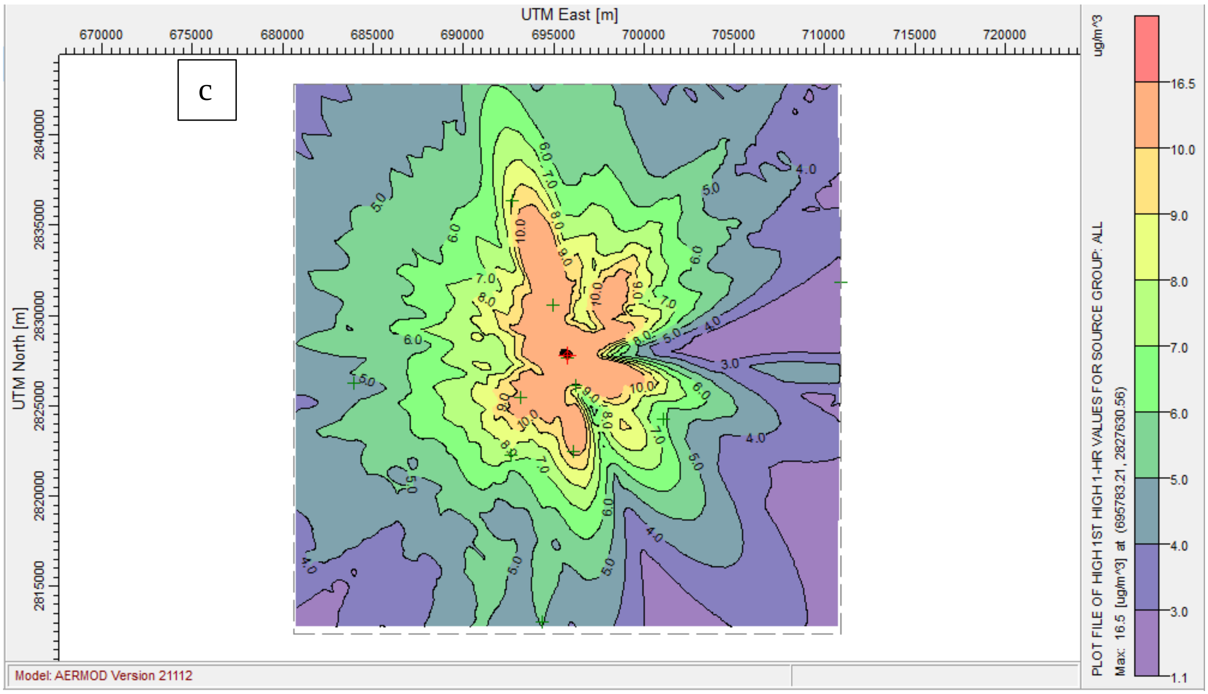


Figure 5.28 (a, b, c): Distribution pattern of maximum 1-hour average concentration of $SO_2$ during (a) winter, (b) summer and (c) monsoon

During winter season, the northeasterly wind carries the pollutants to the S and SW direction; however, light wind and low humidity being the characteristic of this season, the rate of dispersion of pollutants is relatively low compared to summer and monsoon. Meanwhile, in summer season the country experiences low air pressure which results in strong gusty, hot, dry winds blowing towards NE. Hence, the pollutants move linearly with the peak appearing at a distance of 1.2 km from the source. The heavy precipitation and low solar radiation of monsoon results in a central radial distribution of pollutants. The dispersion of the pollutants is consistent with the wind rose diagram of the respective season presented in Figure 5.29.

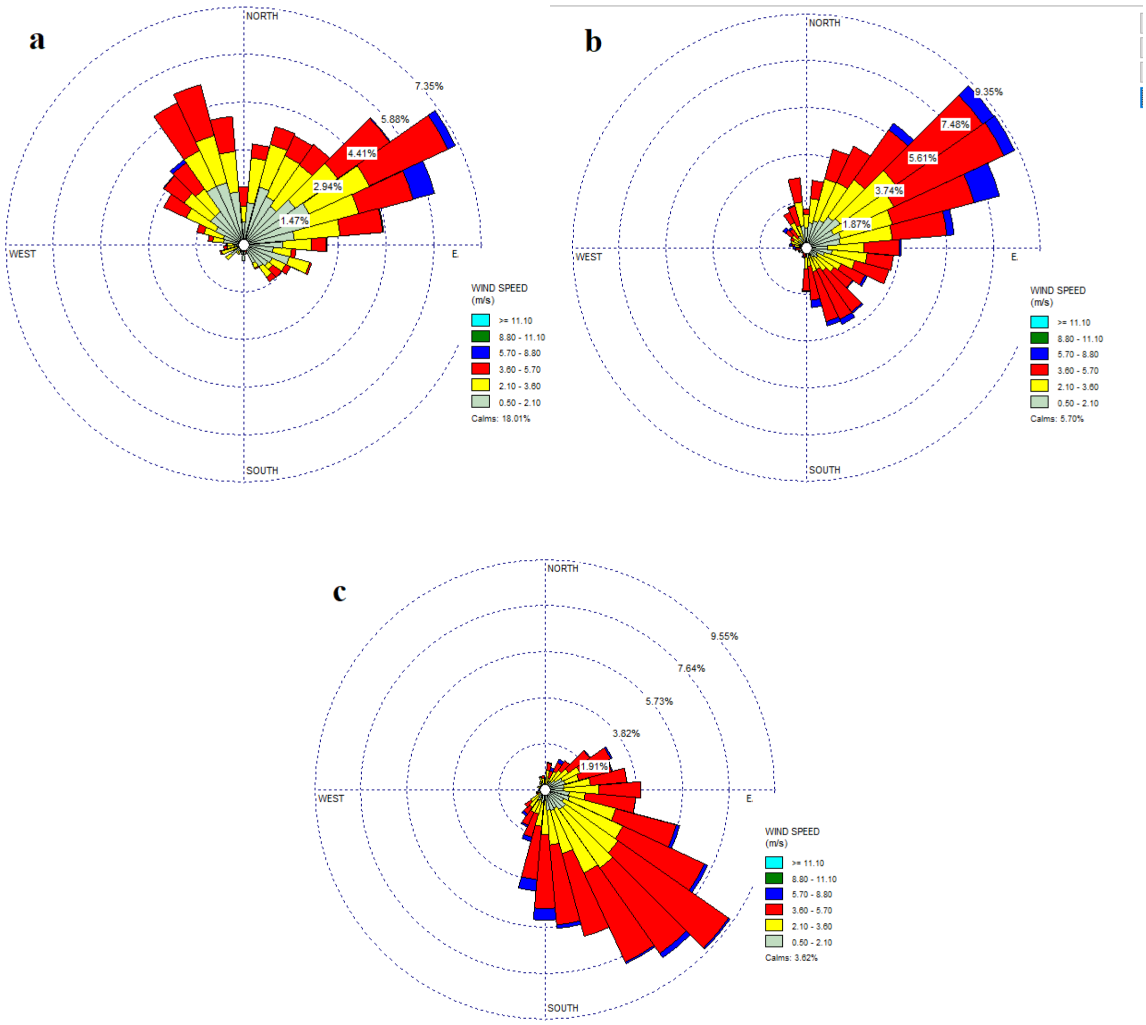


Figure 5.29: Windrose diagram for the study area during (a) winter, (b) summer and (c) monsoon

It is well documented that the dispersion of pollutants is greatly affected by the local meteorological factors (strength and frequency of wind, the intensity of solar radiations) and land surface features (Rahim et al., 2021).

## 5.10 Diurnal Variation of Pollutant Concentration

The diurnal variation of pollutant concentration was assessed on the dates 19 April 2020 and 08 January 2020 to analyze the pollutant dispersion behavior during summer and winter seasons respectively. The analysis was carried out for plant activity only, and the variations have been studied up to a particular distance from the source. The average hourly concentrations have been shown for each distance (from source) over 24 hours. Figure 5.30 shows average hourly concentration of pollutants as a function of time of the day on 19 April 2020. ("0" representing mid night) for different distances from the source (i.e., power plant).

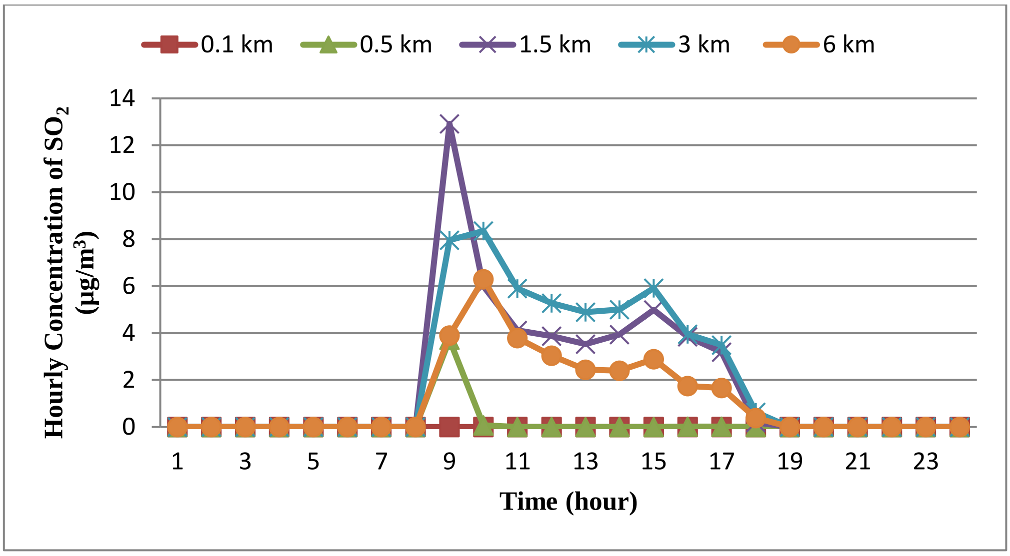


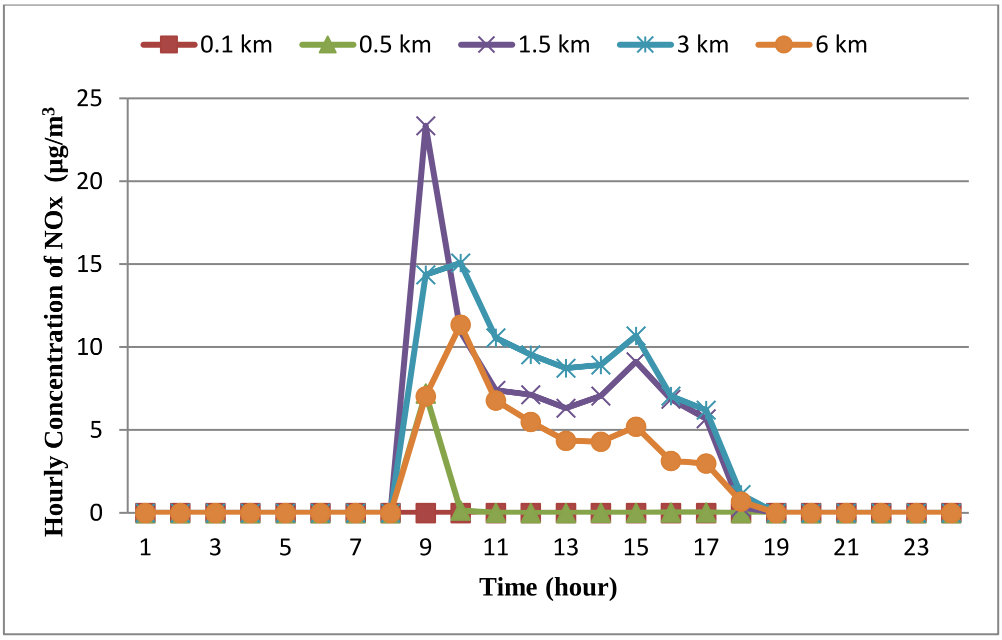

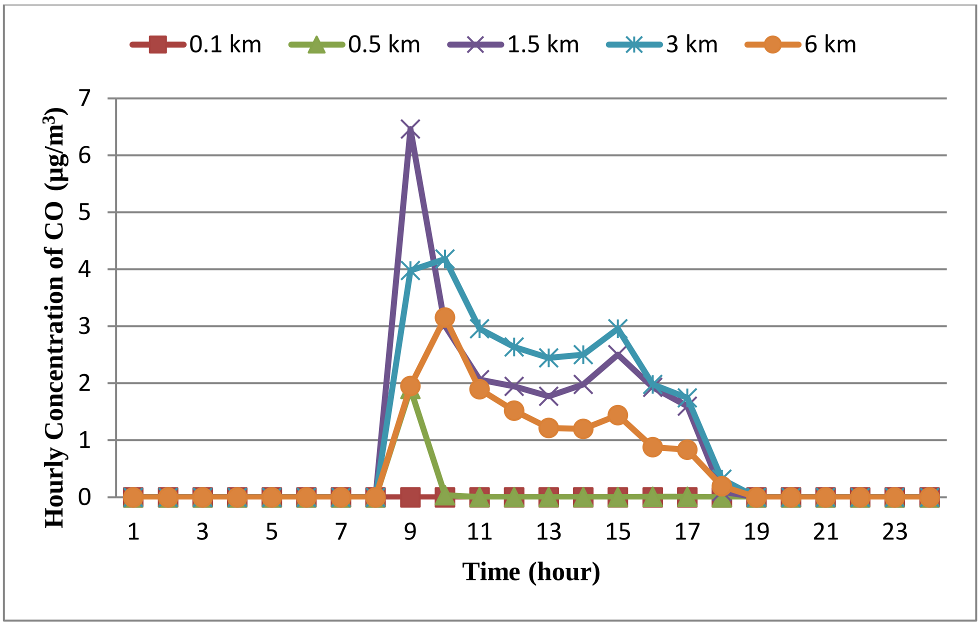


Figure 5.30 (a, b, c): Concentration of pollutants $SO_2$, NOx and CO (due to power plant activity only) as a function of time of the day (on 19 April 2020; "0" representing midnight) at five different distances from the source

Figure 5.30 clearly shows that at a particular distance (0.1 km to 6 km) from the source, the concentration of all three pollutants shows a distinctive trend with time. During the day, after 8 am concentration rise sharply and the peak is reached between 9 am to 11 am. As the day proceeds, the concentrations witness a drastic decline around 12 noon. Again, a slight rise in concentration is observed during the evening period, which eventually undergoes a soft decay during the night.

Meteorology has great importance in transportation, dispersion and natural cleansing of the air pollutants in the atmosphere. Wind speed is an important parameter affecting dispersion of pollutants (Saini and Sharma, 2017). Efforts were therefore made to assess the effect of wind speed on diurnal variation of pollutant concentration.

Figure 5.31 shows variation of wind speed over the day on 19 April 2020. This variation is also consistent with the variation of predicted pollutant concentration shown in Figure 5.30. As the figure describes up to about 8 am in the morning there is virtually no effect of power plant emission on ground level concentration, and ground level concentration is predicted to be near zero. As the day progresses ground level concentration started to increase and about 10 am reaches at its peak.

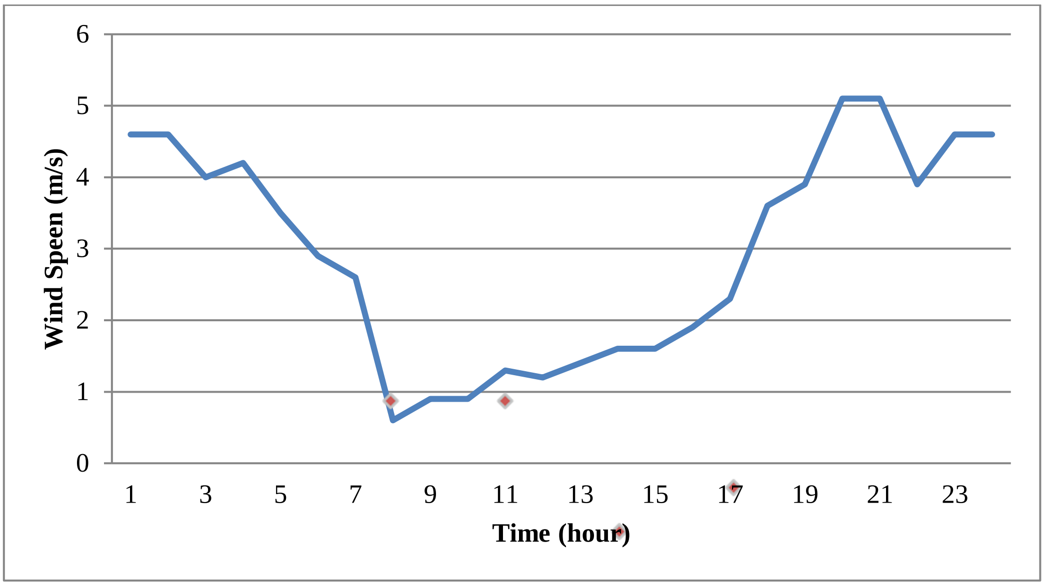


Figure 5.31: Hourly variation of wind speed on 19 April 2020

Wind speed reaches a minimum value at around 8 am. After 8 am wind speed begins to increase and reaches the peak at about 7 pm. From about 8 am to 7 pm, the wind speed is relatively low (from 0.6 m/s to 1.6 m/s). This low wind speed supports higher ground level concentration (as shown in Figure 5.30). As the wind speed increases in the night it contributes to the lowering of pollutant concentration. Pollutant dispersion by higher wind speed has been reported by Tasić et al. (2013).

To assess the diurnal variation of pollutant concentration during winter, the daily variation of $SO_2$ concentration (Figure 5.32) and meteorological parameters for 08 January 2020 were studied. Since all the pollutants exhibits similar diurnal variation, data/graph for the rest of the pollutants have not been shown here. From Figure 5.32 it is observant that pollutants begin to accumulate at ground level from 9 am in the morning. The peak is simultaneously attained at around 11 am at different distances from the source. During afternoon period the concentrations decrease steadily and eventually decline sharply after 5 pm.

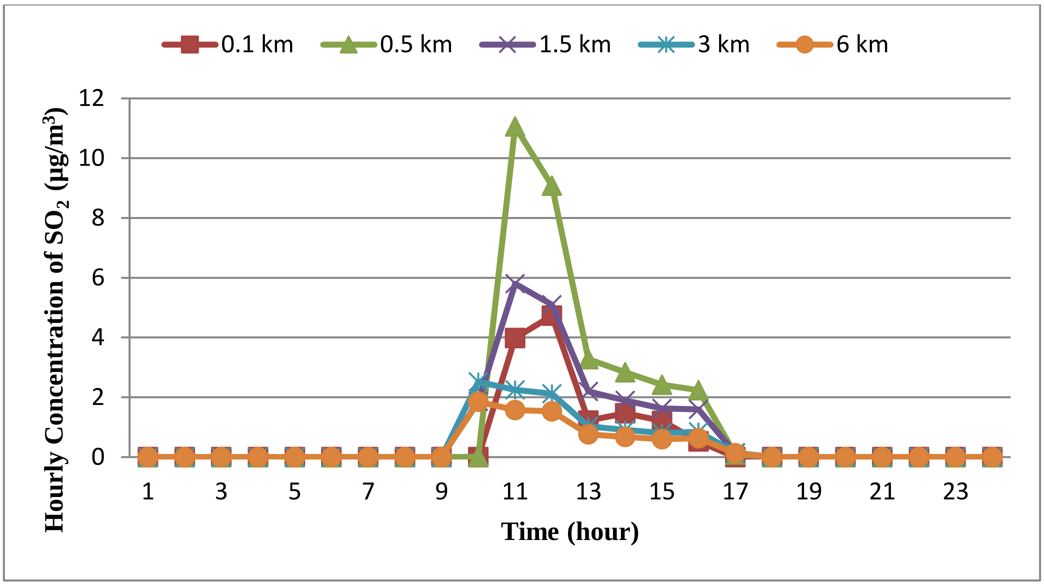


Figure 5.32 (a, b, c): Concentration of pollutants $SO_2$ (due to power plant activity only) as a function of time of the day on 08 January 2020; "0" representing midnight) at five different distances from the source

The pollutant behavior can be explained by the wind speed variation on 08 January. Figure 5.33 shows that high wind (2.5 m/s) speed exists up to 8 am in the morning, which experience a gradual decline afterwards. The appearance of peak $SO_2$ concentration at around 11 am is explained by the presence of light wind (0.5 m/s) along with emission taking place above the mixing height during that period. Furthermore, it is observant that peak $SO_2$ concentration during winter (08 January) is lower than that during summer (19 April).

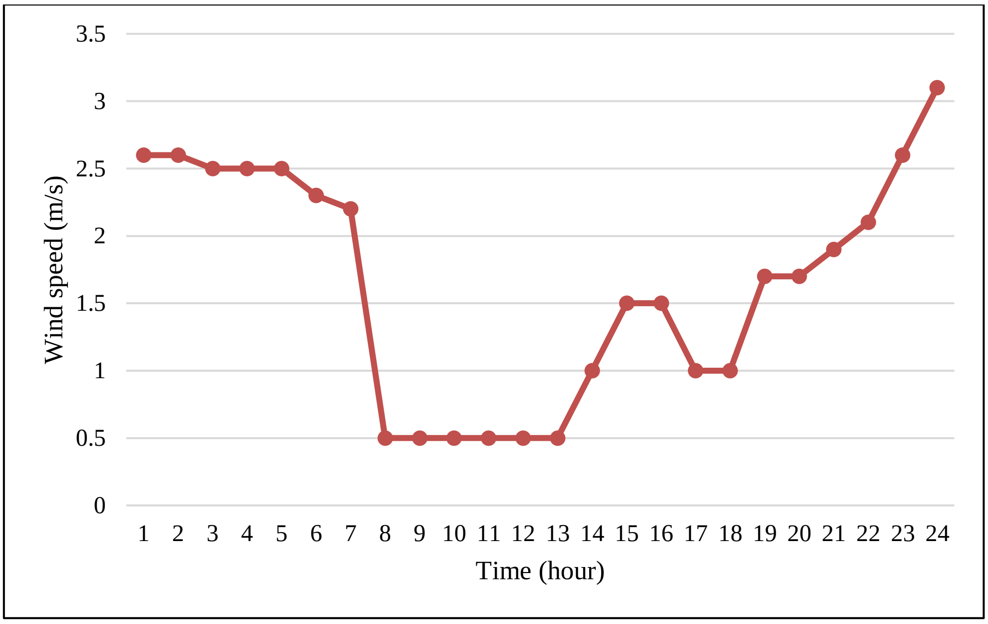


Figure 5.33: Hourly variation of wind speed on 08 January 2020

Hence, it can be concluded that light wind speed confine the pollutants leading to enhanced pollution in the immediate vicinity of the power plant. On the other hand, high wind speed allows dispersion and dilution of pollutants preventing their accumulation at ground level.

## 5.11 Air Quality Index

Air quality index (AQI) provides the understanding of air pollution level at which air can be polluted and the associated health effects that might concern. In Bangladesh AQI is calculated based on 5 criteria pollutants such as particulate matter ($PM_{10}$ and $PM_{2.5}$), $NO_2$, CO, $SO_2$ and Ozone ($O_3$). The Department of Environment (DoE) has also set national ambient air quality standards for these pollutants. These standard aims to protect against adverse human health impact and established national air quality standards to protect public health.

Data obtained from monitoring of ambient air was used to calculate AQI values for $SO_2$ and NOx concentrations (Appendix A-3). Ambient data were collected for continuous 24 hour at three receptor locations (5, 6 and 8) as mentioned in Table 3.1. The measured $SO_2$ and NOx concentrations are presented in Table 5.5.

Table 5.5: Ambient Concentration of $SO_2$ and NOx

| Sampling Location | Date | $SO_2$ (μg/m$^3$) | NOx (μg/m$^3$) |
|---|---|---|---|
| 5 | 5 Dec 2021 | 12.01 | 81.84 |
| 6 | 6 Dec 2021 | 20.39 | 63.93 |
| 8 | 7 Dec 2021 | 41.21 | 73.22 |

The average concentration of $SO_2$ and NOx were 24.53 μg/m$^3$ and 72.99 μg/m$^3$ respectively. The maximum concentration of ambient $SO_2$ and NOx were recorded 41.21 μg/m$^3$ and 81.84 μg/m$^3$ respectively. According to national ambient air quality standard for maximum 24-hr average concentration of $SO_2$ and NOx are 365 μg/m$^3$ and 100 μg/m$^3$. In this regard the ambient air quality was quite below to the standard limit.

Data obtained from monitoring of ambient air was used to calculate the AQI values for 24 hourly averages $SO_2$ and NOx concentrations. The AQI due to the maximum concentration of $SO_2$ and NOx were 11 and 81 respectively which fall in good and moderate category. The AQI for average $SO_2$ and NOx were 6 and 72 which also falls in good and moderate category respectively. From the results it is observant that the AQI fall in moderate category (51-100) which may pose risk for some people particularly those who are unusually sensitive to air pollution.

## 5.12 Model Performance Evaluation

Results of the performance evaluation of AERMOD model has been presented and discussed in this section.

Plot of the comparison between predicted and observed $SO_2$ and NOx are seen in Figure 5.34 and Figure 5.35 respectively.

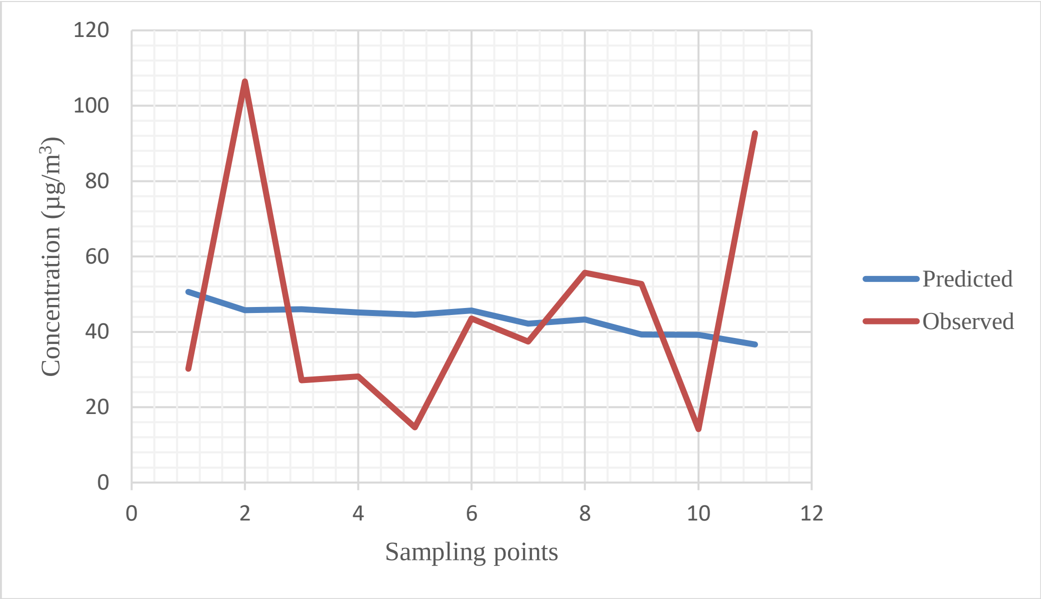


Figure 5.34: Plot of predicted and observed $SO_2$ Concentrations

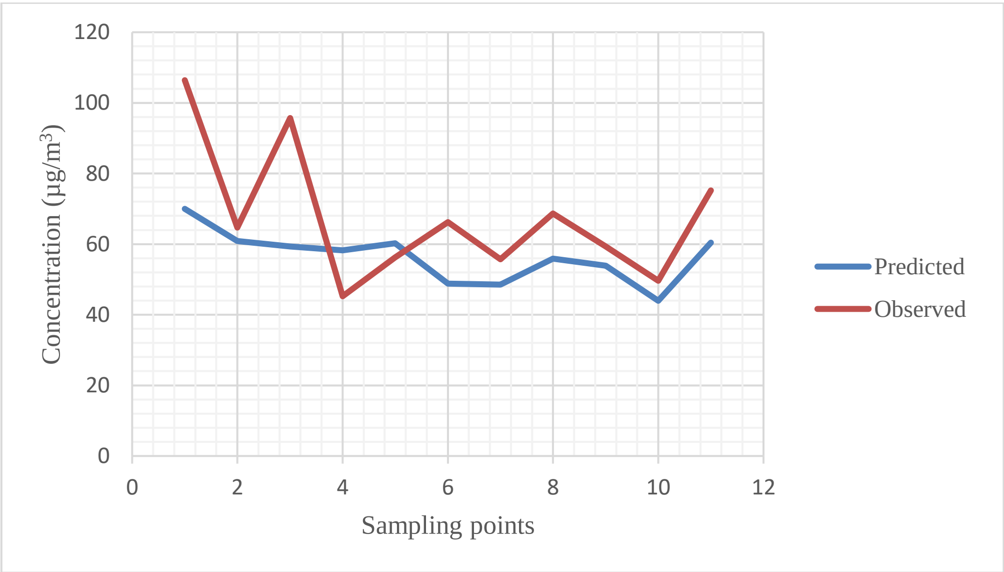


Figure 5.35: Plot of predicted and observed NOx Concentrations

The performance assessment of the model, based on direct quantitative comparisons of observed and predicted mean concentrations as seen in Figure 5.34 and Figure 5.35.

Figures reveal that model predictions for NOx were better than $SO_2$ concentrations. For most of the sampling points predicted NOx concentration closely approached observed concentrations except point 1 and 3. Quantitative agreement between predicted and observed $SO_2$ concentrations were excellent for points 6 and 7, and good for points 8 and 9. However, for points 2 and 11, model significantly under predicted the observed values. Despite these differences between predicted and observed values on some points, the trends in the measurements are accurately predicted especially for NOx.

Results of model performance evaluation after applying the USEPA guideline pertaining to model evaluation protocol are presented in Table 5.6. The indices are the fractional bias (FB), The normalized mean square error (NMSE) and the index of agreement (IOA).

Table 5.6: Statistical Performance Indices of AERMOD model

| **Pollutant** | **FB** | **NMSE** | **IOA** |
|---|---|---|---|
| $SO_2$ | 0.049 | 0.002 | 0.981 |
| NOx | 0.180 | 0.032 | 0.773 |

The index of agreement (IOA) between predicted and observed concentrations is better for $SO_2$ and NOx, since values close to 1 represent a perfect model performance.

However, AERMOD underpredicts $SO_2$ by a small factor than NOx as revealed by their FB values. The positive value of FB indicates underprediction of the model for both the pollutants. The FB values recorded in the model were 0.049 and 0.180. in case of NMSE, better value is recorded for both $SO_2$ than NOx. This shows a reasonable and balanced performance of AERMOD model with the measured values. Both models reasonable predicted the measured values but not perfectly since FB and NMSE should be zero to deemed as perfect model (Chang and Hanna, 2004).

# CHAPTER 6

# DISCUSSIONS

## 6.1 General

This chapter discusses the findings from the dispersion model. Also the effects of the Barapukuria Thermal Power Plant is covered in this chapter.

## 6.2 Comparison with other Coal Fired Power Plant Studies

In the EIA (CPGCL, 2013) report of proposed Matarbari 1200 MW coal fired power plant, yearly average, 24-hour average and 1-hour average values of pollutant concentration were calculated using Guassian diffusion model. Modeling study suggests that the predicted concentration of pollutants from exhaust gases, taking into account the background, will satisfy the ambient air quality standards of Bangladesh as well as environmental standards of the EU.

The Maximum Ground Level Concentration of $SO_2$ and NOx were calculated using SCREEN 3 model in the EIA (EQMS, 2015) report of proposed Payra 2x660 MW coal fired power plant, In Patuakhali district. As the plant was not operational, emission rates of $SO_2$ and NOx were calculated using mass balance method.

Five coal fired power plants each with 1320 MW generation capacity are expected to be installed by 2030 in areas within 5 km radius of Payra, situated in Patuakhali district. Pollutant concentration of these future power plants were predicted by Hossain (2019) by using AERMOD air diffusion model in three different scenarios. Ambient air quality data for the study was collected from EIA report of Payra Power Plant of 2018. But the study was based on theoretical model assumptions as the power plant was not operating at that time. Actual emission rate from the power plant was not available. Ambient air quality data of the study period also was not collected for validation of model.

In the current study actual emission rates from the power plant was collected from the Barapukuria Power Plant authority. Ambient air quality data was also collected for model validation of model and comparison with model predictions.

The findings of these studies are summarized in Table 6.1.

Table 6.1: Comparison of different studies

| Power Plant Study | Studied parameters | Calculated Emission Rates (g/s) | Predicted 24 hour average concentration of pollutants | Bangladesh air quality standard (μg/$m^3$) | WHO guideline (μg/$m^3$) |
|---|---|---|---|---|---|
| EIA of Matarbari 1200 MW Coal Fired Power Plant | SOx | 431 | 40.6 μg/$m^3$ at 3.8 km distance from source | 365 | 20 |
| | NOx | 242 | 25.1 μg/$m^3$ at 3.8 km distance from source | 100 (annual) | 40 (annual) |
| EIA of Payra 2x660 MW coal fired power plant | $SO_2$ | 827 | 264 μg/$m^3$ at 1.36 km from source | 365 | 20 |
| | NOx | 631 | 209 μg/$m^3$ at 1.36 km from source | 100 (annual) | 40 (annual) |
| Study on five coal fired Power plants, in Patuakhali (Phase 1- 1320 MW) | $SO_2$ | 142 | 19.4 μg/$m^3$ at 2.6 km from source | 365 | 20 |
| | NOx | 482 | 38.2 μg/$m^3$ at 2.6 km from source | 100 (annual) | 40 (annual) |
| | CO | 39 | 15.5 μg/$m^3$ at 2.6 km from source | 40000 | 30000 |
| | $PM_{2.5}$ | 20 | 16.6 μg/$m^3$ at 2.6 km from source | 65 | 25 |
| | $PM_{10}$ | 8.95 | 67.9 μg/$m^3$ at 2.6 km from source | 150 | 50 |
| Present study for Barapukuria Coal Fired Power Plant (275 MW) | $SO_2$ | 51.37 | 37.33 μg/$m^3$ at 5 km from source | 365 | 20 |
| | NOx | 92.54 | 45.18 μg/$m^3$ at 5 km from source | 100 (annual) | 40 (annual) |
| | CO | 25.71 | 1.59 μg/$m^3$ at 5 km from source (without background concentration) | 40000 | 30000 |

### 6.3 Impact of Power Plant Emissions on Human Health

This section discusses the effects of power plant operations on human health.

#### 6.3.1 Comparison with Standard Air Quality Values

The predicted peak concentrations of pollutants in the vicinity of the coal-based power plant were obtained from AERMOD simulations. A comparison was then made between cumulative ground level concentration (i.e. summation of peak predicted concentration due to power plant activity and baseline concentration) and the existing WHO, Bangladesh and European Union Standards to ensure compliance with the standards (Table 6.2 and Table 6.3).

Air quality standards provide maximum limits on the amount of a specific pollutant in the air for precise averaging periods. These ambient standards primarily aim at human health protection and have been estimated to permit a margin for citizens susceptible to risk. These values specify harmless daily exposure quantities for the greater part of the population, all over an individual's life period.

In the worst-case scenario, the peak 24 hour predicted concentrations of $SO_2$, $NO_x$ complied the air quality standards. The field data collected at 11 sampling location are also shown in the Table 6.2 and Table 6.3. In case of $SO_2$ the predicted and measured concentrations comply with the Bangladesh and EU standards. In two locations the $SO_2$ value exceeded the WHO guideline. In case of NOx all the values comply with Bangladesh and EU standard and also WHO guideline.

Table 6.2: Comparison of Peak Predicted Concentration of $SO_2$ and Measured Concentration of $SO_2$ with Air Quality Standards (Worst-case scenario)

| Pollutant Considered | Receptor Location | Distance from Source | Predicted Peak Concentration (µg/m3) | Measured Concentration (µg/m3) | Bangladesh Standard (µg/$m^3$) | WHO guideline values (µg/$m^3$) | European Union Standard (µg/$m^3$) |
|---|---|---|---|---|---|---|---|
| $SO_2$ | Base of stack | 0 | 50.60 | 30.22 | 365 | 40 | 125 |
| | Phulbari Primary School | 1.5 | 45.75 | 106.45 | | | |
| | Sherpur Bhabanipur Govt college | 3 | 46.01 | 27.14 | | | |
| | Shibnogor playground | 3 | 45.18 | 28.14 | | | |
| | Phulbari Model High School | 5 | 44.59 | 14.63 | | | |
| | Rangamati jame mosque | 6 | 45.66 | 43.56 | | | |
| | Bhagulpur Bazar | 6 | 42.15 | 37.39 | | | |
| | Parbatipur Upazila Health Complex | 9 | 43.27 | 55.69 | | | |
| | Ambari Bazar Road | 12 | 39.32 | 52.74 | | | |
| | Shuchnipara primary school | 14 | 39.21 | 14.18 | | | |
| | Lohanipara High School | 15 | 36.65 | 92.72 | | | |

Table 6.3: Comparison of Peak Predicted Concentration of NOx and Measured Concentration of NOx with Air Quality Standards (Worst-case scenario)

| Pollutant Considered | Receptor Location | Distance from Source | Predicted Peak Concentration (µg/m3) | Measured Concentration (µg/m3) | Bangladesh Standard ($\mu g/m^3$) | WHO guideline values ($\mu g/m^3$) | European Union Standard ($\mu g/m^3$) |
|---|---|---|---|---|---|---|---|
| NOx | Base of stack | 0 | 69.99 | 106.41 | 100 | 10 | 40 |
| | Phulbari Primary School | 1.5 | 60.87 | 64.64 | | | |
| | Sherpur Bhabanipur Govt college | 3 | 59.36 | 95.69 | | | |
| | Shibnogor playground | 3 | 58.26 | 45.23 | | | |
| | Phulbari Model High School | 5 | 60.20 | 56.23 | | | |
| | Rangamati jame mosque | 6 | 48.78 | 66.26 | | | |
| | Bhagulpur Bazar | 6 | 48.56 | 55.69 | | | |
| | Parbatipur Upazila Health Complex | 9 | 55.92 | 68.69 | | | |
| | Ambari Bazar Road | 12 | 53.86 | 59.32 | | | |
| | Shuchnipara primary school | 14 | 43.95 | 49.65 | | | |
| | Lohanipara High School | 15 | 60.41 | 75.23 | | | |

### 6.3.2 Questionnaire Survey Results

A questionnaire survey was also conducted among the people living within the 10 km distance from the power plant. One to one interview was carried among 40 people of different age groups. Most of them didn't have any severe complaint about the effects of the coal fired power plant on their health. The summary of the questionnaire survey is showed in Table 6.4.

Table 6.4: Disease and symptoms among the people living in the power plant area.

| Disease and symptoms due to increased air pollution | People of age group 0-10 | People of age group 10-20 | People of age group 20-30 | People of age group >30 |
|---|---|---|---|---|
| Respiratory distress | 0 | 2 | 1 | 3 |
| Breathing Problem | 0 | 1 | 2 | 3 |
| Asthma | 1 | 0 | 2 | 2 |
| Coughing | 3 | 2 | 3 | 1 |
| Cardiac Disease | 0 | 0 | 1 | 2 |

As can be seen from the Table that very few peoples have health problems related to air pollution and coal pollution.

### 6.3.3 Air Quality Index (AQI) of the Study Area

The AQI provides information about how clean or polluted the air is, and what associated health effects might be a concern for public. The higher the AQI value, the greater the level of air pollution and the greater the health concern. An AQI value of 100 generally corresponds to the national air quality standard for the pollutant, which is the level that is set by the mandated Environment Protection Agency (e.g., for Bangladesh, Department of Environment) to protect public health. AQI value below 100 (category: moderate) are generally thought of as satisfactory. For the present study the AQI is found to be 81 which falls in the moderate category.

From the comparison of predicted and measured concentration of pollutants with the standard air quality values, it is evident that the maximum emissions of air pollutants ($SO_2$, NOx,) due to the power plant operation is not harmful for the health of the people living in the vicinity of the plant. The questionnaire survey results and the AQI of the study area also indicates the same.

# CHAPTER 7

# CONCLUSIONS AND RECOMMENDATIONS

## 7.1 Conclusions

The overriding purpose of this study was to simulate the dispersion and transport of pollutants emitted due to the operation of Barapukuria Coal Fired Power Plant. The air quality in the vicinity of the power plant was predicted using the dispersion model AERMOD. Meteorological data for the year of 2020 was used in the model simulation. This Chapter summarizes the key findings of the study and presents recommendations for future study.

The major conclusions from the present study are as follows:

- Peak concentration of pollutants ($SO_2$, NOx and CO) over the modeled area were simulated using AERMOD air dispersion model for different averaging periods (Hourly, daily and annual). The predicted peak concentration of $SO_2$ in that area are 18.62 $\mu g/m^3$, 3.19 $\mu g/m^3$, 0.82 $\mu g/m^3$ for 1-hr, 24-hr and annual averaging periods respectively. Similarly, the predicted maximum concentration of NOx in that area are found to be 33.56 $\mu g/m^3$, 5.75 $\mu g/m^3$, 1.48 $\mu g/m^3$ for 1-hr, 24-hr and annual averaging periods respectively. The peak concentrations of CO are 9.32 $\mu g/m^3$, 1.59 $\mu g/m^3$, 0.41 $\mu g/m^3$ for 1-hr, 24-hr and annual averaging period respectively.

- When added to the baseline ambient concentration, it was found that the resultant concentration of NOx exceeds WHO guideline values. Resultant $SO_2$ and CO concentration are in compliance with Bangladesh standard as well as WHO guideline values.

- Predicted peak concentration (hourly average, 24-hr average and annual average) of pollutants ($SO_2$, NOx and CO) over the modeled area (illustrated by iso concentration contours) increases about five times from scenario I (only 3$^{rd}$ unit operating with 150

MW capacity) to Scenario II (all units operating with 525 MW capacity). The predicted CO concentrations due to power plant emissions appears to be negligible.

- The dispersion of $SO_2$, NOx and CO was modeled over a domain of 30 $km^2$ centered around the plant. Based on the primary simulation results it was concluded, that the impact of the power plant was felt highly at the receptor location within a radius of 5 km. Furthermore, receptors located on south western parts of the plant showed relatively higher pollutant concentrations than other parts of the study domain as a result of the predominant north eastern winds in the project area during the study period.

- Comparing with the observed air quality, it was found that 29.4% of total ambient $SO_2$ and 25.2% of total ambient NOx may come from the power plant emission.

- Higher pollutant concentrations were predicted during summer (March-June), while the least concentration appeared during monsoon (July-October). Central radial distribution of pollutants was observed during the monsoon season, whereas north eastern winds linearly carry the pollutants towards north west during winter and summer. The seasonal variation of pollutants is influenced by a number of factors including wind direction and solar radiation.

- There appears to be significant diurnal variation of pollutant concentration in the vicinity of the power plant. Simulated results of the model showed that the peak concentration is reached between 9 to 11 am of a day and the concentrations witnessed a drastic decline around 12 noon. Comparing with the wind speed distribution it was observed that the light winds contribute to enhanced pollutant concentration in the vicinity of the power plant of Barapukuria.

- Air Quality Index (AQI) results showed that AQI for $SO_2$ (11) and NOx (81) during the month of November indicates moderate category (51-100) which may pose risk for some people particularly those who are unusually sensitive to air pollution.

- In order to validate the modeling system, results of the dispersion simulations were compared with the field measurements at the same locations using graphical and statistical measures. The evaluation results revealed a good agreement (98% for $SO_2$ and 77% for NOx) between model and observation leading to the conclusion that AERMOD can be used satisfactorily for air pollution studies for checking compliance of industrial set-ups with standards.

- The maximum predicted concentrations of $SO_2$, NOx and the field measured values of $SO_2$, NOx complied the air quality standards. The questionnaire survey also showed that very few people have problems related to air pollution. The AQI of the study area falls in the moderate category which indicates acceptable air quality. From the results it can be concluded that the maximum emissions of air pollutants ($SO_2$, NOx) due to the power plant operation is not harmful for the health of the people living in the vicinity of Barapukurai Coal Fired Power Plant.

## 7.2 Recommendations for Future Study

From the above given conclusions, the following recommendations could be implied for further studies:

- Due to the increase in coal consumption for power generation, there is a critical need to evaluate the health risks for the population living in the vicinity of a coal fired power plant. Health risk assessment should be conducted for short-term and long-term dispersion of pollutants to investigate population exposure to morbidity and in some cases, premature mortality.
- Ambient air quality data should be collected for longer periods and also season based for better understanding of the surrounding air quality. The emission rate of pollutants from the plant should be collected for longer periods like 6 months or 1 year for a clear view of the emission status.

## REFERENCES


Adappa, S., Tiwari, R. R., Kamath, R. and Guddattu, V. (2017). Health effects and environmental issues in residents around coal-fired thermal power plant, Padubidri: A cross-sectional study, Journal of Environmental and Occupational Science, Vol. 6, No. 1, pp. 611-618.

Adeniran, J. A., Yusuf, R. O., Fakinle, B. S. & Sonibare, J. A. (2018). Air quality assessment and modelling of pollutants emission from a major cement plant complex in Nigeria, Atmospheric Pollution Research, Vol. 10, No. 1, pp. 257-266.

Affum, H. A. (2015). Numerical simulation of dispersion of emissions from Tema oil refinery in Ghana, Ph.D. Thesis, Dept of Nuclear sci and application, University of Ghana.

Ahmed, S. and Hossain, I. (2008). Applicability of air pollution modeling in a cluster of brickfields in Bangladesh, Chemical Engineering Research Bulletin, Vol. 12, pp. 28-34.

Alam, M. J. B., Ahmed, A. A. M., Khan, M. J. H. and Ahmed, B. (2011). Evaluation of possible environmental impacts for Barapukuria thermal power plant and coal mine, Journal of Soil Science and Environmental Management, Vol. 25, pp. 126-131.

APSCL (2016). Environmental Impact Assessment; Ashuganj 400 MW Combined Cycle Power Plant (East), Asian Development bank.

Baig, K. S. and Yousaf, M. (2017). Coal fired power plants: emission problems and controlling techniques, Journal of Earth Science and Climate Change, Vol. 8, No. 7.

BCMCL (2019). Annual Report 2018-2019, Barapukuria Coal Minig Company Ltd.

bdenvironment.com (2013-2021). What is the Bangladesh Clean Air Act?. [Online]. Available https://bdenvironment.com/2020/06/15/what-is-the-bangladesh-clean-air-act/ [Accessed 27 February 2022].

BPDB (2020). Annual Report 2019-2020, Bangladesh Power Development Board.

BPDB (2021). Annual Report 2020-21, Bangladesh Power Development Board.

Brancher, M. (2021). Increased ozone pollution alongside reduced nitrogen dioxide concentrations during Vienna’s first COVID-19 lockdown: Significance for air quality management, Environmental Pollution journal, Vol. 287, pp. 117153.

Burns, D. A., Aherne, J., Gay, D. A. and Lehmann, C. M., (2016). Acid rain and its environmental effects: Recent scientific advances, Atmospheric Environment, Vol. 146, pp. 1-4.

Carbonell, L. T., Ruiz, E. M., Gácita, M. S., Oliva, J. R., Rivero, N.D. (2007). Assessment of the impacts on health due to the emissions of Cuban power plants that use fossil fuel oils with high content of sulfur. Estimation of external costs, Atmospheric Environment, Vol. 41, No. 10, pp. 2202–2213.

CASE (2018). Monthly Air Quality Monitoring Report: July 2018, Ministry of Environment and Forests, Government of the People's Republic of Bangladesh,

CEGIS (2013). Environmental impact assessment of extension of Barapukuria coal fired thermal powewr station by 275 MW to be constructed at the location of Parbatipur, Dinajpur, Ministry of Power, Energy and Mineral Resources; Government of the People's Republic of Bangladesh.

Carqueira, J. d. S., de Albuquerque, H. N. and Salviano de Sousa, F. d. A. (2019). Atmospheric pollutants: modeling with Aermod software, Air Quality, Atmosphere & Health, Vol. 12, pp. 21-32.

Chang, J. C. and Hanna, S. R. (2004). Air quality model performance evaluation, Meteorology and Atmospheric Physics, Vol.87, pp. 167-194.

CPGCL (2013). Environmental impact assessment of construction of Matarbari 600x2 MW coal fired power plant and associated facilities, Coal Power Generation Company of Bangladesh Limited.

Dai, H., Ma, D., Zhu, R., Sun, B., He, J. (2019). Impact of control measures on nitrogen oxides, sulfur dioxide and particulate matter emissions from coal-fired power plants in Anhui Province, China, Atmosphere, Vol. 10, No. 1, pp. 35.

EQMS (2015). Environmental impact assessment (EIA) study of payra 1320 MW thermal power plant project, Bangladesh China Power Company (Pvt.) Ltd.

Fadavi, A., Abari, M. F. and Nadoushan, M. A. (2016). Evaluation of AERMOD for distribution modeling of particulate matters (Case study: Ardestan Cement Factory), International Journal of Pharmaceutical Research & Allied Sciences, Vol. 5, No. 4, pp. 262-270.

Forero López, A. D., Fabiani, M., Lassalle, V. L., Spetter, C. V., Fernandez Severini, M.D. (2022). Critical review of the characteristics, interactions, and toxicity ofmicro/nanomaterials pollutants in aquatic environments, Marine Pollution Bulletin, Vol. 174, pp. 113276.

Guttikunda, S. (2019). Impact analysis of brick kilns on the air quality in Dhaka, Bangladesh. Semantic Scholar.
[Online]. Available: https://www.semanticscholar.org/paper/Impact-Analysis-of-Brick-Kilns-on-the-Air-Quality
Guttikunda/87685662c718f9aa64b9833202e3f2004f5bfd28. [15 August 2022].

Guttikunda, S. K. and Jawahar, P. (2014). Atmospheric emissions and pollution from the coal-fired thermal power plants in India, Atmospheric Environment journal, Vol. 92, pp. 449-460.

Health Effects Institute (2019). State of Global Air 2019: A special report on global exposure to air pollution and its disease burden, Health Effects Institute.

Health Effects Institute (2020). State of Global Air, 2020; A special report on global exposure to air pollution and its health impacts, Health Effects Institute.

Holmes, N. S. and Morawska, L. (2006). A review of Dispersion modelling and its application to the dispersion of particles: An overview of different dispersion models available, Atmospheric Enivronment, Vol. 40, No. 30, pp. 1046-1072.

Hossain, M. N., Paul, S. K. and Hasan, M. M. (2015). Environmental impacts of coal mine and thermal power plant to the surroundings of Barapukuria, Dinajpur, Bangladesh, Environmental Monitoring and Assessessment, Vol. 187.

Hossain, S., Chowdhury, H., Chowdhury, T., Ahamed, J. U., Saidur, R., Sait, S. M. et al. (2020). Energy, exergy and sustainability analyses of Bangladesh's power generation generation sector, Energy Reports, Vol. 6, pp. 868-878.

Hossain, M. (2019). Impact of coal fired power plant emissions on ambient air quality using a diffusion model, M. Sc. Engg. Thesis, Dept. of Civil Engg., BUET.

Hossain, M., Ahmed, T. and Ali, M. A. (2020). Predicting the non-carcinogenic health hazards associated with emissions from developing coal-fired power plants in Payra, Bangladesh, Air Quality, Atmosphere & Health, Vol. 13, No. 11, pp. 1351-1365.

Idris, M., Darma, T. H., Koki, F. S., Suleiman, A., Ali, M. H., Yarima, S. U. et al. (2019). An analysis of air pollution at some industrial areas of Kano using the AERMOD Model, Bayero Journal of Pure and Applied Sciences, Vol. 12, No. 1, pp. 117-127.

Institute for Health Metrics and Evaluation (IHME) (2018). Findings from the global burden disease study.

International Energy Agency (2019). China Power System Transformation Analysis.

IQAir (2020). World Air Quality Report.

Islam, S. and Khan, M. Z. R. (2017). A review of energy sector of Bangladesh, Energy Procedia, Vol. 110, pp. 611-618.

Khatun, M. A., Rashid, M. B. and Hygen, H. O. (2016). Climate of Bangladesh, Bangladesh Meteorological Department.

Kim, H., Byun. G., Choi, Y., Kim, S., Kim, S. Y., Lee, J. T. (2021). Effects of long-term exposure to air pollution on all-cause mortality and cause-specific mortality in seven major cities of South Korea: Korean national health and nutritional examination surveys with mortality follow-up, Environmental Research, Vol. 192, pp. 110290.

Kopas, J., York, E., Jin, X., Harish, S. P., Kennedy, R., Shen, S. V. et al. (2020). Environmental justice in India: incidence of air pollution from coal-fired power plants, Ecological Economics, Vol. 176, pp. 106711.

Kravchenko, J. and Lyerly, H. K. (2018). The Impact of Coal-Powered Electrical Plants and Coal Ash Impoundments on the Health of Residential Communities, NC Medical Journal, Vol. 79, No. 5, pp. 289-300.

Lakes Environmental Consultants Inc (2003). Proposed guidance for air dispersion modeling.

Liu, K., Wu, Q., Wang, L., Wang, S., Liu, T., Ding, D. et al. (2019). Measure-specific effectiveness of air pollution control on China's atmospheric mercury concentration and deposition during 2013-2017, Environmental Science and Technology, Vol. 53, No. 15, pp. 8938-8946.

Li, Z., Ming, T., Liu, S., Peng, C., Richter, R. D., Li, W. et al. (2021). Review on pollutant dispersion in urban areas-part A: Effects of mechanical factors and urban morphology, Building and Environment, Vol. 190, pp. 107534.

López, M. T., Zuk, M., Garibay, V., Tzintzun, G., Iniestra, R., Fernández, A. (2005). Health impacts from power plant emissions in Mexico, Atmospheric Environment, Vol. 39, No. 7, pp. 1199–1209.

Maji, K. J., Arora, M. and Dikshit, A. K. (2018). Premature mortality attributable to PM2.5 exposure and future policy roadmap for 'airpocalypse' affected Asian megacities, Process Safety and Environmental Protection, Vol. 118, pp. (371-383).

Massey, D. D., Kulshrestha, A. and Taneja, A. (2013). Particulate matter concentrations and their related metal toxicity in rural residential environment of semi-arid region of India, Atmospheric Environment, Vol. 67, pp. 278-286.

Masud, M. H., Shakib, M. N. and Rokonuzzaman, M. (2014). Study of environmental impacts of the Barapukuria Thermal Power Plant of Bangladesh, Global Journal of Researches in Engineering Mechanical and Mechanics Engineering, Vol. 14, No. 1.

Ma, T. and Takeuchi, K. (2020). Cleaning up the air for the 2008 Beijing Olympic Games: Empirical study on China's thermal power sector, Resource and Energy Economics, Vol. 60, pp. 101151.

meteoblue (2022). Simulated historical climate & weather data for Dinājpur. [Online]. Available:https://www.meteoblue.com/en/weather/historyclimate/climatemodelled/sliedrecht_netherlands_2747169. [15 August 2022].

Ministry of Environment, Toronto, Ontario (2004). Air dispersion modelling guideline for Ontario.

Mokhtar, M. M., Hassim, M. H. and Taib, R. M. (2014). Health risk assessment of emissions from a coal-fired power plant using AERMOD modeling, Process Safety and Environment Protection, Vol. 92, No. 5, pp. 476-485.

Mousavi, S. S., Goudarzi, G., Sabzalipour, S., Rouzbahani, M. M., Hassan, E. M. (2021). An evaluation of CO, $CO_2$, and $SO_2$ emissions during continuous and non-continuous operation in a gas refinery using the AERMOD, Environmental Science and Pollution Research, Vol. 28, pp. 56996–57008.

Munawer, M. E. (2017). Human health and environmental impacts of coal combustion and post combustion wastes, Journal of Sustainable Mining, Vol. 17, No. 2, pp. 87-96.

Muntaseer Billah Ibn Azkar, M. A., Chatani, S. and Sudo, K. (2012). Simulation of urban and regional air pollution in Bangladesh, Journal of Geophysical Research Atmospheres, Vol. 117, No.7.

North Carolina Department of Environment and Natural Resources, Devision of Air Quality, (2014). Guideline for evaluating the air quality impacts of toxic pollutants in North Carolina.

Petavratzi, E., Kingman, S. and Lowndes, I. (2005). Particulates from mining operations: A review of sources, effects and regulations, Minerals Engineering, Vol. 18, No. 12, pp. 1183-1199.

Power Division (2016). Power System Master Plan 2016, Ministry of Power, Energy and Mineral Resources, Government of the People's Republic of Bangladesh.

Rahim, H. A., Khan, M. F., Ibrahim, Z. F., Shoaib, A., Suradi, H., Mohyeddin, N. et al. (2021). Coastal meteorology on the dispersion of air particles at the Bachok GAW Station, Science of The Total Environment, Vol. 782, pp. 146783.

Rahman, M. M., Howladar M. F., Hossain, M. A., Muzemder, A. T. M. S. H., Numanbakth, M. A. A. (2019). Impact assessment of anthropogenic activities on water environment of Tillai River and its surroundings, Barapukuria Thermal Power Plant, Dinajpur, Bangladesh, Groundwater for Sustainable Development, Vol. 10, pp. 100310.

Rana, M. M., Sulaiman, N., Sivertsen, B., Khan, M. F., Nasreen, S. (2016). Trends in atmospheric particulate matter in Dhaka, Bangladesh, and the vicinity, Environmental Science and Pollution Research, Vol. 23, No. 17, pp. 17393-17403.

Rokonuzzaman, M., Chowdhury, M. S. and Quamruzzaman, C. (2019). Estimating the rate of sulfur dioxide ($SO_2$) emission and its impact on human health in the study area of Barapukuria coal mine, Proc. ICPE 2019, BUET.

Rood, A. S. (2014). Performance evaluation of AERMOD, CALPUFF, and legacy air dispersion models using the Winter Validation Tracer Study dataset, Atmospheric Environment, Vol. 87, pp. 707-720.

Roy, D., Singh, G. and Seo, Y. C. (2019). Carcinogenic and non-carcinogenic risks from $PM_{10}$- and $PM_{2.5}$-bound metals in a critically polluted coal mining area, Atmospheric Pollution Research, Vol. 10, No. 6, pp. 1964-1975.

Safiullah, S., Khan, M. R. R., and Sabur, M. A. (2011). Comparative study of Bangladesh Barapukuria coal with those of various other countries, Journal of Bangladesh Chemical Society, Vol. 24, No. 2, pp. 221-225.

Saini, N. R. and Sharma, B. (2017). Effect of meteorological condiation on NOx pollution of Kota city, India, Indian Journal of Scientific Research, Vol. 15, No. 1, pp. 185-189.

Shaikh, K., Imran, U. and Shaikh, S. (2018). Health risk assessment for emissions from Jamshoro, Journal of Industrial Pollution Control, Vol. 34, No. 2, pp. 2142-2151.

Shindell, D. et. al. (2012). Chapter 2: Atmosphere, The fifth Global Environment Outlook, GEO 5, UNEP, pp. 32-64.

Shi, Z., Zhang, J., Xiao, Z., Lu, T., Ren, X., Wei, H. (2021). Effects of acid rain on plant growth: A meta-analysis, Journal of Environmental Management, Vol. 297, pp. 113213.

SREDA (2016). Energy Efficiency and Conservation Master Plan up to 2030, Ministry of Power, Energy and Mineral Resources, Government of the People's Republic of Bangladesh.

Stern, A. (1976). Air Pollution - Volume III, Academic Press, New York, USA.

Tamim, M. M., Dhar, A. and Hossain, M. S. (2013). Fly ash in Bangladesh- An overview, International Journal of Scientific & Engineering Research, Vol. 4, No. 6, pp. 809-812.

Tasić, V., Kovačević, R. and Milošević, N. (2013). Investigating the impacts of winds on $SO_2$ concentrations in Bor, Serbia, Journal of Sustainable Development of Energy, Water and Environment Systems, Vol. 1, No. 2, pp. 141-151.

USEPA (1995). National air quality and emissions trends report, 1994, United States Environmental Protection Agency, Office of Research and Development.

USEPA (2004). User's Guide for the AERMOD Terrain Preprocessor (AERMAP), United States Environmental Protection Agency, Office of Air Quality Planning and Standard.

USEPA (2016). User's Guide for the AERMOD Meteorological Preprocessor (AERMET), United States Environmental Protection Agency.

USEPA (2021). NAAQS Table. [Online]. Available at: https://www.epa.gov/criteria-air-pollutants/naaqs-table. [30 January 2022].

USEPA (2022). User's guide for the AMS/EPA ragulatory model-AERMOD, United States Environmental Protection Agency, Office of Air Quality Planning and Standard.

Venkatram, A., Brode, R., Cimorelli, A., Lee, R., Paine, R., Perry, S. et al. (2001). A complex terrain dispersion model for regulatory applications, Atmospheric Environment, Vol. 35, No. 24, pp. 4211-4221.

Wang, G., Cheng, S., Wei, W., Yang, X., Wang, X., Jia, J. et al. (2017). Characteristics and emission-reduction measures evaluation of $PM_{2.5}$ during the two major events: APEC and Parade, Science of the Total Environment, Vol. 595, pp. 81-92.

Wang, Y., Wu, R., Liu, L., Yuan, Y., Liu, C. G., Hang Ho, S. S. et al. (2022). Differential health and economic impacts from the COVID-19 lockdown between the developed and developing countries: Perspective on air pollution, Environmental Pollution journal, Vol. 293, pp. 118544.

Wei, X., Tong, Q., Magill, I., Vithayasrichareon, P., Betz, R. et al. (2020). Evaluation of potential co-benefits of air pollution control and climate mitigation policies for China's electricity sector, Energy Economics, Vol. 92, pp. 104917.

World Health Organization (2022). What are the WHO Air quality guidelines?. [Online] Available at: https://www.who.int/news-room/feature-stories/detail/what-are-the-who-air-quality-guidelines. [28 January 2022].

Yue, H., Worrell, E., Crijns-Graus, W. and Zhang, S. (2021). The potential of industrial electricity savings to reduce air pollution from coal-fired power generation in China, Journal of Cleaner Production, Vol. 301, pp. 126978.

Zhao, Y., Wang, S., Duan, L., Lei, Y., Cao, P., Hao, J.(2008). Primary air pollutant emissions of coal-fired power plants in China: Current status and future prediction, Atmospheric Environment journal, Vol. 42, No. 36, pp. 8442–8452.

# APPENDIX

# APPENDIX

A-3: Ambient concentration of $SO_2$ and NOx at 3 receptor locations collected for 24 hour period.

| Sampling Location | 5 | | 6 | | 8 | |
|---|---|---|---|---|---|---|
| Date | 5-Dec-21 | | 6-Dec-21 | | 7-Dec-21 | |
| Hour | $SO_2$ | NOx | $SO_2$ | NOx | $SO_2$ | NOx |
| 1 | 2.660 | 209.920 | 0.000 | 106.830 | 50.540 | 120.330 |
| 2 | 2.660 | 128.288 | 11.900 | 78.590 | 50.540 | 120.330 |
| 3 | 6.340 | 92.826 | 22.335 | 41.380 | 42.560 | 120.330 |
| 4 | 21.901 | 63.189 | 47.330 | 4.800 | 37.240 | 82.130 |
| 5 | 32.674 | 36.386 | 68.430 | 3.820 | 58.520 | 84.040 |
| 6 | 37.462 | 11.524 | 79.300 | 3.820 | 53.200 | 74.490 |
| 7 | 45.929 | 5.284 | 63.650 | 3.820 | 63.840 | 78.310 |
| 8 | 42.383 | 4.107 | 36.650 | 4.170 | 82.460 | 110.780 |
| 9 | 38.393 | 5.635 | 21.439 | 19.800 | 69.160 | 103.140 |
| 10 | 14.275 | 29.350 | 16.700 | 25.560 | 66.500 | 103.140 |
| 11 | 5.808 | 71.275 | 11.730 | 43.450 | 45.220 | 103.140 |
| 12 | 3.547 | 91.585 | 12.350 | 64.640 | 55.860 | 103.140 |
| 13 | 2.926 | 88.210 | 29.260 | 88.019 | 61.180 | 103.140 |
| 14 | 3.015 | 78.565 | 0.000 | 95.370 | 95.760 | 103.140 |
| 15 | 3.236 | 83.085 | 13.300 | 97.630 | 58.520 | 103.140 |
| 16 | 3.680 | 101.994 | 10.640 | 103.070 | 77.140 | 103.140 |
| 17 | 2.660 | 100.243 | 0.000 | 89.030 | 85.120 | 103.140 |
| 18 | 2.749 | 113.486 | 6.650 | 83.560 | 45.220 | 103.140 |
| 19 | 2.660 | 115.682 | 15.960 | 90.050 | 45.220 | 40.110 |
| 20 | 2.660 | 110.621 | 0.000 | 95.460 | 45.220 | 28.650 |
| 21 | 2.660 | 111.035 | 13.830 | 74.960 | 45.220 | 17.190 |
| 22 | 2.660 | 106.610 | 0.000 | 101.930 | 45.220 | 21.010 |
| 23 | 2.660 | 103.968 | 7.980 | 104.380 | 45.220 | 21.010 |
| 24 | 2.660 | 101.421 | 0.000 | 110.350 | 45.220 | 13.370 |